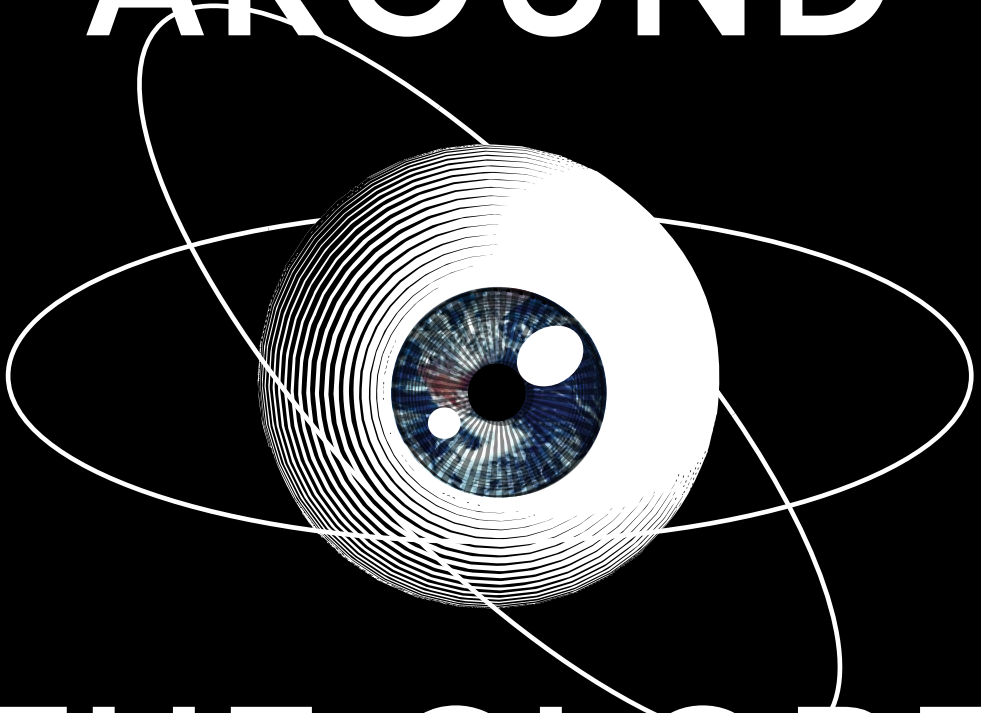


Robin Willaert

AROUND



THE GLOBE

New prospects in diagnosis and treatment planning of orbital diseases:
from imaging analysis to patient-specific treatment.

AROUND THE GLOBE

**New prospects in diagnosis and treatment planning of orbital diseases:
from imaging analysis to patient-specific treatment.**

Robin Willaert

UGent 01813170

KU Leuven u0127785

PROMOTERS GHENT UNIVERSITY

PROMOTERS KU LEUVEN

Prof. Dr. N. Brusselaers

Prof. Dr. R. Jacobs

Prof. Dr. Em. H. Vermeersch

Prof. Dr. I. Mombaerts



JUNE 2020

A dissertation submitted to Ghent University and Catholic University Leuven
in partial fulfilment of the requirements for the Joint Degree of Doctor in Health Sciences
and Biomedical Sciences, respectively.

PROMOTERS

Prof. Dr. N. Brusselsaers	Universiteit Gent
Prof. Dr. Em. H. Vermeersch	Universiteit Gent
Prof. Dr. R. Jacobs	Katholieke Universiteit Leuven
Prof. Dr. I. Mombaerts	Katholieke Universiteit Leuven

SUPERVISORY COMMITTEE

Ir. E. Shaheen	Katholieke Universiteit Leuven
----------------	--------------------------------

EXAMINATION COMMITTEE

Prof. Dr. J. Vande Walle – <i>Voorzitter</i>	Universiteit Gent
Prof. Dr. W. Huvenne – <i>Secretaris</i>	Universiteit Gent
Prof. Dr. B. Leroy	Universiteit Gent
Prof. Dr. P. Demaerel	Katholieke Universiteit Leuven
Prof. Dr. S. De Vleeschouwer	Katholieke Universiteit Leuven
Prof. Dr. T. Maal	Radboud Universiteit Nijmegen

Graphic design by Janine Kopatz
www.janinekopatz.com

© Robin Willaert, 2020

All rights reserved. No part of this thesis may be reproduced or transmitted in any form or by any means, without prior written permission of the authors, or when appropriate, from the publishers of the publications.

Table of contents

List of abbreviations	9
Introduction	11
Rationale and objectives	20
Articles	
1 Three-Dimensional Characterisation of the Globe Position in the Orbit	25
2 Efficacy and complications of orbital fat decompression in Graves' orbitopathy: a systematic review and meta-analysis	37
3 A Systematic Review on Volumetric Analysis in Orbital MRI	61
4 Semi-automatic MRI based Orbital Fat Volumetry: Reliability and Correlation with CT	85
5 Development and Validation of an MRI Protocol for Orbital Soft Tissue Volumetry.....	99
Discussion	119
Summary	127
Samenvatting.....	129
Personal contributions.....	131
Acknowledgements	133
Curriculum vitae	135

“Volens vigilans”

List of abbreviations

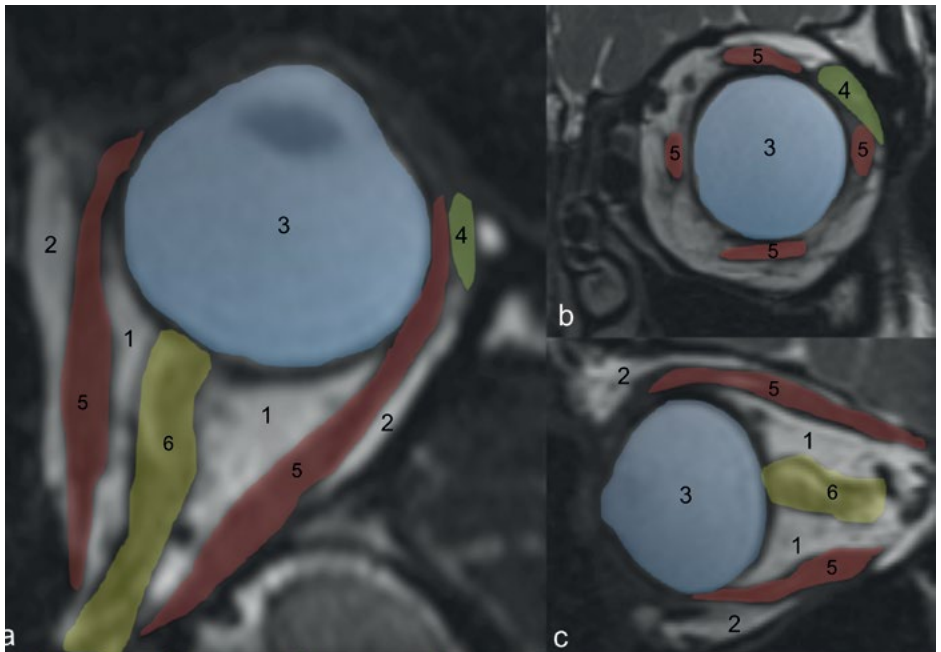
2D	Two Dimensional	MD	Mean difference
3D	Three dimensional	MDT	Multi-dimensional threshold
AP	Anterior-posterior	MINORS	Methodological index for non-randomized studies
BROD	Bone removal orbital decompression	ML	Medial-lateral
CI	Confidence interval	MPRAGE	Magnetisation prepared rapid acquisition gradient echo
CT	Computed tomography	MRI	Magnetic resonance imaging
DICOM	Digital imaging and communications in medicine	PRISMA	Preferred reporting items for systematic reviews and meta-analysis
EOM	Extraocular muscles	QoL	Quality of life
ET	Echo time	RG	Region growing
EUGOGO	European group on graves' orbitopathy	ROI	Region of interest
FLAIR	Fluid-attenuated inversion recovery	RT	Repetition time
FROD	Fat removal orbital decompression	SD	Standard deviation
FSE	Fast spin echo	SE	Standard error
GO	Graves' orbitopathy	SI	Superior-inferior
GP	Globe position	SPACE	Sampling perfection with application-optimized contrasts by using flip angle evolution
GRADE	Grading of recommendations assessment, development and evaluation	T	Tesla
ICC	Intra-class correlation coefficient	TSE	Turbo spin echo
IDEAL	Iterative decomposition of water and fat with echo asymmetry and least-squares estimation	VA	Visual acuity
IOP	Intra-ocular pressure		
IQR	Interquartile range		

Introduction

The concepts of 'globe' and 'orbit', can suggest astrological stories about the universe, the stellar constellations or the navigation of celestial objects. Although this manuscript has been assembled in different parts of the world, the content has not much to do with the universe. The original meaning of 'orbit' is 'ring', which later evolved (i) to describe the elliptical path of a substance in space or (ii) as an anatomical name for the eye socket ('ring around the eye globe')^[1].

The anatomical orbit is centrally located at the intersection between the face (viscerocranium) and braincase (neurocranium). The primary objective of the orbit is the protection of the globe function in order to maintain the perception of vision. This protection is assured by a refined bony and soft tissue construction. The bony pyramid is composed of a three-dimensional (3D) mosaic of seven embryologically different facial bones that vary in thickness. Foramina and fissures, such as inferior orbital fissure, nasolacrimal canal, and optic canal, perforate the walls. Entry to the orbit is outlined by

FIGURE 1 — ILLUSTRATION OF THE ORBITAL ANATOMY ON AXIAL (A), CORONAL (B) AND SAGITTAL (C) SECTIONS OF AN MRI SCAN (T2 SPACE ZOOMIT SEQUENCE) | 1: intra-conal orbital fat; 2: extra-conal orbital fat; 3: globe; 4: lacrimal gland; 5: extraocular muscles; 6: optic nerve.



a curvilinear margin, a strong outer ridge to preserve the contour, but fragile inner walls that can disperse the energy of a traumatic impact and preserve the globe integrity^[2].

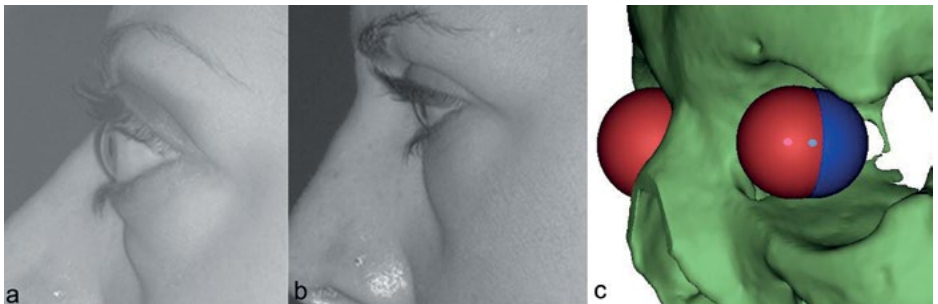
The normal shape of the globe or eyeball is a nearly round sphere with an anteriorly convex bulge, although certain conditions can shorten or elongate the sphere. A variable part of the globe is situated inside the orbital cavity. The wall of the eyeball is three-layered. The most superficial layer is the sclera (continuous with the cornea at the anterior bulge) where the extraocular muscle tendons are inserted. The choroid is the middle vascular layer and the retina is the innermost layer. The largest chamber inside the globe contains the gel-like vitreous body^[3].

The globe is embedded in a cuff of soft tissue structures (figure 1). The orbital fat occupies most of the space inside the orbit. The fat of the orbit consists of extra- and intraconal disbursements. The abundance of fat facilitates the movement of the extraocular muscles (EOM) and maintains the projection of the eye in the orbit^[2,3]. The EOM are comprised of six muscles: four rectus muscles and the superior and inferior oblique muscle. Except from the inferior oblique, all EOM originate at the annulus of Zinn in the orbital apex and travel anteriorly to insert into the globe sclera. The levator palpebrae superioris muscle also attaches to the annulus of Zinn, but its function is lid elevation, not globe movement. As the levator palpebrae muscle is positioned close by the superior rectus, both muscles are often described together as the 'superior rectus-levator complex'^[2]. The optic nerve connects the globe to the brains. It can be subdivided into four main parts: optic nerve head (i.e. intraocular part), intraorbital part, intracanalicular part and intracranial part. The intraorbital part of the optic nerve (approximately 25 mm in length) travels from the posterior part of the eyeball to the intraorbital opening of the optic canal. The optic nerve sheath that contains all three meningeal layers surrounds the intraorbital optic nerve^[3]. The lacrimal gland is located in the superior lateral portion of the orbit and is contained with the periorbita. The gland could be divided in a palpebral and orbital lobe. The smaller palpebral lobe lies close to the eye, along the inner surface of the eyelid^[2].

These soft tissue structures, along with various nerves and blood vessels are incorporated inside the orbit to support the globe function. Every component can be affected by various pathological conditions like inflammatory diseases, traumatic injury or mass lesions. Along with the functional impact on the vision, these diseases will generate aesthetic and social impairments that highly burden the psychosocial status of the patient^[4,5]. The eyes have a central role in personal interaction, facial recognition and emotional expression; hence the influence of ocular or orbital pathology on the quality of life cannot be underestimated. Orbital diseases can cause a change of the globe position, leading to double vision or provoke permanent swelling around the eyes (see Figure 2). Patients with chronic inflammatory orbital diseases report a negative effect on their quality of life and emotional distress that is worse compared to patients suffering from diabetes or heart failure^[4].

An example of a well-known inflammatory orbital disease is Graves' orbitopathy, which is extensively studied in the current thesis. This is an intriguing disease where various orbital components can be involved with a variable disease progression and complex treatment. Graves' orbitopathy, also referred as dysthyroid/thyroid-associated orbitopathy or thyroid eye disease, is part of an autoimmune process that affects orbital tissues in a severe and potentially irreversible manner. Though its pathophysiology remains incompletely understood, two clinical phases can be distinguished including an active followed by an inactive phase^[5,6]. Transition from the active phase to the later inactive stage is often spontaneous in mild cases or can be aided by immunosuppressive medical treatment and/or radiotherapy^[7-10]. Edema and proliferation of the periocular tissues in the active inflammatory phase leads to retrobulbar tissue expansion and proptosis (figure 2). Additional ocular manifestations include eyelid retraction, chemosis, periocular edema and altered ocular motility. Severe disease progression can sometimes cause vision-threatening exposure keratopathy and compressive optic neuropathy. Activated orbital fibroblasts perpetuate these effects by fibrosis, leading to permanent disfigurement, diplopia, functional and social impairment^[5,6]. One of the treatment options for inactive Graves' orbitopathy is surgical decompression, which aims to reduce the orbital content and/or expand the orbital volume in order to shift the position of the globe (decrease proptosis), improve muscular motility and increase visual acuity^[11-13]. With exception of urgent surgical decompression in vision-threatening optic neuropathy or corneal ulceration refractory to steroids, rehabilitative surgery is reserved to the inactive phase.

FIGURE 2 — PATIENT WITH GRAVES' ORBITOPATHY BEFORE AND AFTER SURGICAL TREATMENT



- (a) Clinical pictures of a patient diagnosed with Graves' orbitopathy and explicit proptosis.
 (b) Clinical pictures after surgical orbital decompression with removal of the lateral orbital wall and orbital fat. Marked improvement of the globe position.
 (c) Three-dimensional reconstruction generated from a post-operative CT scan. The red sphere represents the pre-operative globe position and the blue sphere the post-operative position.

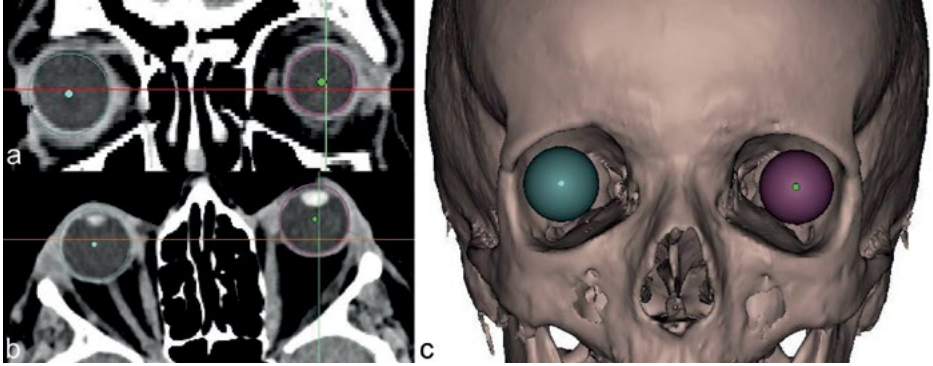
“What gets measured gets managed”

– Peter Drucker, 1954

Similar to any medical condition, the orbital diseases have to be evaluated profoundly in order to manage them in the best possible way. Clinical tools have been developed to measure the orbital dimensions, to assess the soft tissues (e.g. inflammation and swelling of the eyelids or conjunctiva) or to document the position of the globe inside the orbital cavity^[14]. These tools are easily available and protocols have been recommended to obtain the outcomes as objectively as possible. The clinical information, however, only contains a fraction of the full picture and is bounded by 2D measurements of a complex, three-dimensional (3D) structure. Furthermore, the shortcomings inherent to these clinical methods will cause variability amongst different evaluators, hence making the results more subjective^[15,16].

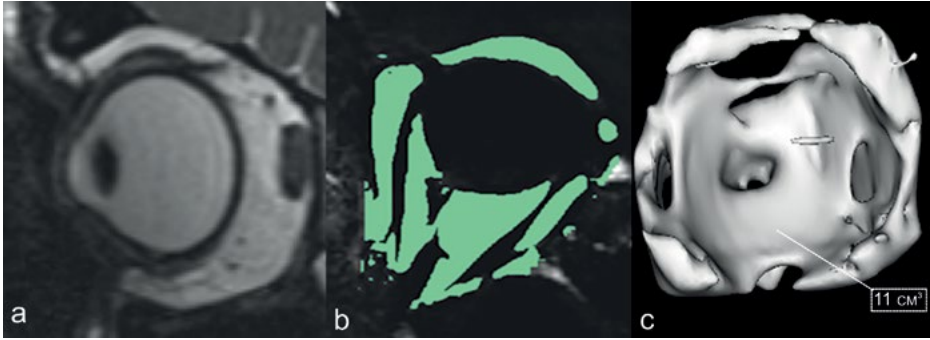
A crucial way to advance clinical information is to supplement the evaluation of the orbit with objective imaging studies. Neuroimaging allows for a more extensive evaluation of the bony and soft tissue orbital structures^[17,18]. Various imaging modalities have been introduced to assess the orbital condition. These methods are continuously developing to improve the accuracy and precision and support the disease management^[19]. Plain x-ray images are the simplest and were most widely used to perform the initial assessment. The absence of proper soft tissue visualization and restriction to only 2D measurements make plain x-ray inferior to more contemporary methods. Since the introduction of Computed Tomography scan (CT), the potential for image analysis has expanded immensely. Nowadays, the CT scan is regarded as the gold standard of orbital imaging in most parts of the world^[20,21]. The CT image acquisition has relatively low cost, is fast and accurate with a high spatial resolution. Paper-thin orbital bones can be clearly visualized and most orbital soft tissue structures can be easily differentiated. Together with the increasing availability of CT data, the post-processing opportunities took a great leap forward^[22-24]. The post-processing methods intend to convert the original data to enhance the interpretation of available information. Since the orbit is an irregular ellipsoidal concavity, volumetric rather than linear determinations are more accurate. For example, 3D bone reconstructions can be rendered from the original CT data, which makes it more accessible to evaluate complex displacements after skeletal trauma (figure 3).

FIGURE 3 — CT SCAN OF THE ORBITAL REGION | Coronal (a) and axial view (b) with two-dimensional segmentation of the globe. The center of the sphere is automatically marked with a green dot (c) Three-dimensional reconstruction of the bony skeleton and spheres representing the globe.



Post-processing methods include, amongst others, the rendering of 3D bone/soft tissue reconstruction, tissue outlining ('segmentation') according to the pixel grey value (Hounsfield Unit (HU)) and morphometric/volumetric analysis of a specific region of interest (ROI). The act of segmentation is an important topic when discussing post-processing analysis and can be accomplished by a variety of methods^[25]. This process will allow grouping the pixels and defining the boundaries of the ROI. The manual segmentation technique requires the operator to determine the borders of the ROI on every single slice of the scan. There is a high level of control, but this approach is also time demanding and impractical for routine use^[26]. Moreover, due to the irregular morphology of orbital tissues, this method is associated with a high inter-observer variation and prone to bias according to the scan plane orientation^[17,27,28]. More advanced methods like regional growing (RG) and multi-dimensional threshold (MDT) algorithms try to overcome these problems through a semi-automatic segmentation process^[29,30]. With RG a seed is set in the ROI to define the reference tissue intensity, which is used by the software to cover the entire ROI (figure 4). MDT segmentation software requires a visual threshold range solely containing the target tissue to segment the ROI. These semi-automatic segmentation techniques, with MDT probably superior to RG, proved to be more convenient and at least as accurate as manual segmentation^[27].

FIGURE 4 — ORBITAL FAT SEGMENTATION AND 3D RECONSTRUCTION



- (a) Orbital MRI scan (T2 Space ZOOMit protocol, sagittal orientation) obtained with a 3T scanner and 64-channel head coil.
- (b) Semi-automatic fat segmentation (green) performed with a region growing algorithm on an axial T1 TSE Dixon sequence (fat images).
- (c) Three-dimensional reconstruction of the orbital fat. The segmentation software automatically generates the orbital fat volume.

The additional information obtained with image post-processing can support the diagnostic pathway, enhance treatment options and monitor the treatment response [31,32]. Furthermore, the development of specialised software made it possible to use this post-processing data and generate virtual simulations to support treatment decisions. Radiation exposure, however, is a significant drawback for orbital CT scanning. Lens opacification and radiation-induced cataract limits its clinical application for repeated scans [30,33]. Magnetic resonance imaging (MRI) emerged in the last decades as an addition to CT scanning. In the absence of radiation exposure, MRI provides excellent soft tissue contrast, with better delineation of the orbital tissues. Moreover, with MRI it is possible to obtain images in all possible (axial, coronal, sagittal and oblique) views without changing the position of the patient's body [27,29,34].

Conventional MRI protocols use T1 weighted, T2 weighted and proton density weighted sequences mainly for morphological analysis. Advances in MRI hardware and new imaging protocols are emerging at high pace, introducing extra opportunities in post-processing methods and quantitative objectification (e.g. signal intensity ratios, fractionated anisotropy, mean diffusivity, volumetric analysis) [35].

These non-invasive assessments are trending in many medical fields because they allow measuring specific tissue responses (e.g. disease activity) and can provide functional tissue characteristics, supporting clinical diagnosis and treatment decision making [36-38]. With the increasing use of MRI to evaluate the orbit, various protocols are being described and a consensus has yet to be reached. The more sophisticated the protocols, the more labour and resource intensive hence difficult to perform in everyday clinical practice. Additionally, MRI is a sensitive imaging technique prone to artifacts. Common artifacts are Gibbs ringing, which present parallel to the edges of abrupt intensity change

^[39,40] and aliasing, where a body part outside the field of view is wrapped inside to the opposite side of the image ^[39] (figure 5).

FIGURE 5 — MRI ARTIFACTS



- (a) T1 weighted TSE sequence, axial orientation, obtained with a 3T MRI scanner and loop coil. Gibbs ringing artifacts (arrows) are visible at the posterior edges of the globe and along the inner side of the extra ocular muscles.
- (b) MPRAGE sequence, axial orientation, obtained with a 3T MRI scanner and 64 channel head coil. Aliasing effect (arrows) inhibits good visualisation of the globe and medial part of the orbit.

These artifacts are important to recognize because they could mask anatomical structures, constrain the segmentation process and should be differentiated from anatomical and functional tissue abnormalities. Various solutions could eliminate this artifacts such as image filters, though this goes beyond the scope of this research project and should be discussed with a MRI technician ^[39].

Although increasing evidence suggests the importance of post-processing analysis, results from various studies may be limited for extrapolation due to differences in scanner performance, sequence acquisition, post-processing protocols or software applications.

In conclusion, the orbit is a sophisticated space packed with many structures, which all have their distinct role. Image processing has the capability to enhance objective documentation of the orbital complex. However, if these outcomes are to be used as an indicator for diagnosis and treatment planning, it is essential that the evaluation is accurate and reliable. Imaging protocols and post-processing methods should be validated and errors implicit in the measurement technique must be defined. This thesis aims to explore the possibilities of processing orbital imaging studies. The introduction of reliable and

feasible post-processing techniques can ameliorate diagnosis and understanding of the mechanism in orbital disorders. These developments should lead to precise quantitative measurements, contributing to a patient-specific treatment.

REFERENCES

-
- [1] Online Etymology Dictionary [Internet]. [cited 2020 May 30]. Available from: etymonline.com
- [2] Turvey TA, Golden BA. Orbital Anatomy for the Surgeon. *Oral Maxillofac Surg Clin North Am.* 2012;24(4):525–36.
- [3] Kenhub Library [Internet]. [cited 2020 Mar 15]. Available from: <https://www.kenhub.com/>
- [4] Wiersinga WM. Quality of life in Graves' ophthalmopathy. *Best Pract Res Clin Endocrinol Metab* [Internet]. 2012 Jun;26(3):359–70. Available from: <http://dx.doi.org/10.1016/j.beem.2011.11.001>
- [5] Weiler DL. Thyroid eye disease: a review. *Clin Exp Optom.* 2017;100(1):20–5.
- [6] Kiran Z, Rashid O, Islam N. Typical graves' ophthalmopathy in primary hypothyroidism. *J Pak Med Assoc.* 2017 Jul;67(7):1104–6.
- [7] Eckstein A, Esser J, Mattheis S, Berchner-Pfannschmidt U. [Graves' Orbitopathy]. *Klin Monbl Augenheilkd.* 2016 Dec;233(12):1385–407.
- [8] Bartalena L, Baldeschi L, Boboridis K, Eckstein A, Kahaly GJ, Marcocci C, et al. The 2016 European Thyroid Association/European Group on Graves' Orbitopathy Guidelines for the Management of Graves' Orbitopathy. *Eur Thyroid J.* 2016;5(1):9–26.
- [9] Phillips ME, Marzban MM, Kathuria SS. Treatment of thyroid eye disease. *Curr Treat Options Neurol.* 2010 Jan;12(1):64–9.
- [10] Marcocci C, Marino M. Treatment of mild, moderate-to-severe and very severe Graves' orbitopathy. *Best Pract Res Clin Endocrinol Metab.* 2012 Jun;26(3):325–37.
- [11] Li EY, Kwok TY, Cheng AC, Wong AC, Yuen HK. Fat-removal orbital decompression for disfiguring proptosis associated with Graves' ophthalmopathy: safety, efficacy and predictability of outcomes. *Int Ophthalmol.* 2015;35(3):325–9.
- [12] Cheng AM, Wei YH, Tighe S, Sheha H, Liao SL. Long-term outcomes of orbital fat decompression in Graves' orbitopathy. *Br J Ophthalmol.* 2018;102(1):69–73.
- [13] Prat MC, Braunstein AL, Dagi Glass LR, Kazim M. Orbital fat decompression for thyroid eye disease: retrospective case review and criteria for optimal case selection. *Ophthal Plast Reconstr Surg.* 2015;31(3):215–8.
- [14] Traber G, Kordic H, Knecht P, Chaloupka K. Hypoglobus - Illusive or real? Etiologies of vertical globe displacement in a tertiary referral centre. *Klin Monbl Augenheilkd.* 2013;230(4):376–9.
- [15] Bingham CM, Sivak-Callcott JA, Gurka MJ, Nguyen J, Hogg JP, Feldon SE, et al. Axial Globe Position Measurement: A Prospective Multicenter Study by the International Thyroid Eye Disease Society. *Ophthal Plast Reconstr Surg.* 2016;32(2):106–12.
- [16] Segni M, Bartley GB, Garrity JA, Bergstralh EJ, Gorman CA. Comparability of proptosis measurements by different techniques. *Am J Ophthalmol.* 2002;133(6):813–8.
- [17] Tian S, Nishida Y, Isberg B, Lennerstrand G. MRI measurements of normal extraocular muscles and other orbital structures. *Graefes Arch Clin Exp Ophthalmol.* 2000;238(5):393–404.
- [18] Firbank MJ, Coulthard A. Evaluation of a technique for estimation of extraocular muscle volume using 2D MRI. *Br J Radiol.* 2000 Dec;73(876):1282–9.
- [19] Müller-Forell W, Kahaly GJ. Neuroimaging of Graves' orbitopathy. *Best Pract Res Clin Endocrinol Metab* [Internet]. 2012;26(3):259–71. Available from: <http://dx.doi.org/10.1016/j.beem.2011.11.009>
- [20] Kontio R, Lindqvist C. Management of Orbital Fractures. *ORAL Maxillofac Surg Clin NORTH Am.* 2009;21(2):209+.
- [21] Hopper RA, Salemy S, Sze RW. Diagnosis of midface fractures with CT: what the surgeon needs to know. *Radiographics.* 2006;26(3):783–93.
- [22] Schiff BA, McMullen CP, Farinhas J, Jackman AH, Hagiwara M, McKellop J, et al. Use of computed tomography to assess volume change after endoscopic orbital decompression for Graves' ophthalmopathy. *Am J Otolaryngol - Head Neck Med Surg* [Internet]. 2015;36(6):729–35. Available from: <http://dx.doi.org/10.1016/j.amjoto.2015.06.005>
- [23] Regensburg NI, Kok PHB, Zonneveld FW, Baldeschi L, Saeed P, Wiersinga WM, et al. A new and validated CT-Based method for the calculation of orbital Soft tissue volumes. *Investig Ophthalmol Vis Sci.* 2008;49(5):1758–62.
- [24] Regensburg NI, Kok PHB, Zonneveld FW, Baldeschi L, Saeed P, Wiersinga WM, et al. A new and validated CT-Based method for the calculation of orbital Soft tissue volumes. *Investig Ophthalmol Vis Sci.* 2008;49(5):1758–62.

- [25] Bentley RP, Sgouros S, Natarajan K, Dover MS, Hockley AD. Normal changes in orbital volume during childhood. *Jo1 Bentley RP, Sgouros S, Natarajan K, Dover MS, Hockley AD Norm Chang orbital Vol Dur childhood J Neurosurg* 2002;96(4):742-746 doi103171/jns20029640742urnal Neurosurg. 2002 Apr;96(4):742-6.
- [26] Garau LM, Guerrieri D, De Cristofaro F, Bruscolini A, Panzironi G. Extraocular muscle sampled volume in Graves' orbitopathy using 3-T fast spin-echo MRI with iterative decomposition of water and fat sequences. *ACTA Radiol OPEN*. 2018 Jun;7(6).
- [27] Tang X, Liu H, Chen L, Wang Q, Luo B, Xiang N, et al. Semi-automatic volume measurement for orbital fat and total extraocular muscles based on Cube FSE-flex sequence in patients with thyroid-associated ophthalmopathy. *Clin Radiol*. 2018;73(8):759.e11-759.e17.
- [28] Firbank MJ, Harrison RM, Williams ED, Coulthard A. Measuring extraocular muscle volume using dynamic contours. *Magn Reson Imaging*. 2001 Feb;19(2):257-65.
- [29] Comerci M, Elefante A, Strianese D, Senese R, Bonavolontà P, Alfano B, et al. Semiautomatic regional segmentation to measure orbital fat volumes in thyroid-associated ophthalmopathy a validation study. *Neuroradiol J*. 2013;26(4):373-9.
- [30] Kaichi Y, Tanitame K, Itakura H, Ohno H, Yoneda M, Takahashi Y, et al. Orbital fat volumetry and water fraction measurements using T2-weighted FSE-IDEAL imaging in patients with thyroid-Associated orbitopathy. *Am J Neuro-radiol*. 2016;37(11):2123-8.
- [31] Siakallis LC, Uddin JM, Miszkil KA. Imaging Investigation of Thyroid Eye Disease. Vol. 34, Ophthalmic plastic and reconstructive surgery. 2018. p. S41-51.
- [32] Gonçalves A, Gebrim E, Monteiro M. Imaging studies for diagnosing Graves' orbitopathy and dysthyroid optic neuropathy. *Clinics [Internet]*. 2012;67(11):1327-34. Available from: <http://clinics.org.br/article.php?id=906>
- [33] Schmutz B, Rahmel B, McNamara Z, Coulthard A, Schuetz M, Lynham A. Magnetic resonance imaging: an accurate, radiation-free, alternative to computed tomography for the primary imaging and three-dimensional reconstruction of the bony orbit. *J Oral Maxillofac Surg*. 2014 Mar;72(3):611-8.
- [34] Nishida Y, Tian S, Isberg B, Tallstedt L, Lennerstrand G. MRI measurements of orbital tissues in dysthyroid ophthalmopathy. *Graefes Arch Clin Exp Ophthalmol*. 2001 Nov;239(11):824-31.
- [35] Watanabe M, Buch K, Fujita A, Jara H, Qureshi MM, Sakai O. Quantitative MR imaging of intra-orbital structures: Tissue-specific measurements and age dependency compared to extra-orbital structures using multispectral quantitative MR imaging. *Orbit (London) [Internet]*. 2017;36(4):189-96. Available from: <http://dx.doi.org/10.1080/01676830.2017.1310254>
- [36] Yokomachi K, Tanitame K, Takahashi Y, Awai K, Akiyama Y, Kaichi Y. Precise size evaluation of extraocular muscles using fat-suppressed fast T1-weighted gradient-recalled echo imaging and multiple gaze fixation targets. *Jpn J Radiol*. 2013;31(12):812-8.
- [37] Shen J, Jiang W, Luo Y, Cai Q, Li Z, Chen Z, et al. Establishment of MRI 3D Reconstruction Technology of Orbital Soft Tissue and Its Preliminary Application in Patients with Thyroid-Associated Ophthalmopathy. *Clin Endocrinol (Oxf)* [Internet]. 2018;(Mv):0-2. Available from: <http://doi.wiley.com/10.1111/cen.13564>
- [38] Lennerstrand G, Tian S, Isberg B, Landau Hogbeck I, Bolzani R, Tallstedt L, et al. Magnetic resonance imaging and ultrasound measurements of extraocular muscles in thyroid-associated ophthalmopathy at different stages of the disease. *Acta Ophthalmol Scand*. 2007 Mar;85(2):192-201.
- [39] Stadler A, Schima W, Ba-Ssalamah A, Kettenbach J, Eisenhuber E. Artifacts in body MR imaging: Their appearance and how to eliminate them. *Eur Radiol*. 2007;17(5):1242-55.
- [40] Dietrich O, Reiser MF, Schoenberg SO. Artifacts in 3-T MRI: Physical background and reduction strategies. *Eur J Radiol*. 2008;65(1):29-35.
-

Rationale and objectives

Aim 1

To improve the three-dimensional visualisation of the globe position in the orbit

Rationale – Assessment of the globe position is an essential step in the management of orbital diseases, yet current methods are limited to only one dimension and could be biased.

Hypothesis – By using computer tomography (CT) data and three dimensional (3D) reconstruction technology, it is possible to illustrate the globe position shift in 3D and evaluate treatment outcome.

Methods – A new 3D model of the globe position will be created using consecutive CT scans and post-processing software (Mimics Medical 21.0, Materialise, Leuven, Belgium). The clinical and imaging data from randomly selected participants (10 patients, 20 orbits) will be used for method validation. Additionally, the CT scans of five patients with inactive Graves' orbitopathy who underwent bony orbital decompression surgery will be analysed according to the proposed method. Development of the virtual model and image analysis will be performed in collaboration with the OMFS-IMPATh research group (KU Leuven).

Aim 2

To assess the potential, consequences and complications of orbital fat removal in Graves' orbitopathy

Rationale – The orbital fat is packed between all orbital structures and contributes to support the globe position as well as to allow harmonious motion of the orbital components. Studying the effects of fat removal could enhance insights in the clinical consequences of volume alterations and mechanisms of action that are important for reconstruction.

Hypothesis – Selective extraction of orbital fat will result in a predictable change of the globe position with a low risk for adverse effects.

Methods – To investigate the importance of orbital fat for the globe position, a systematic review (& meta-analysis) will be conducted on orbital fat decompression. The study protocol is prospectively registered at the international database of PROSPERO (CRD42018084472) and will comply with the Preferred Reporting Items for Systematic Reviews and Meta-Analysis recommendations (PRISMA). Fat only orbital decompression will be included and relationship between lipectomy, globe position and adverse effects (including diplopia) will be studied.

Aim 3

To investigate the contemporary methods of volumetric analysis in orbital MRI

Rationale – Various protocols have been reported to perform volumetric analysis of orbital structures on magnetic resonance imaging (MRI). A lack of homogeneous and validated techniques prevents the common implementation in routine clinical practice.

Hypothesis – A critical analysis of the current knowledge in orbital volumetric techniques can define the pitfalls and contribute to the development of accurate and feasible protocols.

Methods – A systematic review will be performed on post-processing volumetry techniques in orbital MRI. The study protocol is prospectively registered at the international database of PROSPERO (CRD42019127698) and will comply with the PRISMA guidelines. MRI scanning characteristics (scan protocol and acquisition details), and post-processing volumetry technique (software, segmentation methods and volume calculations) will be studied according to the region of interest (muscle, orbital fat, etc.).

Aim 4

To study the feasibility and accuracy of semi-automatic MRI based orbital fat volumetry

Rationale – Measurement of orbital fat can be used as an early marker to assess disease severity, activity and to monitor effectiveness of therapeutic modalities over time. Orbital imaging is an important tool to measure orbital fat, but there is no consensus on the use of different imaging modalities.

Hypothesis – If fat volume is to be used as an indicator for diagnosis and treatment of orbital disorders, it is important that correlation between computed tomography (CT) and magnetic resonance imaging (MRI) measurements are transparent and that the errors implicit in the measurement technique are defined.

Methods – A retrospective, cross-sectional study will include 5 healthy participants (10 orbits) and 6 patients diagnosed with Graves' Orbitopathy. Patients who received both a standard orbital CT and MRI scan will be selected. Results of fat volumetry on MRI will be compared to a validated CT-based measurement method. Image analysis will be accomplished in collaboration with the radiological department (University Hospital Ghent) and OMFS-IMPATh research group (KU Leuven).

Aim 5

To develop and validate a dedicated and accurate MRI protocol for orbital soft tissue volumetry

Rationale – Advances in magnetic resonance imaging (MRI) hardware and developments in post-processing technology make quantitative analysis increasingly valuable for diagnosis, evaluation of disease progression and treatment planning in orbital diseases. However, there is a lack of uniformity and validation of the proposed protocols.

Hypothesis – Dedicated imaging techniques can be selected to improve the post-processing accuracy in orbital MRI scans.

Methods – Twelve different orbital MRI protocols will be qualitatively evaluated on human orbits during a developmental stage. The most optimized protocols will be used for quantitative testing on an animal orbital model (fresh pig cadaver). Technique accuracy will be investigated by comparison with computed tomography (CT) scan and tissue dissection. This work will be performed in cooperation with the Ghent Institute for Functional and Metabolic Imaging (Gifmi- Ghent University).

Articles

Corresponding Author

Robin Willaert

Department of Oral and Maxillofacial Surgery

University Hospitals Leuven

Kapucijnenvoer 33, 3000 Leuven, Belgium

email: robin.willaert@icloud.com

telephone: +32 (0) 474 26 81 47

Publication references: Doi: 10.1007/s00417-020-04631-w - PMID: 32140924

Three-Dimensional Characterisation of the Globe Position in the Orbit

R. WILLAERT MD, DMD^{1,2} | E. SHAHEEN MSc, PHD^{2,3} | J. DEFERM MD, DMD⁴ | H. VERMEERSCH MD, PHD⁵
R. JACOBS DMD, MSc, PHD^{2,3,6} | I. MOMBAERTS MD, PHD⁷

Abstract

Aim — Current methods to analyse the globe position, including Hertel exophthalmometry and computed tomography (CT), are limited to the axial plane and require the lateral orbital rim and cornea as landmarks. This pilot study aimed to design a method to measure the position of the globe in the axial, coronal and sagittal plane and independent from orbital bony and corneal references. **Methods** — With the aid of three-dimensional CT reconstruction technology, we determined the globe position in the orbit based on the center of the globe. Method validation was performed using data of consecutive orbital CT scans from the control group and from patients with Graves' orbitopathy who underwent orbital decompression surgery with removal of the lateral orbital margin. **Results** — The inter- and intra-observer reliability was excellent with a high intraclass correlation coefficient (> 0.99 , 95% CI [0.97; 1.00]). In the decompressed orbits, there was a statistically significant globe position shift along the anterior-posterior axis ($P= 0.0005$, 95% CI [0.63; 3.66]), but not along the medial-lateral and superior-inferior axis. **Conclusion** — The 3D CT method can accurately and reliably characterise the globe position shift in the three dimensions without using orbital and corneal anatomical landmarks. The method can be useful to determine the globe shift in proptosis, enophthalmos, hypoglobus and hyperglobus, even in the presence of strabismus and orbital bone defects.

Key Words

- Orbital disease
- Graves' orbitopathy
- exophthalmometry
- proptosis
- computed tomography

AFFILIATIONS

- 1 Department of Head and Neck Surgery, Ghent University Hospital, Ghent, Belgium
 - 2 Department of Oral and Maxillofacial Surgery, University Hospitals Leuven, Leuven, Belgium
 - 3 OMFS IMPATH Research Group, Department of Imaging and Pathology, Faculty of Medicine, KU Leuven, Leuven, Belgium
 - 4 Department of Oral and Maxillofacial Surgery, Radboud University Hospital, Nijmegen, The Netherlands
 - 5 Department of Plastic and Reconstructive Surgery, Ghent University Hospital, Ghent Belgium
 - 6 Department of Dental Medicine, Karolinska Institutet, Huddinge, Sweden
 - 7 Department of Ophthalmology, University Hospitals Leuven, Leuven, Belgium
- The first two authors contributed equally and we wish to acknowledge them with a shared first authorship.

Introduction

The position of the eyeball in the orbit, also called globe position (GP), is an important marker in the diagnosis and follow-up of patients with Graves' orbitopathy, orbital trauma, and orbital mass lesions. Standardly, GP is assessed with the Hertel exophthalmometer that measures the distance between the anterior vertex of the cornea and the zygomatic process of the lateral orbital rim in the axial plane^[1]. Inter- and intra-observer user variability with Hertel exophthalmometry, however, is common owing to potential horizontal misalignment and parallax error of the device^[1-3]. Alternatively, the GP can be evaluated with two-dimensional (2D) computed tomography (CT) by measuring the vertex of the cornea perpendicular to the interzygomatic line^[2,3]. Both the Hertel and 2D CT method require anatomical integrity of the anterior aspect of the lateral orbital margin and assess the GP in the axial plane only^[4].

Other than the axial deviation, the GP can be deviated in the horizontal axis, as observed from increased interpupillary and CT digitalized interocular distances in patients with Graves' orbitopathy and medial (nasal) shifting of the GP after orbital decompression^[5,6]. On the other hand, deviations of GP in the vertical plane occur in orthotropic hypoglobus and hyperglobus associated with peri-orbital abnormalities and orbital decompression surgery^[7,8]. Horizontal and vertical deviations cannot be accurately detected with currently available tools. The aim of the study is to characterise the GP in the axial, horizontal and vertical plane, independent on bony orbital and corneal landmarks through the use of CT data and 3D reconstruction technology.

Materials and methods

For this pilot study, the clinical and imaging data from randomly selected participants (10 patients, 20 orbits) (5 female; mean age 44 ± 21 years) as controls were retrospectively analysed. The participants had received two serial cranial CT scans, in this study called P1 and P2 scans, at a mean interval of 49 ± 48 days, in the routine follow-up of intracerebral vascular disease ($n=8$) and cerebral (stereotactic brain biopsy) intervention ($n=2$). The exclusion criteria included: orbital, peri-orbital and ocular pathology; previous ocular and peri-ocular surgery; orbital trauma; previous radiotherapy in the head and neck region; long-term use of systemic corticosteroids; and CT scans showing motion artifacts. After validation of the GP characterisation with the 3D CT method in the control group, the CT scans of five patients (7 orbits) (2 female; mean age 52 ± 16 years) with inactive Graves' orbitopathy and euthyroidism who underwent bony orbital decompression surgery were analysed. Using a transcutaneous upper eyelid approach, the lateral rim and wall were removed en-bloc, with additional removal of the lateral floor and orbital fat from the lateral inferior quadrant where required. Preoperative proptosis was measured with Hertel exophthalmometry. The CT scans of each patient were obtained before (P1) and after (P2) the orbital decompression at a mean time interval of 159 ± 122 days. The non-decompressed orbits of the 3 patients with Graves' orbitopathy who had received unilateral decompression were not included in the study. The study adhered to the tenets of the declaration of Helsinki. Institutional review board approval and informed consents were obtained (B670201733474).

All CT scans were obtained through the multidetector technique with a field of view containing the orbital structures. A single volume of data was acquired in the axial plane at 1-2mm thickness (Supplementary Table A). All non-contrast images were recorded in Digital Imaging and Communications in Medicine (DICOM) format, anonymized and transferred to a workstation for the analysis.

SUPPLEMENTARY TABLE A — SPATIAL RESOLUTION DETAILS CT SCANS

Kernel	H30s
Focal spots	1.2
Single Collimation width (mm)	0.6
α Total Collimation width (mm)	38.4
Pixel spacing (mm, Mean \pm SD)	0.42 \pm 0.03
Samples per pixel	1
Slice thickness (mm)	1 or 1.5 or 2
Reconstructed images (pixel)	512 x 512
Pitch factor	0.8

FIGURE I.1 — PROCEDURAL STEPS TO EVALUATE 3D CHANGES OF THE GLOBE POSITION

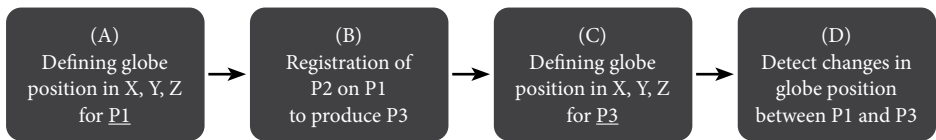
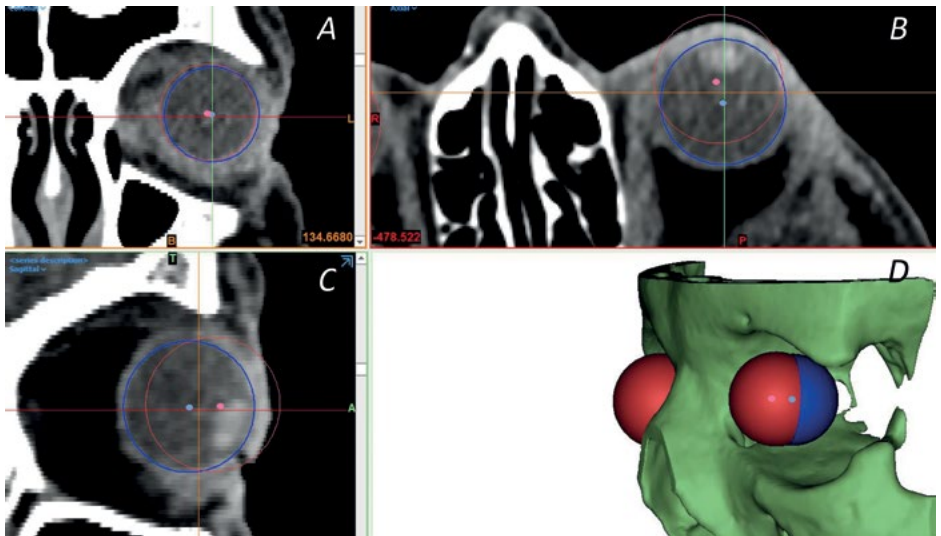


FIGURE I.2 — CHARACTERISATION OF THE GLOBE POSITION BEFORE AND AFTER ORBITAL DECOMPRESSION |



The position of the left globe within the orbit as defined on the preoperative CT scan (red circle, P1) and after orbital decompression with removal of the lateral orbital wall and rim (blue circle, P3). The center of the globe (red and blue dot for respectively, P1 and P3) was generated with software (Mimics 21.0 innovation suite). (A) A minimal lateral and inferior globe deviation after decompression is shown in the coronal CT slide. (B, C) Posterior globe displacement after decompression is illustrated in the axial and sagittal CT slides. (D) 3D reconstruction of the globe and bony orbit illustrating the postoperative proptosis reduction.

The 3D CT method for GP assessment comprised the following process (Figure 1.1 and 1.2):

- (A) **Defining GP for P1:** The DICOM files were uploaded into Mimics Medical 21.0 software (Materialise, Leuven, Belgium). Contrast was adjusted for optimal visualization of the sclera. After centering the globe in 3 orthogonal planes, the slices with maximum globe diameter were identified. Four landmarks were used to create a sphere from the inner border of the sclera: the upper and lower border of the globe diameter for the sagittal plane; the medial border at the level of the medial rectus muscle insertion for the coronal plane; and the optic disc entry into the sclera for the axial plane. The center of the globe was automatically generated by the software and was recorded in an X, Y and Z coordinate system, representing respectively the anterior-posterior, medial-lateral and superior-inferior direction.
- (B) **Registration of P2 on P1 to produce P3:** The DICOM data from P1 and P2 CT scans were imported into Amira software (ThermoFisher Scientific, Massachusetts, USA). The base of the skull was identified on the P1 scan and a voxel based registration procedure was used to align the skull base from the P2 scan on the P1, obtaining a new registered dataset, called P3, that was exported in DICOM format^[9,10]. The registration procedure prevented bias from variability in skeletal orientation and head positioning during scanning and ensured that possible changes in globe center are caused by a shift in GP.
- (C) **Defining GP for P3:** The GP was determined by defining the globe center on the registered P3 DICOM dataset, following the same procedure as described in step (A).
- (D) **Evaluation of changes in GP:** Changes in GP were detected by calculating the difference between the center of the globe of P1 and P3 for the X, Y and Z-axis. To present the 3D shift of the globe center as a single value, the Euclidean distance, i.e., the ordinary or straight-line distance between two points in Euclidean space, was calculated.

Statistical analysis

The data were analyzed using MedCalc statistical software (Version 12.0, Ostend, Belgium). For inter- and intra-observer variability tests, the mean and standard deviation (SD) of the error between two measurements were analyzed in the X, Y, and Z-axis separately, and the intraclass correlation coefficient (ICC) with 95% confidence interval (CI) was calculated (two-way mixed-effects model). The ICC estimate is interpreted as following: values of <0.5 represent poor reliability, values of 0.5 to 0.74 moderate, values of 0.75 to 0.9 good, and >0.90 excellent reliability^[11,12]. There is a 95% chance that the true ICC

value is included in the 95% CI. The mean and SD of the GP changes (i.e., differences between P1 and P3) were separately computed for the X, Y, and Z-axis and the Euclidean distance. The Mann-Whitney U test was used to compare changes of GP in the decompressed orbits with those of the control orbits. The mean, 95% CI and interquartile range (IQR) were calculated. Differences were considered statistically significant at P-values of <0.05.

Results**Reliability of globe position characterisation**

The results of the observer reliability in characterising the GP are shown in Table 1.1. The mean error for inter- and intra-observer variability was <0.5 mm (SD <0.5 mm) for each axis, and the mean Euclidean distance error was <1 mm. The two-sided confidence interval of the ICC estimates of the inter- and intra-observer analysis for the P1 and P3 scans showed excellent agreement (0.97-1.00).

Shift of the globe position

The GP shifts, i.e. changes in globe position between P1 and P3, of the control group (10 patients, 20 orbits) and decompression group (5 patients, 7 orbits) are presented in Table 1.2. The mean shift in the control group does not exceed 0.6 mm in each orthogonal axis. In the decompression group, a statistically significant GP shift between the pre- and postoperative positions was recorded in the X-axis (anterior-to-posterior shift) and in the Euclidean movement (>2.5 mm, $P < 0.001$). GP changes along the Z-axis, i.e. superior-to-inferior shift, are slightly elevated in the decompression group but do not reach a statistically significant difference.

The patients' characteristics and their GP shifts, i.e. change in globe position between pre- and postoperative situation, are outlined in Table 1.3. Patients with severe proptosis, i.e., Hertel measurements of 24mm and more, had the highest anterior-posterior displacement (X-axis) and Euclidean change after decompression. Inferior displacement of the globe (Z-axis) was observed in the orbits where the orbital floor was removed.

Discussion

Exophthalmometry is a routinely performed exam in the diagnosis and follow-up of orbital diseases and disorders and relies on the distance from the corneal apex to the lateral canthal area in the axial plane. In this study we showed that 3D CT data can accurately and reliably characterise the GP in the three dimensions of space without using orbital and corneal anatomical landmarks.

While Hertel exophthalmometry is considered the standard, various alternative techniques have been introduced to measure GP. Fichter et al., and Takahashi and Kakizaki, investigated the horizontal GP using respectively digital pupillometry and keratometry between the two eyes [6,13]. Alsuhaibani et al. described a 2D CT technique to measure the distance between the medial parts of both globes in patients undergoing orbital decompression surgery [5]. Guo et al. proposed a CT-based craniofacial 3D coordinate system to evaluate the axial GP in patients with thyroid orbitopathy [14]. The coordinate system, however, requires orbital bony landmarks, limiting its use in defects involving the zygomatic process. Our method relies on the center of the globe without additional reference planes and is independent of gaze direction. In particular, gaze cannot be accurately controlled in patients with strabismus and limited ocular motility. Moreover, it is practically impossible to repeat the same gaze between consecutive CT scans. Abnormal corneal position from strabismus influences the readings of Hertel and 2D CT exophthalmometry but not of 3D CT GP characterisation. The 3D CT method is not applicable when the eyeball morphology would change in between 2 consecutive

TABLE I.I — OBSERVER VARIABILITY TESTING AND MEASUREMENT ERROR OF 3D CT GLOBE POSITION CHARACTERISATION IN 20 HEALTHY ORBITS (CONTROL GROUP)

		X-axis AP (mm)	Y-axis ML (mm)	Z-axis SI (mm)	Euclidean error (mm)
PI Inter-observer variability	Mean± SD	0.34±0.21	0.32±0.22	0.30±0.28	0.65±0.22
	IQR	0.20-0.46	0.17-0.37	0.09-0.36	0.47-0.78
	ICC (95% CI)	0.99 (0.97-1.00)	1.00 (0.99-1.00)	1.00 (0.99-1.00)	
PI Intra-observer variability	Mean± SD	0.19±0.15	0.27±0.21	0.24±0.16	0.47±0.18
	IQR	0.08-0.28	0.09-0.33	0.10-0.36	0.31-0.60
	ICC (95%CI)	1.00 (0.99-1.00)	1.00 (0.99-1.00)	1.00 (0.99-1.00)	
P3 Inter-observer variability	Mean± SD	0.38±0.28	0.36±0.27	0.50±0.36	0.80±0.41
	IQR	0.17-0.50	0.18-0.37	0.25-0.60	0.51-1.17
	ICC (95%CI)	0.99 (0.97-1.00)	1.00 (0.99-1.00)	0.99 (0.97-1.00)	
P3 Intra-observer variability	Mean± SD	0.30±0.33	0.37±0.44	0.32±0.28	0.65±0.53
	IQR	0.08-0.40	0.10-0.41	0.09-0.46	0.25-0.92
	ICC (95%CI)	0.99 (0.97-1.00)	1.00 (0.99-1.00)	0.99 (0.97-1.00)	

AP: anterior-posterior; ML: medial-lateral; SI: superior-inferior; PI: First CT scan; P3: Registered second CT scan; ICC: Intraclass correlation; SD: Standard deviation; IQR: Interquartile range.

TABLE I.2 — COMPARISON OF SHIFT OF 3D CT GLOBE POSITION IN THE CONTROL AND DECOMPRESSION GROUP

	N (Orbits)		X-axis AP (mm)	Y-axis ML (mm)	Z-axis SI (mm)	Euclidean change (mm)
Control group	20	Mean± SD	0.58±0.41	0.50±0.31	0.46±0.36	1.02±0.36
		IQR	0.32-0.76	0.28-0.68	0.22-0.69	0.75-1.21
Decompression group	7	Mean± SD	2.59±1.78	0.46±0.27	0.88±0.83	2.98±1.59
		IQR	1.21-4.18	0.27-0.69	0.33-1.21	1.51-4.19
		P-value (95% CI)	0.0005 (0.63; 3.66)	0.87 (-0.31; 0.24)	0.16 (-0.12; 0.84)	0.0009 (0.50; 3.26)

AP: anterior-posterior; ML: medial-lateral; SI: superior-inferior. SD: Standard deviation; IQR: Interquartile range; CI: Confidence interval. The P-values are calculated with the Mann-Whitney U test.

TABLE I.3 — PATIENT CHARACTERISTICS AND 3D GLOBE SHIFT OF THE DECOMPRESSION GROUP

Age (years)	Side	Hertel at PI (mm)	2D CT proptosis at PI (mm)	Time interval surgery to P2 (days)	Orbital decompression procedure	X-axis AP (mm)	Y-axis ML (mm)	Z-axis SI (mm)	Euclidean change (mm)
44	L	24	23	58	Lateral wall, lateral rim, floor and fat removal	1.69*	0.74	2.56*	3.15
	R	21	20	58	Lateral wall, lateral rim and floor removal	1.31*	0.55	1.32*	1.94
48	L	26	25	133	Lateral wall, lateral rim, floor and fat removal	5.27*	0.43	0.89	5.36
	R	24	24	133	Lateral wall, lateral rim and fat removal	4.42*	0.00	0.24	4.43
65	L	21	20	70	Lateral wall and rim removal	1.17*	0.50	0.48	1.37
33	L	18	17	364	Lateral wall and rim removal	0.81	0.73	0.32	1.14
72	L	23	23	156	Lateral wall and rim removal	3.45*	0.22	0.37	3.48

AP: anterior-posterior; ML: medial-lateral; SI: superior-inferior. L: Left; R: Right. PI: Preoperative CT scan; P2: Postoperative CT scan. *GP changes of more than 1mm are considered clinically relevant.

scans, e.g. after post-scleral buckling, staphyloma, and phthisis. The deviation of the globe center will inherently cause bias and inaccurate results. Otherwise, in distorted eyeballs that can be considered morphologically stable (e.g. refractive error), the center of the reconstructed sphere will be the same in every scan and the method could be applied accurately.

In the 7 decompressed orbits, GP changes were observed along the X-axis (anterior-posterior). Globe displacement along Y- (medial-lateral) and Z-axis (superior-inferior), however, appears to be insignificant after removal of the lateral orbital wall and rim. Although decompression with removal of the orbital floor can inadvertently result in orthotropic hypoglobus with the clinical sign of “setting sun” appearance of the globe, deepening of the superior sulcus and eyelid malposition, this was not encountered in our patients [7,8,15].

Quantification of a vertical and horizontal GP shift is hitherto estimated with a ruler. Our 3D CT method, however, allows detection and quantification of the GP along these axes too.

The 3D CT method to study GP has a high inter- and intra-observer reproducibility, with a mean error not exceeding 0.5 mm for each axis. ICC values of >0.9 are considered ideal to be used in a clinical setting. Compared to standard methods such as Hertel and 2D CT exophthalmometry, the 3D CT error can be considered acceptable for research purposes as well as for routine clinical use [1,2]. The Euclidean distance is a novel value to describe the globe shift. By combining the 3D CT GP change of the axial, horizon-

tal and vertical axis, the Euclidean distance shift renders the 3D movement in one single value. The Euclidean distance shift was significantly increased after decompression surgery, with the amount corresponding with the amount of preoperative Hertel values. Therefore, it is likely a sensitive marker to expose unusual GP shifts, but future studies are needed to understand its relevance.

There are several limitations of the study. The design requires consecutive CT scans. While orbital CT is routinely used for surgical planning of orbital trauma and Graves' orbitopathy, the cumulative radiation dose remains a concern particularly in children, young adults and pregnant women [15]. In the future, magnetic resonance imaging as a radiation-free alternative can be studied for the purpose of 3D GP. Another limitation of this study was the lack of a gold standard for comparison. Correlations to Hertel and 2D CT exophthalmometry were not made as they rely on the lateral orbital rim, which was removed during the decompression in our study population. However, Hertel exophthalmometry will not pose any problems in patients receiving a 'rim-sparing' deep lateral wall orbital decompression. In the future, alternative devices such as the superior and inferior orbital rim-based exophthalmometer developed by Naugle and Couvillion can be used to validate our design in cases with damage to the lateral rim [16-18]. Furthermore, the series of decompressed orbits was small. While various techniques of orbital decompression are currently employed, the choice depending on specific conditions of the patient, surgeon's experience and institutional tradition, we included in this study only those decompressed orbits

with a removed lateral orbital rim to illustrate the feasibility of the 3D CT method in these cases [19–21]. On the other hand, the sample size is equivalent to other validation studies in virtual planning and computer-assisted analysis [22–24]. Finally, the presence of large orbital implants (e.g. titanium mesh after orbital trauma) could provoke image artefacts limiting the use of this technique.

Conclusion

In conclusion, 3D CT technology can accurately characterise the position of the globe in the orbit, independent of the lateral canthal area and cornea. As orbital decompression surgery assumes dramatic changes of GP along the axial axis, subsequent studies may focus on detecting changes of GP in the “unusual” axes, i.e. vertical and horizontal. This may be relevant in patients with hypoglobus, hyperglobus, and enophthalmos, and with concomitant strabismus. In the future, improved documentation of the eyeball position can possibly assist surgical planning and monitor disease progression in patients with Graves’ orbitopathy, orbital trauma, and orbital mass lesions.

ACKNOWLEDGEMENTS

Funding: This research did not receive any specific grant from funding agencies in the public, commercial, or not-for-profit sectors.

Conflict of interest: The authors declare that they have no conflict of interest.

Ethical approval: All procedures performed in studies involving human participants were in accordance with the ethical standards of the institutional and/or national research committee (Ethical review board University Hospital Ghent, reference number

B670201733474) and with the 1964 Helsinki declaration and its later amendments or comparable ethical standards.

Informed consent: Informed consent was obtained from all individual participants included in the study.

This article does not contain any studies with animals performed by any of the authors.

REFERENCES

- [1] Bingham CM, Sivak-Callcott JA, Gurka MJ, et al (2016) Axial Globe Position Measurement: A Prospective Multi-center Study by the International Thyroid Eye Disease Society. *Ophthal Plast Reconstr Surg* 32:106–12. doi:10.1097/IOP.0000000000000437
- [2] Segni M, Bartley GB, Garrity JA, et al (2002) Comparability of proptosis measurements by different techniques. *Am J Ophthalmol* 133:813–8. doi:10.1016/S0002-9394(02)01429-0
- [3] Ramli N, Kala S, Samsudin A, et al (2015) Proptosis - Correlation and Agreement between Hertel Exophthalmometry and Computed Tomography. *Orbit* 34:257–62. doi:10.3109/01676830.2015.1057291
- [4] Nkenke E, Maier T, Benz M, et al (2004) Hertel exophthalmometry versus computed tomography and optical 3D imaging for the determination of the globe position in zygomatic fractures. *Int J Oral Maxillofac Surg* 33:125–33. doi:10.1054/ijom.2002.0481
- [5] Alsuhaibani AH, Carter KD, Policeni B, et al (2011) Orbital volume and eye position changes after balanced orbital decompression. *Ophthal Plast Reconstr Surg* 27:158–63. doi:10.1097/IOP.0b013e3181e72b3
- [6] Takahashi Y, Kakizaki H (2014) Horizontal eye position in thyroid eye disease: A retrospective comparison with normal individuals and changes after orbital decompression surgery. *PLoS One* 9:1–11. doi:10.1371/journal.pone.0114220
- [7] Traber G, Kordic H, Knecht P, et al (2013) Hypoglobus - Illusive or real? Etiologies of vertical globe displacement in a tertiary referral centre. *Klin Monbl Augenheilkd* 230:376–9. doi:10.1055/s-0032-1328385
- [8] Long JA, Baylis HI (1990) Hypoglobus following orbital decompression for dysthyroid ophthalmopathy. *Ophthal Plast Reconstr Surg* 6:185–9. doi:10.1097/00002341-199009000-00006
- [9] Pluim JPW, Maintz JBA, Viergever MA (2003) Mutual-information-based registration of medical images: a survey. *IEEE Trans Med Imaging* 22:986–1004. doi:10.1109/TMI.2003.815867

- [10] Collignon A, Marchal G, Maes F, et al (2002) Multimodality image registration by maximization of mutual information. *IEEE Trans Med Imaging* 16:187–98. doi:10.1109/42.563664
- [11] Kottner J, Audige L, Brorson S, et al (2011) Guidelines for Reporting Reliability and Agreement Studies (GRRAS) were proposed. *Int J Nurs Stud* 64: 96–106. doi:10.1016/j.ijnurstu.2011.01.016
- [12] Koo TK, Li MY (2016) A Guideline of Selecting and Reporting Intraclass Correlation Coefficients for Reliability Research. *J Chiropr Med* 15:155–63. doi:10.1016/j.jcm.2016.02.012
- [13] Fichter N, Krentz H, Guthoff RF (2013) Functional and esthetic outcome after bony lateral wall decompression with orbital rim removal and additional fat resection in graves' orbitopathy with regard to the configuration of the lateral canthal region. *Orbit* 32:239–46. doi:10.3109/01676830.2013.788662
- [14] Guo J, Qian J, Yuan Y, et al (2017) A Novel Three-Dimensional Vector Analysis of Axial Globe Position in Thyroid Eye Disease. *J Ophthalmol* e-pub ahead of print 9 April 2017. doi:10.1155/2017/7253898
- [15] Siakallis LC, Uddin JM, Miszkial KA (2018) Imaging Investigation of Thyroid Eye Disease. *Ophthal Plast Reconstr Surg* 34:S41–51. doi:10.1097/IOP.0000000000001139
- [16] Jeon HB, Kang DH, Oh SA, et al (2016) Comparative Study of Naugle and Hertel Exophthalmometry in Orbitozygomatic Fracture. *J Craniofac Surg* 27:2015–7. doi:10.1097/SCS.0000000000002334
- [17] Genders SW, Mourits DL, Jasem M, et al (2015) Parallax-free Exophthalmometry: A Comprehensive Review of the Literature on Clinical Exophthalmometry and the Introduction of the First Parallax-Free Exophthalmometer. *Orbit* 34:23–9. doi:10.3109/01676830.2014.963877
- [18] Naugle TCJ, Couvillion JT (1992) A superior and inferior orbital rim-based exophthalmometer (orbitometer). *Ophthalmic Surg* 23:836–7.
- [19] Bartalena L, Baldeschi L, Boboridis K, et al (2016) The 2016 European Thyroid Association/European Group on Graves' Orbitopathy Guidelines for the Management of Graves' Orbitopathy. *Eur Thyroid J* 5:9–26. doi:10.1159/000443828
- [20] Mourits MP, Bijl H, Altea MA, et al (2009) Outcome of orbital decompression for disfiguring proptosis in patients with Graves' orbitopathy using various surgical procedures. *Br J Ophthalmol* 93:1518–23. doi:10.1136/bjo.2008.149302
- [21] Boboridis KG, Uddin J, Mikropoulos DG, et al (2015) Critical Appraisal on Orbital Decompression for Thyroid Eye Disease: A Systematic Review and Literature Search. *Adv Ther* 32:595–611. doi:10.1007/s12325-015-0228-y
- [22] Xi T, Luijn R Van, Baan F, et al (2019) Landmark-Based Versus Voxel-Based 3-Dimensional Quantitative Analysis of Bimaxillary Osteotomies: A Comparative Study. *J Oral Maxillofac Surg* Epub ahead of print. doi:10.1016/j.joms.2019.10.019
- [23] Stokbro K, Thygesen T (2018) A 3-Dimensional Approach for Analysis in Orthognathic Surgery — Using Free Software for Voxel-Based Alignment and Semiautomatic Measurement. *J Oral Maxillofac Surg* 76:1316–1326. doi:10.1016/j.joms.2017.11.010
- [24] Baan F, Liebregts J, Xi T, et al (2016) A New 3D Tool for Assessing the Accuracy of Bimaxillary Surgery: The OrthoGnathicAnalyser. *PLoS One* 11: e0149625. doi:10.1371/journal.pone.0149625
-

Corresponding Author

Robin Willaert

Department of Oral and Maxillofacial Surgery

University Hospitals Leuven

Kapucijnenvoer 33, 3000 Leuven, Belgium

email: robin.willaert@icloud.com

telephone: +32 (0) 474 26 81 47

Publication references: Doi: 10.1016/j.ijom.2019.08.009. -PMID: 31474503

Efficacy and complications of orbital fat decompression in Graves' orbitopathy: a systematic review and meta-analysis

R. WILLAERT MD, DMD^{1,2} | T. MALY MD³ | V. NINCLAUS MD⁴ | W. HUVENNE MD, PHD¹
H. VERMEERSCH MD PHD⁵ | N. BRUSSELAERS MD PHD^{1,6}

Abstract

In Graves' orbitopathy, surgical decompression is often needed for functional and esthetic reasons. This meta-analysis assesses effectiveness and safety of only fat removal orbital decompression to treat exophthalmos in Graves' orbitopathy. A systematic search was conducted in Pubmed/MEDLINE, Web of Science and Cochrane Library for studies published before August 2018. Random effects meta-analyses were applied, weighted means and weighted proportions with corresponding 95% confidence intervals (CI) were calculated. Study quality and quality of evidence for each individual outcome was analyzed. Of 1908 initial records, thirteen observational studies were selected, representing 4820 orbits in 2583 patients.

Weighted pre-operative Hertel exophthalmometry was 23.10 mm (95% CI 21.77-24.43) and post-operative 19.31 mm (95% CI 17.81-20.81). The weighted mean difference was 3.81 mm (3.41-4.21). Five studies reported on improvement of diplopia after surgery, in 943 of 1165 patients (weighted proportion 0.50, 95% CI 0.15-0.85). Persistent new onset diplopia was reported in 5 studies, or 124 of 1184 patients (weighted proportion 0.15, 95% CI 0.03-0.27). No serious adverse events were reported. Results support the effectiveness and safety of fat removal orbital decompression to treat mild-to-moderate exophthalmos in Graves' orbitopathy. Prospective and controlled trials are needed to improve level of evidence.

Key Words

- Graves' Orbitopathy
- Endocrine ophthalmopathy
- Fat removal
- Orbital Decompression

AFFILIATIONS

- 1 Department of Head and Neck Surgery, Ghent University Hospital, Belgium
- 2 Department of Oral and Maxillofacial Surgery, University Hospitals Leuven, Leuven, Belgium
- 3 Faculty of Medicine and Health Sciences, Ghent University, Belgium
- 4 Department of Ophthalmology, Ghent University Hospital, Belgium
- 5 Department of Plastic and Reconstructive surgery, Ghent University Hospital, Belgium
- 6 Department of Microbiology, Tumour and Cell Biology, Karolinska Institutet, Stockholm, Sweden

This systematic review was preregistered at the PROSPERO database (CRD42018084472).

Introduction

Graves' orbitopathy (GO), also referred to as dysthyroid/thyroid-associated orbitopathy or thyroid eye disease, is part of an autoimmune process that affects orbital tissues in a severe and potentially irreversible manner. Though its pathophysiology remains incompletely understood, two clinical phases can be distinguished including an active followed by an inactive phase^[1,2]. Transition from the active phase to the later inactive stage is often spontaneous in mild cases or can be aided by immunosuppressive medical treatment and/or radiotherapy^[3-6].

Edema and proliferation of the periorbital tissues in the active inflammatory phase leads to retrobulbar tissue expansion and proptosis. Additional ocular manifestations include eyelid retraction, chemosis, periorbital edema and altered ocular motility. Severe disease progression can sometimes cause vision-threatening exposure keratopathy and compressive optic neuropathy. Activated orbital fibroblasts perpetuate these effects by fibrosis, leading to permanent disfigurement, diplopia and functional, social and aesthetic impairment^[1,2].

Surgical decompression aims to reduce orbital content and/or expand orbital volume in order to shift the position of the globe (decrease exophthalmos), restore venous drainage, improve muscular motility and increase visual acuity^[7-9]. With exception of urgent surgical decompression in vision-threatening optic neuropathy or corneal ulceration refractory to steroids, rehabilitative surgery is reserved to the inactive phase. An abundance of decompressive techniques encompassing both adipose and/or osse-

ous tissue removal have been described in literature^[3,4,10]. Bone removal orbital decompression (BROD) would be characterized by larger effect size (proptosis reduction), though more complications have been reported, such as diplopia, sinusitis, hypoglobus, cerebrospinal fluid leakage and infraorbital hypoesthesia^[1,4,11]. As surgical indications expanded, less invasive techniques such as orbital fat removal became increasingly popular. As no bone is removed in fat removal orbital decompression (FROD), the potential for side effects could be minimized^[12,13]. The Olivari technique was first described in 1988 and remains the most cited method for adipose decompression^[14]. Multiple surgical teams have reported favorable outcomes regarding safety and efficacy^[1,3,4,8,10,15].

At present, several approaches are in use, including combinations of fat removal and single or multiple orbital wall decompression^[10]. The choice of surgical technique mostly depends on personal training, experience and institutional tradition. It remains unclear which technique is superior, with regards to distinct disease presentations and a patient specific, tailored approach^[16]. To our knowledge, no previous or ongoing systematic review concerns orbital decompression via adipose tissue removal. This systematic review aims to identify and summarize the efficacy and safety of orbital decompression by means of only adipose tissue removal for treatment of Graves' orbitopathy.

Materials and methods

A systematic review of literature was performed, compliant to the Preferred Reporting Items for Systematic Reviews and Meta-Analysis recommendations (PRISMA). The study protocol was prospectively registered at the international database of PROSPERO (registration number CRD42018084472).

Primary outcomes were (i) description of post-operative exophthalmos and proptosis reduction (quantitative, continuous data, clinical measurement recorded in millimeter); (ii) amount of fat removal (quantitative, continuous data, recorded in mL) and relation to proptosis reduction (iii) status of visual acuity (qualitative data; no changes, better or worse) and (iiii) status of diplopia (qualitative data; no changes/worse, improved/resolved or new onset). Secondary outcomes consisted of (i) changes in intra-ocular pressure (IOP) (quantitative; continuous data); (ii) assessment of additional sequelae or complications (descriptive data); (iii) changes in quality of life (QoL) (quantitative; continuous data using validated checklists). Possible factors that could modify outcome parameters such as smoking behavior, orbital radiation therapy and the use of imaging analysis, were additionally noted.

Studies were eligible if they were original papers, in English, German, Dutch or French, published before August 2018, describing at least 4 orbits operated through orbital fat decompression as only surgical treatment option in GO patients. Included studies were selected on assessment of surgical technique, reporting of at least one primary outcome and covering a minimum post-operative follow-up of

three months. Non-interventional publications, including editorials, commentaries, review articles and those not subject to peer review were excluded.

The Pubmed/MEDLINE, Cochrane Library and Web of Science databases were searched for a combination of subject headings, in which a first term denominates Graves' orbitopathy; associated to a second term denominating fat decompression. No additional date or publication limits were applied. The references of the included articles and the Web of Science citation index were cross-checked to identify additional eligible articles. (The complete search strategy can be found in Supplementary Table A).

Data collection

One author (RW) performed a first screening on title to remove all clearly irrelevant articles. Two authors (RW, TM) independently conducted selection on title and abstract, followed by full-text critical appraisal, applying the selection criteria to determine eligibility and final in- or exclusion. In the event of duplicate publications, companion papers or an overlap between studies regarding the same patient population, only the most recent and complete study was included. Disagreements among reviewers were settled by additional discussions and by consulting a third reviewer (VN, NB) if necessary. Two reviewers (RW, TM) extracted data independently using standardized lists according to Cochrane Collaboration guidelines^[17]. Research design, study period, demographic data (number of subjects and orbits, ethnicity, gender ratio, age range) and interventional data (indication for treatment, surgical tech-

nique, primary and secondary outcomes, length of follow-up) were recorded.

Quality assessment

The quality of each eligible study was critically appraised by two authors (RW, TM) independently using the Methodological Index for Non-Randomized Studies (MINORS) criteria to assess non-RCTs [18]. The smallest study samples (less than 10 patients or less than 20 orbits) were analyzed for quality using a modified DELPHI checklist reported by Moga et al [19]. In addition, the quality of the evidence for each outcome was evaluated separately using the Grading of Recommendations Assessment, Development and Evaluation (GRADE) criteria and GRADEprofiler software [20].

Because this review concerns one distinct surgical intervention while there are many alternative procedures described, we are aware of possible susceptibility bias (extent of treatment could depend on disease severity) and performance bias (surgical technique and outcome depends on skills and expertise of the operator) [21]. When appropriate, subgroup analyses were performed to check for outcome agreement between large studies (≥ 50 included orbits) and small studies.

Statistical analysis

Descriptive statistics and calculation of correlations between continuous outcomes were provided using SPSS Version 25.0, IBM Corp. Armonk, New York. Meta-analysis was conducted using Stata MP version 14 (Stata Corporation, Texas), using the packages `metan` and `metaprop` [22]. If studies were judged to be clinically and

methodologically sufficiently similar with at least 2 studies reporting the outcome, weighted means and weighted proportions with corresponding 95% confidence intervals (CI) were calculated. Random effect meta-analyses are applied because of the expected high clinical and statistical heterogeneity. Statistical heterogeneity was assessed by visual inspection of forest plots and by examining of the I-squared (I²) statistic, with values above 75% considered as high heterogeneity [17,23].

Results

Included studies

The search resulted in 1908 unique articles, of which 22 were included for qualitative assessment for inclusion (Figure 2.1). Nine studies were excluded because of overlapping study populations or insufficient reporting of outcome data. Thirteen observational studies were included in the meta-analysis. One study was prospective [24]. Eleven articles were published in English, one in German [25] and one in French [26]. In terms of location, seven studies were European, four Asian and two North American. The study designs and population characteristics of the included studies are described in Table 2.1.

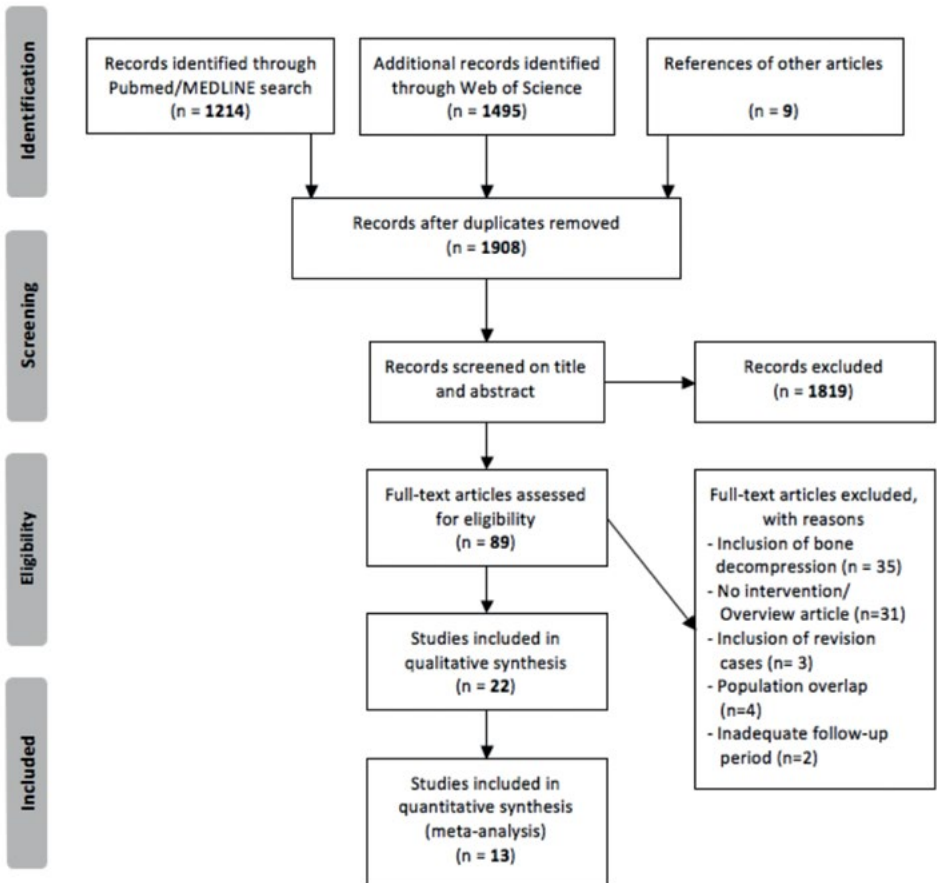
Adipose decompression was performed in 2583 patients on 4820 orbits. The smallest study included 5 orbits in 4 patients [27], whereas the largest included 2697 orbits in 1374 patients [28]. The earliest included study was published in 1998 [15], whereas 6 studies were published in the last 10 years. Average age was 40.1 years (range 15-80 years). Female to male ratio was 2.99:1 (range 1.0-7.0). Average follow-up was 32.6 months (range 3-132).

Risk of bias

Two criteria were insufficiently reported in all articles: calculation of the study size and unbiased assessment of the study endpoints (Supplementary data – Table B1/2). All included studies stated a clear objective/aim, sufficiently described eligibility criteria, intervention, outcome measures and had an appropriate follow-up period. Three studies had one or more comparative interventions^[29–31].

Because all trials were non-randomized, all outcomes started at ‘low quality’ evidence (Supplementary data – Table C). Two outcomes (Hertel exophthalmometry and amount of orbital fat removal) were upgraded in GRADE score, as a clear dose-response relation was apparent. The level of evidence for all other outcomes (intraocular pressure, diplopia, visual acuity, complications) was downgraded as a large heterogeneity was present and patient numbers were lower.

FIGURE 2.1 — PRISMA FLOW DIAGRAM | Databases were searched for relevant studies using predefined inclusion criteria. After removing duplicates and screening on title and abstract, 89 articles were eligible for full-text examination. Finally, 13 studies were considered suitable for inclusion in the meta-analysis.



AUTHORS, COUNTRY, YEAR	DESIGN	PERIOD OF DATA COLLECTION	INTERVENTION OR COMPARISON	N (PATIENTS)	N (ORBITS)
Adenis et al., France, 1998 [15]	Retrospective, observational	1992-1996	FROD only (Modified Olivari technique)	25	41
Kazim et al., US, 2000 [32]	Retrospective, case series	NR	FROD only	5	8
Adenis et al., France, 2003 [26]	Retrospective, observational	1999	FROD only (Modified Olivari technique)	35	58
Ivekovic et al., Croatia, 2005 [27]	Retrospective, case series	2003-2004	FROD only (Full-thickness anterior blepharotomy)	4	5
Balázs et al., Hungary, 2006 [25]	Retrospective, observational	1999-2004	FROD only (Modified Olivari technique)	33	50
Robert et al., France, 2006 [24]	Prospective, observational	NR	FROD only (Modified Olivari technique)	39	64
Richter et al., Germany, 2007 [28]	Retrospective, observational	1984-2004	FROD only (Olivari technique)	1374	2697
Sagilli et al., UK, 2008 [30]	Retrospective, observational, comparative	NR	Group I: FROD (Lower eyelid approach)	3	6
			Group II: FROD+2-wall	4	7
			Group III: FROD+3-wall	4	5
Chang et al., South Korea, 2013 [29]	Retrospective, observational, comparative	2004-2008	Group I: FROD (Lower eyelid approach)	13	13
			Group II: FROD+2-wall	20	20
Prat et al., US, 2015 [9]	Retrospective, observational	1990-2010	FROD only (Lower eyelid approach)	109	217
Li et al., China, 2015 [7]	Retrospective, observational	2009-2012	FROD only (Lower eyelid approach)	11	21
Cheng et al., Taiwan, 2018 [8]	Retrospective, observational	2003-2014	FROD only (Lower eyelid approach)	845	1604
Woo et al., South Korea, 2017 [31]	Retrospective, observational, comparative	2011-2014	Group I: FROD (Lower eyelid approach)	18	36
			Group II: FROD+2-wall	11	22
			Group III: FROD+3-wall	30	60

GENDER (%M)	AGE (YEARS) MEAN (RANGE)	FOLLOW-UP (MONTHS) MEAN (RANGE)
67	51 (27-72)	9 (3-28)
67	52 (27-67)	>3
52	50 (27-77)	18
67	53 (44-78)	>3
32	48 (18-67)	37 (3-59)
50	53 (27-80)	6
20	45 (22-75)	32 (6-132)
All patients: 11	All patients: 49 (32-70)	All patients: >3
18	45	All patients: >36
67	45	
39	44 (15-73)	>3
38	45 (28-65)	22 (12-36)
33	40	37
6	32 (17-55)	21 (3-40)
0	37 (22-60)	21 (3-42)
36	35 (20-59)	20 (3-50)

TABLE 2.1 — BASIC CHARACTERISTICS OF STUDIES PERFORMING ORBITAL FAT DECOMPRESSION FOR GRAVES' ORBITOPATHY

M: Man. N: Number. FROD: fat removal orbital decompression. BROD: Bone removal orbital decompression.

NR: Not Reported.

Hertel Exophthalmometry

Pre- and post-operative measurements by Hertel exophthalmometry (including standard deviations) were reported in 9 of 13 included studies and mean differences with standard deviations in 11 studies enabling pooling the weighted means of 1812 treated orbits (Table 2.2). Weighted pre-operative Hertel exophthalmometry was 23.10 mm (95% CI 21.77-24.43) and post-operative 19.31 mm (95% CI 17.81-20.81) (Table 2.3). The weighted mean reduction was 3.81 mm

(3.41-4.21) (Figure 2.2); and both by inspection of the pre- and post-operative values and the pooled difference, it is apparent that the gain was slightly higher in the larger studies. Heterogeneity values were high in all analyses.

Resected adipose tissue

In 8 studies out of 13 included studies (1857 orbits) (Table 2.2), information on the amount of resected adipose tissue was available, with a pooled average resected volume of 5.09 mL (95% CI 4.18-6.01).

TABLE 2.2 — SUMMARY OF MAIN OUTCOME PARAMETERS

AUTHORS	N (ORBITS)	PREOPERATIVE HERTEL VALUE (MM) MEAN ± SD	POSTOPERATIVE HERTEL VALUE (MM) MEAN ± SD	PROPTOSIS REDUCTION (MM) MEAN ± SD	AMOUNT ORBITAL FAT REMOVED (ML) MEAN ± SD	NEW ONSET DIPLOPIA (%)	DIPLOPIA BETTER OR RESOLVED (%)
Adenis et al [15]	41	24.5 ± 2.8	19.8 ± 2.5	4.7 ± 2.4	73 ± 1.9	2/11 (18)	5/14 (36)
Kazim et al. [32]	8	24.5 ± 2	21.3 ± 2.1	3.0 ± 1.3	'4 -6 mL'	NR	NR
Adenis et al. [26]	58	NR	NR	4.5 ± 2.0	72 ± 1.8	9/28 (32)	0/7 (0)
Ivekovic et al. [27]	5	22.8 ± 1.9	19.4 ± 1.5	3.4 ± 0.8	> 6 mL'	0/4 (0)	NR
Balázs et al. [25]	50	24.3 ± 2.6	21.0 ± 2.3	3.2 ± 1.3	4.5 ± 1.1	0/20 (0)	7/13 (54)
Robert et al. [24]	64	24.3 ± 2.5	19.9 ± 3.1	4.4 ± 2.8	6.4 ± 4.5	NR	NR
Richter et al. [28]	2697	24.3 ± (NR)	18.4 ± (NR)	5.9 ± (NR)	6.3 ± (NR)	89/440 (20)	859/934 (92)
Sagilli et al. [30]	13	21.8 ± 2.0	18.9 ± 2.4	5.2 ± 1.3	5.4 ± 1.3	1/13 (8)	NR
Chang et al. [29]	13	21.8 ± 2.0	18.9 ± 2.4	5.2 ± 1.3	5.4 ± 1.3	1/13 (8)	NR
Prat et al. [9]	217	23.6 ± (NR)	20.3 ± (NR)	3.3 ± 1.5	3.2 ± (NR)	0/58 (0)	15/51 (30)
Li et al. [7]	21	21.3 ± 3.6	17.0 ± 2.8	4.2 ± 1.3	4.0 ± 1.1	0/11 (0)	NR
Cheng et al. [8]	1604	21.2 ± 1.6	16.9 ± 1.2	4.1 ± 1.3	4.5 ± 1.1	23/ 692 (3)	57/153 (37)
Woo et al. [31]	36	19.9 ± (NR)	16.3 ± (NR)	3.5 ± (?)	6.7 ± (NR)	NR	NR

N: Number. ; NR: Not Reported.

A slightly higher amount of fat was resected in larger studies (5.59 mL 95% CI 4.51-6.68) compared to smaller studies (4.59 mL 95% CI 2.23-6.96) (Table 2.3). Six studies individually checked for a possible correlation between amount of fat removal and proptosis reduction. One article reports a 1:1 ratio^[9], whereas 2 articles^[7,8] describe a good prediction on Hertel change when using an equation which includes age, gender and preoperative diplopia, proposed by Liao^[13]. Because of the heterogeneity of the data, these correlations were not pooled by means of meta-analysis.

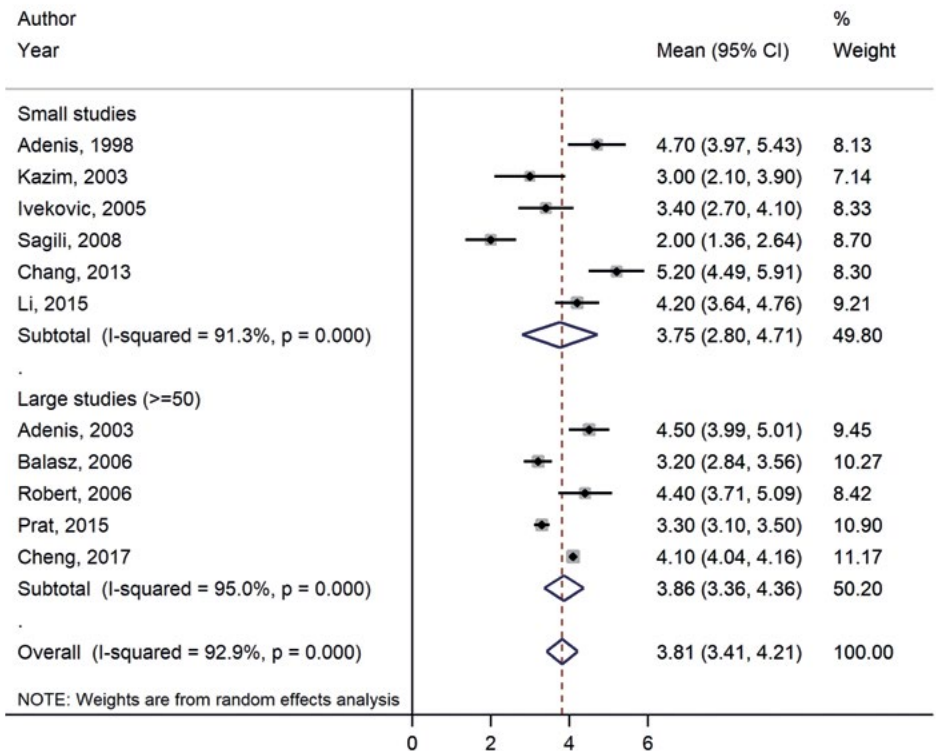
Visual acuity

Four of 13 studies (75 of 2524 patients) provided detailed information about pre- and postoperative visual acuity^[7,15,27,32]. Due to the small amount of patients and heterogeneity in patient population (inclusion of patients with and without optic neuropathy), this outcome was not subjected to meta-analysis.

Diplopia

Diplopia and/or ocular motility disturbances were reported in 9 of 13 included studies^[7-9,15,25-29] (2421 patients) (Table 2.2),

FIGURE 2.2 — FOREST PLOT ILLUSTRATING THE POOLED MEAN PROPTOSIS REDUCTION AFTER ORBITAL FAT DECOMPRESSION | The post-operative change in Hertel exophthalmometry is calculated by random-effect meta-analysis, separately for large and small study samples, and presented with corresponding 95% confidence intervals (CI). Values are in mm.



of which 3 studies [7,27,29] only included individuals without diplopia before surgery. All studies showed high heterogeneity in definition, assessment of ocular motility and occurrence of diplopia. The weighted proportion of individuals presenting with diplopia at the time of surgery was 0.41 (0.15-0.68). Of these, 50% improved after surgery (0.50, 95% CI 0.15-0.85). Of those without diplopia before surgery 15% developed persistent new onset diplopia after surgery (0.15, 95% CI 0.03-0.27) (Table 2.4).

Intra-ocular pressure

Five studies reported on IOP values [15,24,25,27,30] yet only 3 studies reported both pre- and post-operative values with standard deviations required for meta-analysis [24,27,30]. The weighted mean pre-operative

IOP (reported in 3/13 studies) was 17.22 mmHg (13.57-20.87) and post-operative 16.07 mmHg (15.26-16.88), with respectively $I^2=97.3\%$ and $I^2=16.7$ (Table 2.3). Measurements of intraocular pressure were highly variable in timing and different measurement techniques were reported.

Other complications

Data on other complications was available in 9 of 13 studies included (Supplementary data — Table D); yet heterogeneously reported, so only a descriptive (unweighted) overview is presented. After fat decompression procedures in 2336 patients, a total of 161 other complications were reported, of which 103 occurred in the largest study of 1274 individuals [28]. The cut-off for defining complications as ‘temporary’

TABLE 2.3 — WEIGHTED MEANS FOR EXOPHTHALMOMETRY MEASUREMENTS, EXCISED FAT VOLUME AND INTRA-OCULAR PRESSURE.

	N STUDIES	N OR-BITS	PRE-OPERATIVE (95% CI)	I^2 (%)	POSTOPERATIVE (95% CI)	I^2 (%)	MEAN DIFFERENCE (95% CI)	I^2 (%)
HERTEL MEASUREMENTS (IN MM)	11	1812	23.10 (21.77-24.43)	96.7	19.31 (17.81-20.81)	97.8	3.81 (3.41-4.21)	92.9
Small studies	8	94	23.04 (21.87-24.21)	78.5	19.33 (18.33-20.33)	79.0	3.75 (2.80-4.71)	91.3
Large studies	3	1718	23.25 (20.77-25.72)	98.8	19.27 (16.29-22.24)	99.1	3.86 (3.36-4.36)	95.0
AMOUNT OF FAT REMOVED (IN ML)	8	1857			5.09 (4.18-6.01)	98.1		
Small studies	4	81			4.59 (2.23-6.96)	98.7		
Large studies	4	1776			5.59 (4.51-6.68)	97.0		
INTRA-OCULAR PRESSURE (IN MMHG)	3	75	17.22 (13.57-20.87)	97.3	16.07 (15.26-16.88)	16.7		
Small studies	2	11	16.08 (12.67-19.50)	89.9	16.31 (14.65-17.97)	53.7		

N: Number. I^2 : I-squared statistic heterogeneity assessment. Weighted means with corresponding 95% confidence intervals (CI) were calculated using random effect meta-analyses.

(n=80) and ‘permanent’ (n=81) varied between studies, from 3 to 6 months after surgery. Ten studies did not report any temporary complications, while the other 3 reported temporary complications in 0,01% to 16% of all patients [15,25,28]. The temporary complications which occurred in these studies included bleeding [25,28], infection [28], sensory nerve damage [15,25] and conjunctivitis/chemosis requiring treatment [28]. Four studies did not report any permanent complications [9,26,30,31], while the remaining 9 studies reported permanent complications in 2-22% of all patients. The permanent complications that occurred include sensory nerve damage [25,28], palpebral position disorder [15,25], proptosis recurrence [8,28,29] and one patient with new onset presbyopia [7]. No loss of vision or other serious adverse events (CSF leak, hypoglobus, meningitis, sinusitis, scarification, lacrimal nerve damage) were reported.

Quality of Life

Quality of life was not systematically described in the included articles. Only one study assessed quality of life, in which the validated GO-Qol questionnaire was used

in a small portion of the studied population (n=43/845 patients, 5.09%) [8].

Confounding

Smoking status was only assessed in 2 studies. One mentions active smoking behavior in 16 of 154 patients (10.4%), without further analysis [9], the other reports a multivariate analysis including smoking, though no significant association with treatment success (proptosis reduction and diplopia status) was objectified [8].

In six included studies orbital radiation therapy could precede surgical decompression [9,15,24,25,28,32]. All studies display a considerable variation in timing, indication and proportion of patients who are treated with orbital irradiation. Two studies [15,32] state no clear effect of radiotherapy on surgical outcome, while an increased risk of complications was reported in one study [28]. Another study suggests a history of radiation therapy could be of benefit and increase proptosis reduction [9].

The application, timing and clinical consequences of orbital imaging (CT or

TABLE 2.4 — WEIGHTED PROPORTIONS OF DIPLOPIA OCCURRENCE BEFORE AND AFTER SURGERY.

	N studies (*)	n/N (patients)	Weighted proportion (95% CI)	I ² (%)
Diplopia before surgery	6	1172/2421 I	0.41 (0.15-0.68)	99.3
Diplopia <u>resolved</u> after surgery	6 (5*)	943/1172	0.50 (0.15-0.85)	98.7
Diplopia <u>remained or worsened</u> after surgery	6 (5*)	229/1172	0.50 (0.15-0.85)	98.7
No diplopia before surgery	6	1249/2421 I	0.59 (0.32-0.85)	99.3
<u>New onset</u> diplopia after surgery	9 (5*)	124/1277	0.15 (0.03-0.27)	95.0

(*) = Number of studies in weighted proportion since studies with proportion of 0 or 1 are disregarded. Weighted proportions are calculated by random effects analysis. N: Number. NR: Not Reported. I²: I-squared statistic heterogeneity assessment.

MRI) for fat removal is highly variable when analyzing the included studies. Some authors use pre-operative imaging analysis to select the most appropriate decompression technique [7,29,32], others define different subgroups based on imaging but perform lipectomy in all groups [8,9,15,24]. All studies where subgroups (fat vs. muscle predominant or combined) were defined using orbital imaging, did not find a significant difference in proptosis reduction after performing fat removal decompression [8,9,15,24].

Discussion The results of this review indicate that an effective proptosis reduction is possible through orbital fat decompression in patients with mild-to-moderate Graves' orbitopathy. No conclusive statements remain regarding impact of fat decompression on visual acuity, quality of life or intra-ocular pressure. To our knowledge, this is the first meta-analysis reviewing the effects of orbital decompression by only fat removal in GO.

Normal values of Hertel exophthalmometry range 15-20 mm. The average proptosis reduction achieved by two-wall orbital bone decompression is 4.0 to 5.0 mm [10,11,16,33]. As this result compares to the outcome in the current analysis, FROD can be considered effective and clinically meaningful to reduce mild-to-moderate proptosis. Only few reports included patients with severe proptosis (>26 mm) for FROD treatment. That is why many authors recommend a tailored approach when larger exophthalmos reduction is needed in severe proptosis. Either a per-operative, stepwise decompression, with additional bone removal when fat removal is insufficient [28,29,31,34] or stratifi-

cation based on preoperative evaluation is suggested [35-37]. The effect of adipose decompression on visual acuity and IOP in GO remains debated [38-41]. Due to the small number of patients, differences in clinical assessment and statistical heterogeneity, a very low level of evidence certainty is administered to these outcomes and additional research is needed. One important remark concerns the use of FROD in urgent decompression for vision loss caused by dysthyroid optic neuropathy. Current therapeutic guidelines advise use of intravenous steroids for first-line medical decompression [42,43]. However, in cases of insufficiency or contraindication of corticotherapy, several authors report good results after FROD for urgent decompression in dysthyroid optic neuropathy [9,12,24,25,28,32].

Some severe complications, as optic nerve damage, cerebrospinal fluid leak and meningitis, are described after bony orbital decompression. None of these complications could be withheld after FROD. Overall, the selected studies presented the complications inconsistently, which prevents meta-analysis and makes underreporting presumable. New onset or worsening diplopia is the most highlighted complication in this review results. Incidence reports of new onset diplopia in literature vary between 10% and 20% [11,16,33]. The exact pathophysiological mechanism is debated, but dislocation of the globe axis and disturbance of the extraocular muscle path make it probably more common following BROD [28]. In contrast to FROD, where removal of several adipose tissue pockets could maintain the central position of the globe, while possibly alleviating tension on the extraocular muscles. This review suggests

a lower risk of new onset diplopia comparing to earlier reports and shows improvement after FROD in most patients with existing diplopia. However, no reliable prediction on change of diplopia status is possible, whether or not this problem existed before FROD. Standardized measurement methods (interval time, scoring systems and technique) could provide new insights on development and prevention of diplopia status.

An interesting, yet complex, debate concerns the suggestion of a linear association between adipose tissue removal and proptosis reduction, which could be very helpful in planning a tailored approach. Several included studies reported on this topic and their findings complement previous statements of a correlation between resected adipose volume and change in exophthalmometry^[12,13]. However, interpretation in terms of causality and individual prediction remains difficult. Many confounders, as ethnic anatomical differences, the role of patient subgroups (fat- or muscle predominance) and site of fat removal (post- or pre-equatorial fat) remain debated factors^[28,37,44]. Future imaging studies with quantification of intra-orbital tissue volumes could probably enhance understanding to make proptosis reduction more predictable.

GO may cause severe psychological impairment^[45], thus surgical outcome and success of treatment go beyond reduction in proptosis. Quality of Life assessment may provide a novel approach to bypass the large variability in clinical measurements. However, despite accumulating evidence of its importance, this tool is not yet applied in routine clinical practice. Further research is required to intensify the clinical

implementation of QoL assessment as a major outcome parameter to evaluate surgical interventions^[7,8,45].

It is important to point out that several factors are believed to alter disease progression and possibly therapeutic outcome, including smoking status and orbital radiotherapy^[46,47]. Orbital radiotherapy is a common preoperative treatment modality. An increase in adhesions due to fibrosis might increase procedure difficulty and could jeopardize outcome prognosis^[48,49]. Due to underreporting and ambiguous results, the impact of these factors on treatment outcome requires more investigation. Orbital imaging and computer analysis could improve treatment strategy and outcome of FROD. CT and MRI are performed to confirm diagnosis, though might be useful for treatment stratification as well. Fat-, muscle- or mixed predominant edema types can be distinguished, greatly aiding in patient-specific, tailored surgical therapy. The application of orbital imaging, however, is variable and studies where subgroups were stratified using orbital imaging, could not show a significant difference in outcome. Therefore, no consensus is reached over the added value of image-based segregation of subtypes of GO.

A large number of patients could be withheld from 13 studies with equivalent surgical procedures, but a great discrepancy in study size was displayed. Supplementary subgroup analysis revealed a slight increase of resected fat volume in the large cohorts, although the gain in proptosis reduction was not clinically relevant. Another limitation is the absence of a gold standard technique to compare the results. A multitude of surgical (bone

and/or fat) decompression techniques have been described and no consensus exists on which surgical technique could be applied for which disease presentation. Other limitations inherent to this study are attributable to the inclusion of non-randomized, interventional studies. Extensive analysis of study quality and of evidence for each outcome parameter separately was performed to extract valuable scientific and clinical meaningful information. Despite high heterogeneity in reporting certain parameters (visual acuity, diplopia status and IOP) and risk of selection bias due to un-identified confounders, 2 main outcome measures (Hertel value and amount of fat removed) are recognized as moderate level evidence.

Conclusion In conclusion, orbital decompression by fat removal can be considered an effective procedure to treat mild-to-moderate exophthalmos in patients with Graves' Orbitopathy. The current evidence is low to assume that orbital fat removal consistently improves the postoperative outcome in terms of intraocular pressure, diplopia, QoL and visual acuity. Future research should focus on well-designed, prospective studies with uniform clinical outcome assessment to improve data interpretation and synthesis.

ACKNOWLEDGEMENTS

This work has not been submitted simultaneously to another journal and has not been published before. All authors have read and approved this work before submitting to IJOMS.

No ethical approval was required.

This study received no funding. No conflicts of interest are to be disclosed.

REFERENCES

- [1] Weiler DL. Thyroid eye disease: a review. *Clin Exp Optom.* 2017;100(1):20–5.
- [2] Kiran Z, Rashid O, Islam N. Typical graves' ophthalmopathy in primary hypothyroidism. *J Pak Med Assoc.* 2017 Jul;67(7):1104–6.
- [3] Eckstein A, Esser J, Mattheis S, Berchner-Pfannschmidt U. [Graves' Orbitopathy]. *Klin Monbl Augenheilkd.* 2016 Dec;233(12):1385–407.
- [4] Bartalena L, Baldeschi L, Boboridis K, Eckstein A, Kahaly GJ, Marcocci C, et al. The 2016 European Thyroid Association/European Group on Graves' Orbitopathy Guidelines for the Management of Graves' Orbitopathy. *Eur Thyroid J.* 2016;5(1):9–26.
- [5] Phillips ME, Marzban MM, Kathuria SS. Treatment of thyroid eye disease. *Curr Treat Options Neurol.* 2010 Jan;12(1):64–9.
- [6] Marcocci C, Marino M. Treatment of mild, moderate-to-severe and very severe Graves' orbitopathy. *Best Pract Res Clin Endocrinol Metab.* 2012 Jun;26(3):325–37.
- [7] Li EY, Kwok TY, Cheng AC, Wong AC, Yuen HK. Fat-removal orbital decompression for disfiguring proptosis associated with Graves' ophthalmopathy: safety, efficacy and predictability of outcomes. *Int Ophthalmol.* 2015;35(3):325–9. 7.
- [8] Cheng AM, Wei YH, Tighe S, Sheha H, Liao SL. Long-term outcomes of orbital fat decompression in Graves' orbitopathy. *Br J Ophthalmol.* 2018;102(1):69–73.
- [9] Prat MC, Braunstein AL, Dagi Glass LR, Kazim M. Orbital fat decompression for thyroid eye disease: retrospective case review and criteria for optimal case selection. *Ophthal Plast Reconstr Surg.* 2015;31(3):215–8.
- [10] Boboridis KG, Uddin J, Mikropoulos DG, Bunce C, Mangouritsas G, Voudouragkaki IC, et al. Critical Appraisal on Orbital Decompression for Thyroid Eye Disease: A Systematic Review and Literature Search. *Adv Ther.* 2015;32(7):595–611.
- [11] Menconi F, Marcocci C, Marino M. Diagnosis and classification of Graves' disease. *Autoimmun Rev.* 2014;13(4–5):398–402.
- [12] Wu CH, Chang TC, Liao SL. Results and Predictability of Fat-Removal Orbital Decompression for Disfiguring Graves Exophthalmos in an Asian Patient Population. *Am J Ophthalmol.* 2008;145(4):755–9.
- [13] Liao SL, Huang SW. Correlation of retrobulbar volume change with resected orbital fat volume and proptosis reduction after fatty decompression for graves ophthalmopathy. *Am J Ophthalmol.* 2011;151(3):465–469.e1.
- [14] Olivari N. Endokrine Orbitopathie: Chirurgische Therapie. *HNO.* 2010;58(1):8–14.

- [15] Adenis JP, Robert PY, Lasudry JG, Dalloul Z. Treatment of proptosis with fat removal orbital decompression in Graves' ophthalmopathy. *Eur J Ophthalmol*. 1998;8(4):246–52.
- [16] Mourits MP, Bijl H, Altea MA, Baldeschi L, Boboridis K, Currò N, et al. Outcome of orbital decompression for disfiguring proptosis in patients with Graves' orbitopathy using various surgical procedures. *Br J Ophthalmol*. 2009;93(11):1518–23.
- [17] Higgins J, Green S. *Cochrane Handbook for Systematic Reviews of Interventions* [Internet]. The Cochrane Library. The Cochrane Collaboration; 2006. Available from: <https://training.cochrane.org/handbook/> [Accessibility verified May, 2019]
- [18] Slim K, Nini E, Forestier D, Kwiatkowski F, Panis Y, Chipponi J. Methodological index for non-randomized studies (minors): development and validation of a new instrument. *ANZ J Surg*. 2003 Sep;73(9):712–6.
- [19] Moga C, Guo B, Schopflocher D, Harstall C. Development of a quality appraisal tool for case series studies using a modified Delphi technique [Internet]. Edmonton (AB): Institute of Health Economics; 2012. Available from: <https://www.ihe.ca/advanced-search/development-of-a-quality-appraisal-tool-for-case-series-studies-using-a-modified-delphi-technique/> [Accessibility verified May, 2019]
- [20] Ryan R, Hill S. How to GRADE the quality of the evidence. Version 3.0. *Cochrane Consumers and Communication Group*; 2016.
- [21] Paradis C. Bias in surgical research. *Ann Surg*. 2008 Aug;248(2):180–8.
- [22] Nyaga VN, Arbyn M, Aerts M. Metaprop : a Stata command to perform meta-analysis of binomial data. *Arch ofPublic Heal*. 2014;72(39):1–10.
- [23] Higgins JPT, Thompson SG, Deeks JJ, Altman DG. Measuring inconsistency in meta-analyses. *BMJ*. 2003 Sep;327(7414):557–60.
- [24] Robert PYR, Rivas M, Camezind P, Rulfi JY, Adenis JP. Decrease of intraocular pressure after fat-removal orbital decompression in Graves disease. *Ophthal Plast Reconstr Surg*. 2006;22(2):92–5.
- [25] Balázs E, Nagy E V., Tóth K, Steiber Z, Kertész K, Szucs-Farkas Z, et al. Erfahrungen mit transpalpebraler orbitaler Lippektomie. *Ophthalmologie*. 2006;103(6):517–22.
- [26] Adenis JP, Camezind P, Robert P-Y. [Is incidence of diplopia after Fat Removal Orbital Decompression a predictive factor of choice of surgical technique for Graves' ophthalmopathy?]. *Bull Acad Natl Med*. 2003;187(9):1649–60.
- [27] Ivekovic R, Novak-Laus K, Tedeschi-Reiner E, Masnec-Paskvalin S, Saric D, Mandic Z. Full-thickness anterior blepharotomy and transpalpebral fat decompression in Graves' orbitopathy. *Coll Antropol*. 2005;29 Suppl 1:33–6.
- [28] Richter DF, Stoff A, Olivari N. Transpalpebral decompression of endocrine ophthalmopathy by intraorbital fat removal (olivari technique): Experience and progression after more than 3000 operations over 20 years. *Plast Reconstr Surg*. 2007;120(1):109–23.
- [29] Chang M, Baek S, Lee TS. Long-term outcomes of unilateral orbital fat decompression for thyroid eye disease. *Graefes Arch Clin Exp Ophthalmol*. 2013;251(3):935–9.
- [30] Sagili S, DeSousa J-L, Malhotra R. Intraocular Pressure and Refractive Changes Following Orbital Decompression with Intraorbital Fat Excision. *Open Ophthalmol J*. 2008;2(1):73–6.
- [31] Woo YJ, Yoon JS. Changes in pupillary distance after fat versus bony orbital decompression in Graves' orbitopathy. *Can J Ophthalmol*. 2017;52(2):186–91.
- [32] Kazim M, Trokel SL, Acaroglu G, Elliott A. Reversal of dysthyroid optic neuropathy following orbital fat decompression. *Br J Ophthalmol*. 2000;84(6):600–5.
- [33] Rootman DB. Orbital decompression for thyroid eye disease. *Surv Ophthalmol*. 2018 Jan;63(1):86–104.
- [34] Clauser L, Galie M, Sarti E, Dallera V. Rationale of treatment in Graves ophthalmopathy. *Plast Reconstr Surg*. 2001 Dec;108(7):1880–94.
- [35] Imburgia A, Elia G, Franco F, Perri P, Franco E, Galie M, et al. Treatment of exophthalmos and strabismus surgery in thyroid-associated orbitopathy. *Int J Oral Maxillofac Surg*. 2016 Jun;45(6):743–9.
- [36] Krastinova-Lolov D, Bach CA, Hartl DM, Coquille F, Jansinski M, Cecchi P, et al. Surgical strategy in the treatment of globe protrusion depending on its mechanism (Graves' disease, nonsyndromic exorbitism, or high myopia). *Plast Reconstr Surg*. 2006;117(2):553–64.
- [37] Lee KH, Jang SY, Lee SY, Yoon JS. Graded Decompression of Orbital Fat and Wall in Patients with Graves' Orbitopathy. *Korean J Ophthalmol*. 2014;28(1):1.
- [38] Dev S, Damji KF, DeBacker CM, Cox TA, Dutton JJ, Allingham RR. Decrease in intraocular pressure after orbital decompression for thyroid orbitopathy. *Can J Ophthalmol*. 1998 Oct;33(6):314–9.
- [39] Danesh-Meyer H V, Savino PJ, Deramo V, Sergott RC, Smith AF. Intraocular pressure changes after treatment for Graves' orbitopathy. *Ophthalmology*. 2001 Jan;108(1):145–50.
- [40] Cockerham KP, Pal C, Jani B, Wolter A, Kennerdell JS. The prevalence and implications of ocular hypertension and glaucoma in thyroid-associated orbitopathy. *Ophthalmology*. 1997 Jun;104(6):914–7.
- [41] Kalmann R, Mourits MP. Prevalence and management of elevated intraocular pressure in patients with Graves' orbitopathy. *Br J Ophthalmol*. 1998 Jul;82(7):754–7.
- [42] Perumal B, Meyer DR. Treatment of severe thyroid eye disease: a survey of the American Society of Ophthalmic Plastic and Reconstructive Surgery (ASOPRS). *Ophthal Plast Reconstr Surg*. 2015;31(2):127–31.

- [43] Wakelkamp IMMJ, Baldeschi L, Saeed P, Mourits MP, Prummel MF, Wiersinga WM. Surgical or medical decompression as a first-line treatment of optic neuropathy in Graves' ophthalmopathy? A randomized controlled trial. *Clin Endocrinol (Oxf)*. 2005 Sep;63(3):323-8.
- [44] Liao SL, Kao SCS, Hou PK, Chen MS. Results of orbital decompression in Taiwan. *Orbit*. 2003;20(4):267-74.
- [45] Wiersinga WM. Quality of life in Graves' ophthalmopathy. *Best Pract Res Clin Endocrinol Metab*. 2012 Jun;26(3):359-70.
- [46] Bartalena L, Marcocci C, Tanda ML, Manetti L, Dell'Unto E, Bartolomei MP, et al. Cigarette smoking and treatment outcomes in Graves ophthalmopathy. *Ann Intern Med*. 1998 Oct;129(8):632-5.
- [47] Eckstein A, Quadbeck B, Mueller G, Rettenmeier AW, Hoermann R, Mann K, et al. Impact of smoking on the response to treatment of thyroid associated ophthalmopathy. *Br J Ophthalmol*. 2003 Jun;87(6):773-6.
- [48] Olivari N. Transpalpebral decompression of endocrine ophthalmopathy (Graves' disease) by removal of intraorbital fat: experience with 147 operations over 5 years. *Plast Reconstr Surg*. 1991 Apr;87(4):623-7.
- [49] Clauser LC, Galie M, Tieghi R, Carinci F. Endocrine orbitopathy: 11 years retrospective study and review of 102 patients & 196 orbits. *J Craniomaxillofac Surg*. 2012 Feb;40(2):134-41.

SUPPLEMENTARY MATERIAL

SUPPLEMENTARY TABLE A — DETAILED SEARCH STRATEGY FOR PUBMED AND WEB OF SCIENCE

PUBMED SEARCH

The following key terms were combined with Boolean operators in the Pubmed search regarding Graves' ophthalmopathy and adipose tissue removal. Mesh terms included 'graves disease[MeSH]'; 'graves ophthalmopathy[MeSH]'; graves disease, 'graves ophthalmopathy', 'graves', 'dysthyroid', 'thyroid', 'thyroid-associated', 'exophthalmos', 'ophthalmopathy', 'eye disease', 'keratopathy', 'orbitopathy', 'exophthalmy', 'proptosis', combined with search terms as 'fat removal', 'fat decompression', 'surgical', 'surgery', 'decompression', 'removal', 'fat', 'lipectomy' or 'liposuction'. An additional search of the references of included studies was performed to find relevant studies.

PUBMED: Mesh terms : [graves disease] [graves ophthalmopathy] ("graves ophthalmopathy"[Mesh] OR "graves disease"[Mesh] OR "graves" [Tiab] OR "dysthyroid" [Tiab] OR "thyroid" [Tiab] OR "thyroid-associated" [Tiab]) AND ("orbitopathy" [Tiab] OR "exophthalmy" [Tiab] OR "exophthalmos"[Tiab] OR "ophthalmopathy"[Tiab] OR " eye disease" [Tiab] OR "keratopathy" [Tiab] OR "proptosis" [Tiab]) AND ("fat removal"[Tiab] OR "fat decompression"[Tiab] OR "surgical"[Tiab] OR "surgery"[Tiab] OR "decompression"[Tiab] OR "removal"[Tiab] OR "fat"[Tiab] OR "lipectomy"[Tiab] OR "liposuction"[Tiab])

WEB OF SCIENCE SEARCH

WOS: TOPIC: (graves ophthalmopathy OR graves disease OR graves OR dysthyroid OR thyroid OR thyroid-associated) AND (orbitopathy OR exophthalmy OR exophthalmos OR ophthalmopathy OR eye disease OR keratopathy OR proptosis) AND (fat removal OR fat decompression OR surgical OR surgery OR decompression OR removal OR fat OR lipectomy OR liposuction). Timespan: All years. Indexes: SCI-EXPANDED, SSCI, A&HCI, CPCI-S, CPCI-SSH, ESCI

SUPPLEMENTARY TABLE B — QUALITATIVE ANALYSIS**I/ QUALITATIVE ANALYSIS MINOR CRITERIA**

MINORS			
Studies N=9 [7-9, 15, 23-25, 27, 30]			
	Not reported	Indequetely reported	Adequetely reported
Clearly stated aim	0	0	9
Inclusion of consecutive patients	0	3	6
Prospective collection of data	8	0	1
Endpoints appropriate to the aim of the study	0	0	9
Unbiased assessment of the study endpoint	0	9	0
Follow-up period appropriate to the aim of the study	0	0	9
Loss to follow-up less than 5%	0	0	9
Prospective calculation of the study size	9	0	0
Additional criteria in the case of comparative study N=1 [30]			
An adequate control group	0	0	1
Contemporary groups	0	1	0
Baseline equivalence of groups	0	0	1
Adequate statistical analysis	0	0	1

2/ QUALITATIVE ANALYSIS MDELPHI SCORING SYSTEM

MDELPHI SCORE	27	29	30	32
Studies n = 4				
TOTAL SCORE (x/36)	33	27	26	30
Is the hypothesis/aim/objective of the study stated in the abstract, introduction, or methods section?	2	2	2	2
Study population				
Are the characteristics of the participants included in the study described?	2	2	2	2
Were the cases collected in more than one centre?	0	0	0	0
Are the eligibility criteria (inclusion and exclusion criteria) to entry the study explicit and appropriate?	2	1	1	2
Were patients recruited consecutively?	1	2	1	1
Did patients enter the study at a similar point in the disease?	2	2	2	2
Intervention and co-intervention				
Was the intervention clearly described in the study?	2	2	2	2
Were additional interventions (co-interventions) clearly reported in the study?	2	0	2	2
Outcome measures				
Are the outcome measures clearly defined in the introduction or methods section?	2	2	2	2
Were relevant outcomes appropriately measured with objective and/or subjective methods?	2	2	2	2
Were outcomes assessed before and after intervention?	2	2	2	2
Statistical analysis				
Were the statistical tests used to assess the primary outcomes appropriate?	2	2	0	0
Results and conclusions				
Was the length of follow-up reported?	2	2	2	2
Was the loss to follow-up reported?	2	0	2	2
Does the study provide estimates of the random variability in the data of relevant outcomes?	2	2	0	1
Are adverse events reported?	2	2	2	2
Are the conclusions of the study supported by results?	2	2	2	2
Are both competing interest and source of support for the study reported?	2	0	0	2

SUPPLEMENTARY TABLE C — GRADE QUALITY ASSESSMENT

I/ HERTEL EXOPHTHALMOMETRY

GRADE criteria	Rating (circle one)	Footnotes (explain reasons for down- or upgrading)	Quality of the evidence (circle one)
OUTCOME: HERTEL EXOPHTHALMOMETRY			
Study design	RCT (starts as high quality) Non-RCT (starts as low quality)	Non-RCT	@@@@ High @@@@ Moderate @@@@ Low @@@@ Very low
Risk of Bias (use the Cochrane Risk of Bias tables and figures)	No Serious (-1) Very serious (-2)	Plausible bias is unlikely to seriously alter the results.	
Inconsistency	No Serious (-1) Very serious (-2)	Low degree of variability between studies, low heterogeneity (23%).	
Indirectness	No Serious (-1) Very serious (-2)	All findings apply to the review question.	
Imprecision	No Serious (-1) Very serious (-2)	Sufficient number of participants, confidence interval indicates a meaningful benefit.	
Publication Bias	Undetected Strongly suspected (-1)	Limited publication bias is possible. Funnel plot is available	
Other (upgrading factors, circle all that apply)	Large effect (+1 or +2) Dose response (+1 or +2) No plausible confounding (+1 or +2)	Dose-response relationship with adipose decompression	

2/ AMOUNT OF FAT REMOVAL

GRADE criteria	Rating (circle one)	Footnotes (explain reasons for down- or upgrading)	Quality of the evidence (circle one)
OUTCOME: AMOUNT OF FAT REMOVAL			
Study design	RCT (starts as high quality) Non-RCT (starts as low quality)	Non-RCT	
Risk of Bias (use the Cochrane Risk of Bias tables and figures)	No Serious (-1) Very serious (-2)	Plausible bias is unlikely to seriously alter the results.	⊕⊕⊕⊕ High
Inconsistency	No Serious (-1) Very serious (-2)	Low degree of inconsistency in narrative data, no large variations in the degree to which the outcome is affected.	⊕⊕⊕⊙ Moderate
Indirectness	No Serious (-1) Very serious (-2)	All findings apply to the review question.	⊕⊕⊕⊙ Low
Imprecision	No Serious (-1) Very serious (-2)	Sufficient number of participants, confidence interval indicates a meaningful benefit.	⊕⊕⊕⊙ Low
Publication Bias	Undetected Strongly suspected (-1)	Limited publication bias is possible. Funnel plot is available.	⊕⊕⊕⊙ Very low
Other (upgrading factors, circle all that apply)	Large effect (+1 or +2) Dose response (+1 or +2) No plausible confounding (+1 or +2)	Dose-response relationship with Hertel exophthalmometry	

3/ INTRAOCULAR PRESSURE

GRADE criteria	Rating (circle one)	Footnotes (explain reasons for down- or upgrading)	Quality of the evidence (circle one)
OUTCOME: INTRAOCULAR PRESSURE			
Study design	RCT (starts as high quality) Non-RCT (starts as low quality)	Non-RCT	
Risk of Bias (use the Cochrane Risk of Bias tables and figures)	No Serious (-1) Very serious (-2)	Plausible bias is unlikely to seriously alter the results.	⊕⊕⊕⊕ High
Inconsistency	No Serious (-1) Very serious (-2)	Large variability, considerable heterogeneity (88%).	⊕⊕⊕⊙ Moderate
Indirectness	No Serious (-1) Very serious (-2)	All findings apply to the review question.	⊕⊕⊕⊙ Low
Imprecision	No Serious (-1) Very serious (-2)	Small number of total participants, wide confidence interval includes 'no effect'.	⊕⊕⊕⊙ Low
Publication Bias	Undetected Strongly suspected (-1)	Only small studies included. No large studies available. Limited publication bias possible. Funnel plot is available.	⊕⊕⊕⊙ Very low
Other (upgrading factors, circle all that apply)	Large effect (+1 or +2) Dose response (+1 or +2) No plausible confounding (+1 or +2)	/	

4/ DIPLOPIA

GRADE criteria	Rating (circle one)	Footnotes (explain reasons for down- or upgrading)	Quality of the evidence (circle one)
OUTCOME: DIPLOPIA			
Study design	RCT (starts as high quality) Non-RCT (starts as low quality)	Non-RCT	
Risk of Bias (use the Cochrane Risk of Bias tables and figures)	No Serious (-1) Very serious (-2)	Plausible bias is unlikely to seriously alter the results.	⊕⊕⊕⊕ High
Inconsistency	No Serious (-1) Very serious (-2)	Large variability, considerable heterogeneity (98%).	⊕⊕⊕⊙ Moderate
Indirectness	No Serious (-1) Very serious (-2)	All findings apply to the review question.	
Imprecision	No Serious (-1) Very serious (-2)	Wide confidence interval includes 'no effect'.	⊕⊕⊙⊙ Low
Publication Bias	Undetected Strongly suspected (-1)	Limited publication bias possible. Funnel plot is available	⊕⊙⊙⊙
Other (upgrading factors, circle all that apply)	Large effect (+1 or +2) Dose response (+1 or +2) No plausible confounding (+1 or +2)	/	Very low

5/ VISUAL ACUITY

GRADE criteria	Rating (circle one)	Footnotes (explain reasons for down- or upgrading)	Quality of the evidence (circle one)
OUTCOME: VISUAL ACUITY			
Study design	RCT (starts as high quality) Non-RCT (starts as low quality)	Non-RCT	
Risk of Bias (use the Cochrane Risk of Bias tables and figures)	No Serious (-1) Very serious (-2)	Plausible bias is unlikely to seriously alter the results.	⊕⊕⊕⊕ High
Inconsistency	No Serious (-1) Very serious (-2)	Large variability, considerable het- erogeneity (91%).	⊕⊕⊕⊙ Moderate
Indirectness	No Serious (-1) Very serious (-2)	All findings apply to the review question.	
Imprecision	No Serious (-1) Very serious (-2)	Small number of total participants, wide confidence interval includes 'no effect'.	⊕⊕⊙⊙ Low
Publication Bias	Undetected Strongly suspected (-1)	Only small studies included. No large studies available. Limited publication bias possible. Funnel plot is available.	⊕⊙⊙⊙ Very low
Other (upgrading factors, circle all that apply)	Large effect (+1 or +2) Dose response (+1 or +2) No plausible confounding (+1 or +2)	/	

6/ COMPLICATIONS

GRADE criteria	Rating (circle one)	Footnotes (explain reasons for down- or upgrading)	Quality of the evidence (circle one)
COMPLICATIONS			
Study design	RCT (starts as high quality) Non-RCT (starts as low quality)	Non-RCT	
Risk of Bias (use the Cochrane Risk of Bias tables and figures)	No Serious (-1) Very serious (-2)	Plausible bias is unlikely to seriously alter the results.	⊕⊕⊕⊕ High
Inconsistency	No Serious (-1) Very serious (-2)	High degree of inconsistency in narrative data.	⊕⊕⊕⊙ Moderate
Indirectness	No Serious (-1) Very serious (-2)	All findings apply to the review question.	
Imprecision	No Serious (-1) Very serious (-2)	Inconsistent rapport of complications in narrative data.	⊕⊕⊙⊙ Low
Publication Bias	Undetected Strongly suspected (-1)	Narrative data, many small studies included. Funnel plot not possible.	⊕⊙⊙⊙
Other (upgrading factors, circle all that apply)	Large effect (+1 or +2) Dose response (+1 or +2) No plausible confounding (+1 or +2)	/	Very low

SUPPLEMENTARY TABLE D — TEMPORARY AND PERMANENT COMPLICATIONS (UNWEIGHTED PROPORTIONS) AFTER ORBITAL FAT DECOMPRESSION

	N studies	n/N patients (%)
Temporary Complication		
Bleeding	2 ^{25,28}	13/1407 (0.01)
Infection	1 ²⁸	12/1374 (0.01)
Sensory nerve damage	2 ^{5,25}	9/58 (15.5)
Conjunctivitis/ chemosis requiring therapy	1 ²⁸	46/1374 (3.3)
Total temporary complications	3 ^{5,25,28}	80/1432 (5.6)
Permanent Complication		
Sensory nerve damage	2 ^{25,28}	21/1407 (1.5)
Palpebral position disorder	2 ^{5,25}	13/58 (22.4)
Proptosis recurrence	3 ^{8,28,29}	46/2232 (2.0)
New onset presbyopia	1 ⁷	1/11 (9.0)
Loss of vision	8 ^{7,8,15,24,25,27,28,32}	0/2336
Other (CSF leak, hypoglobus, meningitis, sinusitis, scarification, lacrimal nerve damage)	NR	
Total permanent complications	9 ^{7,8,15,24,25,27-29,32}	81/2336 (3.5)
Overall complications	9 ^{7,8,15,24,25,27-29,32}	161/2336 (6.9)

Corresponding Author

Robin Willaert
Department of Oral and Maxillofacial Surgery
University Hospitals Leuven
Kapucijnenvoer 33, 3000 Leuven, Belgium
email: robin.willaert@icloud.com
telephone: +32 (0) 474 26 81 47

A Systematic Review on Volumetric Analysis in Orbital MRI

R. WILLAERT MD, DMD^{1,2} | M. DEGRAEVE MD³ | J. DEFERM MD, DMD⁴ | K. ORHAN DMD, MSc, PHD^{5,6}
I. MOMBAERTS MD, PHD⁷ | R. JACOBS DMD, MSc, PHD^{2,6,8} | N. BRUSSELAERS MD, PHD⁹

Abstract

Aim — Volumetric analysis of orbital soft tissues with magnetic resonance imaging (MRI) can contribute to the diagnostic pathway and understanding of the pathophysiological mechanism of orbital inflammation, trauma and tumors. It is not clear, however, which MRI method should be used for which condition. **Methods** — A systematic search was conducted in Pubmed/MEDLINE, Web of Science and Cochrane Library for all studies published before November 2019. The review was prospectively registered, compliant to the PRISMA guidelines and included extensive quality control. Primary outcomes were (i) MRI scanning characteristics (scan protocol and acquisition details), (ii) post-processing volumetry technique (software, segmentation methods and volume calculations), (iii) studied region of interest (ROI). Secondary outcomes consisted of (i) clinical relevance and indication for volumetric analysis and (ii) method of validation. **Results** — Of 2830 initial records, 27 articles were selected, of which 48% were published in the last 5 years. Large heterogeneity exists in MRI characteristics as well as post-processing technique. Technological advances drive an evolution towards more ‘dedicated’ volumetric methods according to the specific ROI and clinical indication. Volumetry of extraocular muscles and orbital fat is most common, but the ROI borders are variable. Sporadic studies report analysis of the globe, orbital cavity, optic nerve and lacrimal gland. Few studies include a proper validation such as phantom verification and observer variability of the proposed volumetry protocol. **Conclusions** — Proper understanding of all variables affecting the volumetric results is primordial for accurate interpretation of clinical and research outcome parameters. These study findings can contribute to a more solid translation of volumetric analysis. Increasing automatized volumetric techniques could provide more convenient and reliable ways of assessment.

Key Words

- Orbit
- Magnetic Resonance Imaging
- Computer-Assisted Image Processing
- Quantitative Evaluation

AFFILIATIONS

- 1 Department of Head and Neck Surgery, Ghent University Hospital, Ghent, Belgium
- 2 Department of Oral and Maxillofacial Surgery, University Hospitals Leuven, Leuven, Belgium
- 3 Faculty of Medicine and Health Sciences, Ghent University, Ghent, Belgium
- 4 Department of Oral and Maxillofacial Surgery, RadboudUMC, Nijmegen, the Netherlands
- 5 Department of Dentomaxillofacial Radiology, Faculty of Dentistry, Ankara University, Ankara, Turkey
- 6 OMFS IMPATH Research Group, Department of Imaging and Pathology, Faculty of Medicine, KU Leuven, Leuven, Belgium
- 7 Department of Ophthalmology, University Hospitals Leuven, Leuven, Belgium
- 8 Department of Dental Medicine, Karolinska Institutet, Stockholm, Sweden
- 9 Department of Microbiology, Tumour and Cell Biology, Karolinska Institutet, Stockholm, Sweden

This systematic review was preregistered at the PROSPERO database (CRD42019127698)

Introduction

Imaging studies like computed tomography (CT) and magnetic resonance imaging (MRI) are indispensable in the management of orbital mass lesions, inflammatory diseases, trauma and developmental disorders. MRI scanning of the orbit is commonly preferred to CT because the soft tissue resolution is much higher and any slice direction can be selected. In addition, the patient is not exposed to radiation^[1,2]. Conventional MRI protocols mainly provide morphological characteristics, which allow interpreting pathologic changes and describing the proper diagnosis. Developments in post-processing techniques, however, enhance the potential of MRI facilitating quantitative objectification such as signal intensity ratios, fractionated anisotropy, mean diffusivity, and volumetric analysis. Non-invasive assessment of anatomical and functional anomalies support the understanding and differentiation of orbital pathologies^[3]: to identify soft tissue inflammation of the retrobulbar tissue and the extraocular muscles^[4]; to measure the enlargement of the extraocular muscles in Graves' Orbitopathy^[6]; or to document orbital fat volume changes in patients with Graves' orbitopathy^[7]. Post-processing analysis often necessitates specific imaging software and acquisition protocols. These techniques are precise and reliable but also time-consuming and resource and labor intensive, hampering its routine clinical use. Although increasing evidence for the importance of post-processing, there is no current consensus on scanner performance, sequence acquisition, post-processing software, and unvalidated protocols are use^[8-10].

The aim of this paper is to review the current knowledge on MRI post-processing techniques in orbital volumetry. We describe the contemporary volumetry methods according to the intra-orbital structures of interest. Technical developments in MRI hardware, availability of software and time investment are being taken into account to make recommendations and suggest improvements for future research.

Materials and Methods

A systematic review of literature was performed, compliant to the Preferred Reporting Items for Systematic Reviews and Meta-Analysis recommendations (PRISMA). The study protocol was prospectively registered at the international database of PROSPERO (CRD42019127698).

Primary outcomes were (i) MRI scanning characteristics (hardware, scan protocol and acquisition details), (ii) post-processing volumetry technique (software, segmentation methods and volume calculations), and (iii) studied regions of interest (ROI) (extraocular muscles, orbital fat, globe, optic nerve, orbital cavity and lacrimal gland). Secondary outcomes consisted of (i) clinical relevance and indication for volumetric analysis and (ii) method of validation for the proposed post-processing volumetry technique.

Studies were eligible if they were original papers written in English, German, Dutch or French, published before November 2019, describing at least one intra-orbital ROI by quantitative volumetric assessment. Studies were included if primary outcomes were reported. Non-interventional publications, including editorials, commentaries, review arti-

cles and those not subject to peer review were excluded. The Pubmed/MEDLINE, Cochrane Library and Web of Science databases were searched for a combination of subject headings, in which a first term denominates 'Orbit'; associated to a second and third term denominating 'MRI' and 'post-processing'. No additional date or publication limits were applied. The references of the included articles and the Web of Science citation index were cross-checked to identify additional eligible articles. The complete search strategy can be found in Supplement A.

Data collection

One author (RW) performed a first screening on title to remove all clearly irrelevant articles. Two authors (RW, MD) independently conducted selection on title and abstract, followed by full-text critical appraisal, applying the selection criteria to determine eligibility and final in- or exclusion. In the event of duplicate publications, companion papers or an overlap between studies regarding the same patient population, only the most recent and complete study was included. Disagreements among reviewers were settled by additional discussions and by consulting a third reviewer (JD or KO) if necessary. Two reviewers (RW, MD) extracted data independently using standardized lists according to the Cochrane Collaboration guidelines^[11].

Research design, study period, demographic data (number of subjects and amount of orbits, study location) and interventional data (ROI, MRI hardware, imaging protocol, acquisition details, segmentation method and volume calculation) were recorded.

Quality assessment

The quality of the articles were critically appraised by two authors (RW, MD) independently using the Methodological Index for Non-Randomized Studies (MINORS) criteria to assess non-Randomized clinical trials^[12].

Results Included articles

The search resulted in 27 English articles for qualitative analysis (Figure 3.1 - PRISMA flow Chart). The study designs and population characteristics are described in Table 3.1. The earliest included article was published in 2000, whereas 48% of articles were published in the last 5 years.

Quality analysis and risk of bias

All articles reported the objectives, endpoints and inclusion criteria, but did not prospectively calculate the study size. Eighteen studies were based on unvalidated measurement methods using new scanning protocols, software or segmentation techniques. Therefore, there could be a high risk for bias in the assessment of study endpoints. (Supplement B). Eighteen studies used comparative analysis with control groups.

MRI scanning characteristics

From 2002 the images for orbital volumetry were obtained with a 1.5T MRI scanner instead of the 1.0T. From 2014 the 3T MRI scanner was used in six articles (Table 3.2-4). All but one study^[13] reported the use of additional radiofrequency coils, head coil or surface loop coils, to improve signal-to-noise ratio. Two studies com-

bined both a head coil and surface loop coil^[14,15]. The surface loop coil is a simple, receive-only loop wire, positioned over the ROI and commonly used for small body parts. The head coil can have a variable amount of channels from 1 to 64, to enhance signal sensitivity and parallel imaging, hence reducing acquisition time^[16].

All studies provided a detailed acquisition protocol including information about repetition time (RT), echo time (ET), matrix and field-of-view. The scan time ranged from 2.5 to 18.0 minute^[17-18]. Slice thickness varied from 0.5-4.0 mm and most studies used continuous slices with no or only minimal (0.1/0.3mm) interslice gap. Reported voxel dimensions varied from 0.13 to 3.00 mm³. Five studies reported the use of isotropic voxel dimensions^[6,9,19-21].

Fourteen studies reported to control for gaze during the scanning process. Gaze control could be achieved by the use of a fixation target at the inside of the gantry, by instructing the patient to keep eyes in central gaze or close the eyes and maintain still in primary position.

Post-processing technique

Tissue segmentation involves the process of outlining the ROI on the scan images. The included articles report a myriad of different software programs for manual or semi-automatic segmentation of the orbital tissues (Table 3.6-7). Three research groups operated with in-house developed software^[13,19,22] and twenty-one (77 %) used commercially or freely available post-processing software. One research group described the use of an overhead projector instead of computer software^[23-24].

Half of the included articles describe the use of a semi-automatic segmentation process combining multi-dimensional threshold (MDT) or region growing (RG) techniques with manual adjustments. To assess the actual volume of the segmented ROI, 63% of the articles (17/27) describe a volumetric calculation by multiplying the sum of the ROI cross-sectional areas by the image plane thickness^[25]. Other articles performed volumetric analysis by multiplying the number of pixels by the voxel dimensions (6 studies) or used post-processing software to deduct the volume automatically.

Extraocular muscles

The EOM were the most analysed ROI, in 70% of the studies (19/27). Evaluations of the EOM volume are reported in the diagnosis and follow-up of inflammatory orbital diseases (e.g. Graves' orbitopathy), for evaluation of limited eye motility and to study the changes in tissue morphology during eye movement/muscle contraction.

T1 as well as T2 weighted sequences, both contrast-enhanced and non-enhanced, were used to measure muscles volumes (Table 3.2). Other less frequently used sequences included proton density weighted (PDw)^[9], Magnetisation Prepared - Rapid Acquisition Gradient Echo (MPRAGE)^[19] and Cube-Fast Spin Echo (FSE) flex^[20]. The orientation of the muscle axis was the main factor to select the optimal scanning plane. Axial, sagittal, coronal and 'quasi-coronal' (= perpendicular to the long axis of each orbit/optic nerve) scanning planes are proposed to segment the particular EOM (Table 3.2). The volume can be evaluated for each muscle separately or all muscles together as a single volume (Table 3.5). Most au-

thors suggest calculating the EOM volume separately, although in 10 studies the levator palpebrae and the superior rectus were assessed together as the superior rectus-levator complex. The inferior oblique muscle is often discarded, as this muscle is the smallest and has an oblique orientation in all sections, which makes it difficult to accurately delineate. Eight studies analyse the partial muscle volume only including the muscle belly not the tendinous parts. Two studies assessed the total muscle volume of one orbit by subtracting the other orbital tissues (globe,

lacrimal gland, optic nerve and orbital fat) from the entire orbital volume^[20,26].

The most used techniques (in 12/19 studies) for outlining the muscles was manual segmentation (Table 3.6). If a semi-automatic segmentation method was applied, it mostly involved an MDT method with manual adjustments on each slide. The duration for muscle segmentation and volume calculation was reported 4 to 7 min with the semi-automatic techniques, compared to 20 min with the manual technique^[19].

FIGURE 3.1 — PRISMA FLOW DIAGRAM

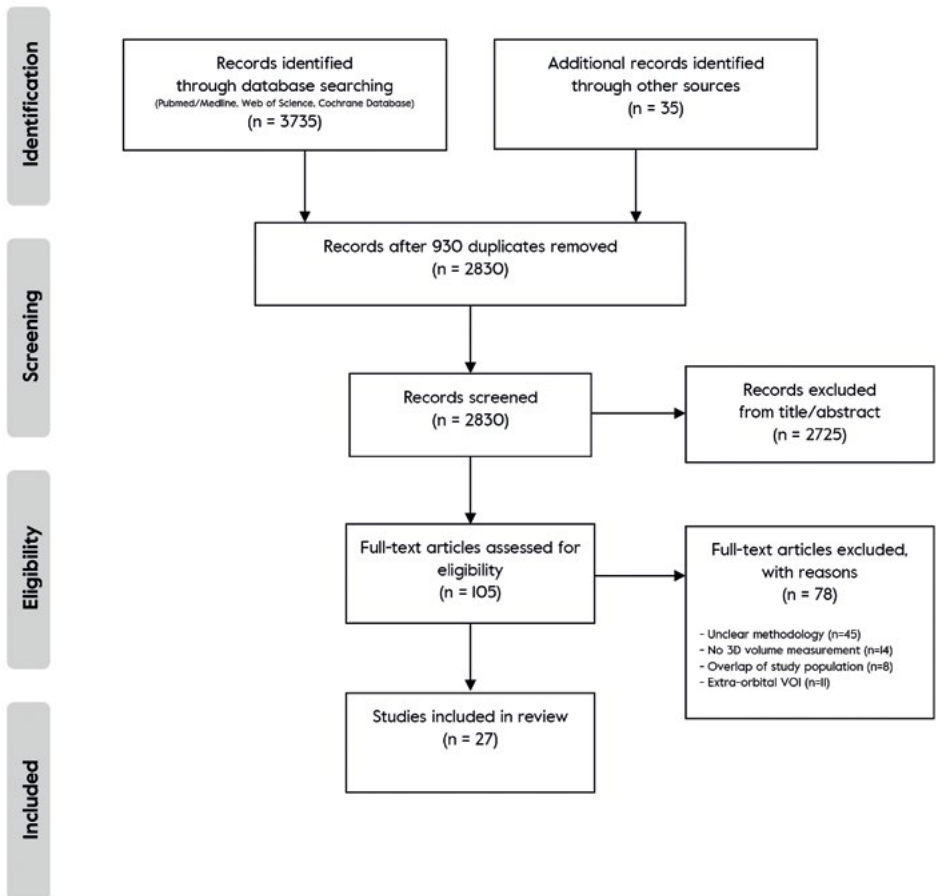


TABLE 3.1 — CHARACTERISTICS OF INCLUDED STUDIES

AUTHOR, DATE	STUDY TYPE/ DESIGN	ROI	PARTICIPANTS	STUDY LOCA- TION	STUDY GOAL
Firbank et al., 2000	Retrospective Case-control Method validation	EOM	26 (incl. 19 controls)	Europe	Define errors in EOM volumetry in GO
Firbank et al., 2001	Retrospective Case-control Method validation	EOM	6 (incl. 1 control)	Europe	Introduce new technique for EOM volumetry
Nishida et al., 2001	Retrospective Case-control	EOM Orbital fat	14 (incl. 8 controls)	Europe	Evaluate EOM and orbital fat volume changes in GO
Nishida et al., 2002	Retrospective Case-control	EOM Fat Orbital cavity	23 (incl. 13 controls)	Europe	Correlate exophthalmos with EOM and fat volume
Szucs-Farkas et al., 2002	Retrospective Case-control Method Validation	EOM	55 (incl. 20 controls)	Europe	Identify the optimal EOM parameter to monitor treatment response in GO
Ortube et al., 2006	Prospective Case-control	EOM	46 (incl. 10 controls)	North America	Evaluate volume changes in EOM palsy
Lennerstrand et al., 2007	Retrospective Case-control	EOM	50 (incl. 18 controls)	Europe	Evaluate EOM volume in GO
Majos et al., 2007 (part I)	Retrospective Cohort	EOM	45	Europe	Introduce new technique for EOM volumetry
Majos et al., 2007 (part II)	Retrospective Cohort	Orbital fat Eye globe	45	Europe	Introduce new technique for orbital fat and eye globe volumetry
Kolk et al., 2008	Prospective Cohort Method validation	EOM Orbital fat Eye globe Orbital cavity	37	Europe	Volumetric changes after orbital trauma
Clark et al., 2011	Prospective Case-control	EOM	48 (incl. 36 controls)	North America	Evaluate volume changes in EOM palsy
Clark et al., 2012	Retrospective Cohort	EOM	15	North America	Correlate EOM volume to muscle contractility in healthy participants
Comerci et al., 2013	Retrospective Case-control Method validation	Orbital fat	24 (incl. 12 controls)	Europe	Introduce new technique for orbital fat volumetry in GO
Stojanov et al., 2013	Prospective Case-control	Orbital fat	100 (incl. 50 controls)	Europe	Correlate orbital fat volume and intra-ocular pressure to obesity
Buch et al., 2014	Retrospective Case-control	Lacrimal gland	25 (incl. 12 controls)	North America	Evaluate lacrimal gland volume in SCD
Hoffmann et al., 2014	Retrospective Case-control Method validation	Optic nerve	46 (incl. 23 controls)	Europe	Evaluate optic nerve volume in ICH
Schmutz et al., 2014	Prospective Cohort Method validation	Orbital cavity	11	Australia	Compare MRI-based orbital 3D model to CT-based model in orbital trauma
Loba et al., 2015	Retrospective Cohort Method validation	EOM	10	Europe	Define normal EOM values for different gaze positions in healthy participants

Volumetry in orbital MRI

AUTHOR, DATE	STUDY TYPE/ DESIGN	ROI	PARTICIPANTS	STUDY LOCA- TION	STUDY GOAL
Shin et al., 2015	Prospective Case-control	EOM	74 (incl. 12 controls)	North America	Evaluate volume changes in EOM palsy
Clark et al., 2016	Retrospective Cohort	EOM	15	North America	Correlate EOM volume to muscle contractility in healthy participants
Higashiyama et al., 2016	Retrospective Cohort	EOM	25	Asia	Evaluate EOM volume to monitor treatment response in GO
Hu et al., 2016	Retrospective Case-control	Lacrimal gland	57 (incl. 24 controls)	Asia	Evaluate lacrimal gland volume in GO
Kaichi et al., 2016	Prospective Case-control Method validation	Orbital fat	39 (incl. 30 controls)	Asia	Evaluate orbital fat volume in GO
Suh et al., 2016	Prospective Case-control	EOM	38 (incl. 19 controls)	North America	Evaluate volume changes in EOM palsy
Higashiyama et al., 2018	Prospective Cohort	EOM Orbital fat Eye globe Optic nerve	9	Asia	Evaluate EOM and orbital fat volume to monitor treatment response in GO
Shen et al., 2018	Retrospective Case-control Method validation	EOM Orbital fat	20 (incl. 10 controls)	Asia	Introduce new technique for EOM and orbital fat volumetry
Tang et al., 2018	Retrospective Case-control Method validation	EOM Orbital fat Eye globe Optic nerve Lacrimal gland	30 (incl. 15 controls)	Asia	Evaluate volumetry accuracy with different segmentation techniques

ROI: region of interest

ICH: idiopathic intracranial hypertension

SCD: Sickle cell disease

TABLE 3.2 — SCAN PROTOCOLS FOR EOM VOLUMETRY

Author, date	MRI hardware	Coil	Sequence	Plane	Slice thickness (mm)	Inter-slice gap (mm)	Scan time (min:sec)	Voxel dimensions (mm ³)
Firbank et al., 2000	I.0T, Siemens	Head coil	T1w 2D SE	Coronal	3	0.3	NR	Anisotropic; 2.43
Firbank et al., 2001	I.0T, Siemens	Head coil	3D MPRAGE	Coronal	1	0	8	Isotropic; 1.00
Nishida et al., 2001	1.5T, Siemens	Surface coil	T1w SE	Quasi-coronal	2	0	4-5	Anisotropic; 0.50
Nishida et al., 2002	1.5T, Siemens	Surface coil	T1w	Coronal+ Axial+ Sagittal	2 or 3	0	NR	NR
Szucs-Farkas et al., 2002	I.0T, Shimadzu	Head coil	T1w SE	Axial	3	0	NR	NR
Ortube et al., 2006	1.5T, GE	Surface coil	T1w	Quasi-coronal	2	0	NR	NR
Lennerstrand et al., 2007	1.5T, GE	Head coil	T1w SE	Coronal	2	0	NR	Isotropic; 0.92
Majos et al., 2007 (part I)	1.5T, Siemens	Head coil	T1w SE	Coronal + Axial	3	0.1	9:24	Anisotropic; 3.00
Kolk et al., 2008	1.5T, Philips	Head coil + Surface coil	PDw/ T2w	Coronal+ Axial+ Sagittal	1	0	6:15	Isotropic; 1.00
Clark et al., 2011	1.5T, GE	Surface coil	T1w/ T2w FSE	Quasi-coronal	2	0	NR	Anisotropic
Clark et al., 2012	1.5T, GE	Surface coil	T2w FSE	Quasi-coronal	2	0	NR	Anisotropic
Loba et al., 2015	1.5T, Siemens	Head coil	T2w	Quasi-coronal	2	0	1:18	NR
Shin et al., 2015	1.5T, GE	Surface coil	T1w/T2w FSE	Quasi-coronal	2	0	NR	Anisotropic
Clark et al., 2016	1.5T, GE	Surface coil	T2w FSE	Quasi-coronal	2	0	NR	NR
Higashiyama et al., 2016	3.0T, Philips	Head coil	T2w SE	Axial+ Sagittal	2.5	NR	NR	NR
Suh et al., 2016	1.5T, GE	Surface coil	T1w/ T2w FSE	Quasi-coronal	2	0	NR	Anisotropic
Higashiyama et al., 2018	3.0T, GE	Head coil	T2w SE	Coronal+ Axial+ Sagittal	1.5	NR	NR	NR
Shen et al., 2018	1.5T, Philips	Head coil	T1w 3D FFE	NR	0.8	0	NR	NR
Tang et al., 2018	3.0T, GE	Head coil	Cube FSE flex	Axial	0.5	0	5:59	Isotropic; 0.13

NR: Not reported; GE: General Electric; 2D: two-dimensional; (F)(T)(C)SE: (fast)(turbo)(conventional)spin echo; FFE: fast field echo; MPRAGE: Magnetisation Prepared - Rapid Acquisition Gradient Echo; FS : fat suppression; PD : proton density

TABLE 3.3 — SCAN PROTOCOLS FOR ORBITAL FAT VOLUMETRY

Author, date	MRI hardware	Coil	Sequence	Plane	Slice thickness (mm)	Inter-slice gap (mm)	Scan time (min:sec)	Voxel dimensions (mm ³)
Nishida et al., 2001	1.5T, Siemens	Surface coil	T1w SE	Coronal	2	0	4-5	Anisotropic; 0.50
Nishida et al., 2002	1.5T, Siemens	Surface coil	T1w	Axial	2 or 3	0	NR	NR
Majos et al., 2007 (part II)	1.5T, Siemens	Head coil	T1w SE	Coronal + Axial	3	0.1	9:24	Anisotropic; 3.00
Kolk et al., 2008	1.5T, Philips	Head coil + Surface coil	PDw/ T2w	Coronal+ Axial+ Sagittal	1	0	6:15	Isotropic; 1.00
Comerci et al., 2013	1.5T, Philips	NR	T1w CSE/ T2w/ PDw CSE	Axial	4	4	NR	NR
Stojanov et al., 2013	1.5T, Siemens	Head coil	FLAIR	Axial	0.5	NR	18	NR
Kaichi et al., 2016	3.0T, GE	Head coil	T2w FSE IDEAL	Axial	2	0	2:42	NR
Higashiyama et al., 2018	3.0T, GE	Head coil	T2w SE	Axial	1.5	NR	NR	NR
Shen et al., 2018	1.5T, Philips	Head coil	T1w 3D FFE	NR	0.8	0	NR	NR
Tang et al., 2018	3.0T, GE	Head coil	Cube FSE flex	Axial	0.5	0	5:59	Isotropic; 0.13

NR: Not reported; GE: General Electric; 2D: two-dimensional; (F)(T)(C)SE: (fast)(turbo)(conventional)spin echo; FFE: fast field echo; MPRAGE: Magnetisation Prepared - Rapid Acquisition Gradient Echo; FLAIR : fluid attenuated inversion recovery; FS : fat suppression; PD : proton density; IDEAL: iterative decomposition of water and fat with echo asymmetry and least-squares estimation

Seven articles included validation of the volumetry method, either by using a model (computer simulation or anatomical), variability testing or comparison with other imaging techniques. Semi-automatic techniques are reported to be sufficiently accurate in a phantom controlled comparison^[20,26], matching manual segmentation^[19,20] but are faster and more practical in use.

Orbital fat

The orbital fat tissue is the largest component in the orbit, divided in extraconal and intraconal components. The volume of orbital fat is the second most analysed ROI, to study the etiopathology and treatment in exophthalmos/changes of globe position, in Graves' orbitopathy and after maxillofacial trauma (Table 3.1). Regular T1, T2 and proton density (PD) weighted sequences are reported for determining the orbital fat volume (Table 3.3). Others suggest more specific sequences: CUBE

TABLE 3.4 — SCAN PROTOCOLS FOR EYE GLOBE, OPTIC NERVE, ORBITAL CAVITY AND LACRIMAL GLAND VOLUMETRY

Author, date	ROI	MRI hardware	Coil	Sequence	Plane	Slice thickness (mm)	Inter-slice gap (mm)	Scan time (min:sec)	Voxel dimensions (mm ³)
Nishida et al., 2002	Orbital cavity	1.5T, Siemens	Surface coil	T1w	Axial	2 or 3	0	NR	NR
Majos et al., 2007 (part II)	Eye globe	1.5T, Siemens	Head coil	T1w SE	Coronal+ Axial	3	0.1	9:24	Anisotropic; 3.00
Kolk et al., 2008	Eye globe Optic nerve Orbital cavity	1.5T, Philips	Head coil + Surface coil	PDw/T2w	Coronal+ Axial+ Sagittal	1	0	6:15	Isotropic; 1
Hoffmann et al., 2014	Optic nerve	1.5T, Siemens	Head coil+ Surface coil	T2w TSE	Coronal	2	0	7:20	Anisotropic
Schmutz et al., 2014	Orbital cavity	3.0T, Siemens	Head coil	T1w	NR	0.5	0	5:00	Isotropic; 0.13
Buch et al., 2014	Lacrimal gland	1.5T, Philips	Head coil	T1w/T2w mixed TSE	Axial	3	0	9:50	Anisotropic; 2.65
Hu et al., 2016	Lacrimal gland	3.0T, Siemens	Head coil	T2w FS	Coronal+ Axial	3	0	NR	Anisotropic
Higashiyama et al., 2018	Eye globe Optic nerve	3.0T, GE	Head coil	T2w SE	Axial	1.5	NR	NR	NR
Tang et al., 2018	Eye globe- Optic nerve Orbital cavity Lacrimal gland	3.0T, GE	Head coil	Cube FSE flex	Axial	0.5	0	5:59	Isotropic; 0.13

NR: ROI: Region of interest; NR: Not reported; GE: General Electric; 2D: two-dimensional; (F)(T)(C)SE: (fast)(turbo)(conventional)spin echo; FFE: fast field echo; MPRAGE: Magnetisation Prepared - Rapid Acquisition Gradient Echo; FLAIR : fluid attenuated inversion recovery; FS : fat suppression; PD : proton density; IDEAL: iterative decomposition of water and fat with echo asymmetry and least-squares estimationdensity

FSE flex, Fluid-attenuated inversion recovery (FLAIR) or a T2w FSE Iterative Decomposition of water and fat with Echo Asymmetry and Least-squares estimation) (IDEAL).

All studies calculated the entire orbital fat volume. One study on exophthalmos measurement in Graves' orbitopathy separately evaluated the anterior orbital fat tissue, which is the amount of fat outside the bony orbital cavity^[23]. The orbital fat volume could be assessed by manual or semi-automatic segmentation. Shen et al. combined two semi-automatic segmentation methods by first performing a MDT selection which could be manually adjusted by a RG segmentation^[26]. This method enabled the distinction between fat tissue and orbital blood vessels. Higashiyama et al. and Ohji et al. included the lacrimal gland, vessels and connective tissue in the fat volume^[10]. Another option is segmenting all except the orbital fat tissue (EOM, globe, lacrimal gland and optic nerve) and subtracting these structures

from the whole orbital volume (Table 3.5). Semi-automatic segmentation of the orbital fat is reported to take between 5 to 15 min. Five studies validated the method for fat volumetry by testing the operator variability or studying the accuracy by comparing with a (virtual) phantom model. All studies reported a sufficient reliability of the proposed volumetric method.

Globe

The normal shape of the globe or eyeball is a nearly round sphere with an anteriorly convex bulge, although certain conditions can shorten or elongate the sphere.

To study the relation of the globe volume with exophthalmos Majos and co-authors outlined the outer contour of the globe on T1w images with a semi-automatic, MDT segmentation procedure^[27]. Other studies assessed the globe volume as a part of more extensive post-processing analysis: to evaluate volumetry accuracy with different segmentation

TABLE 3.5 — VARIATION IN ROI SEGMENTATION BOUNDARIES

ROI		N studies	
EOM	Separate muscle segmentation	Complete muscle volume (belly+tendon)	7
		Partial muscle volume	8
		Not reported	10
	All EOM together through subtraction method		2
	Distinct muscle variations	Inferior oblique muscle excluded	5
		Superior and inferior muscle excluded	8
		Levator palpebrae muscle included	10
< 3 muscles evaluated		2	
Orbital fat	Exclusive fat tissue segmentation	7	
	Fat volume through subtraction method	3	
	Lacrimal gland included in fat volume	4	

TABLE 3.6 — POST-PROCESSING DETAILS FOR MANUAL SEGMENTATION

Author, date	Post-processing software	Volumetric analysis	Method validation
Nishida et al., 2001	ROI outlined with overhead projector. Cross-sectional area calculation with software.	Summation of area method.	NR
Nishida et al., 2002	ROI outlined with overhead projector. Cross-sectional area calculation with software.	Summation of area method.	NR
Szucs-Farkas et al., 2002	Software (NOS) specially developed for post-processing on MRI.	Summation of area method.	Variability testing
Ortube et al., 2006	ImageJ (W.Rasband, National institutes of health, Bethesda, Maryland)-freeware.	Summation of area method.	NR
Lennerstrand et al., 2007	Measuring tools of workstation (Advantage Windows ®).	Summation of area method.	NR
Clark et al., 2011	Image J (W.Rasband, National institutes of health, Bethesda, Maryland)- freeware.	Summation of area method.	NR
Clark et al., 2012	Image J (W.Rasband, National institutes of health, Bethesda, Maryland)-freeware. Matlab (The Mathworks Inc., Natick, MA, USA).	Summation of area method.	NR
Buch et al., 2014	3D slicer (version 2.6, http://www.slicer.org)-freeware.	Multiplying number of pixels by the corresponding voxel volumes.	NR
Shin et al., 2015	ImageJ (W.Rasband, National institutes of health, Bethesda, Maryland)-freeware.	Summation of area method.	NR
Clark et al., 2016	ImageJ (W.Rasband, National institutes of health, Bethesda, Maryland)-freeware.	Summation of area method.	NR
Higashiyama et al., 2016	ImageJ (W.Rasband, National institutes of health, Bethesda, Maryland)-freeware.	Summation of area method.	NR
Hu et al., 2016	NR	Summation of area method.	Variability testing
Suh et al., 2016	Adobe Photoshop (Adobe Systems Inc., San Jose, CA, USA). Image J (W.Rasband, National institutes of health, Bethesda, Maryland)-freeware. Matlab (The Mathworks Inc., Natick, MA, USA).	Summation of area method.	NR
Higashiyama et al., 2018	ImageJ (W.Rasband, National institutes of health, Bethesda, Maryland)	Summation of area method.	NR

Summation of area method= multiply the 2D segmented area by the value of the slice thickness and sum all slices of the ROI.
NR: Not reported. ROI: Region of interest. NOS: Not otherwise specified.

TABLE 3.7 — POST-PROCESSING DETAILS FOR SEMI-AUTOMATIC SEGMENTATION

Author, date	Post-processing software	Volumetric analysis	Method validation	Comments
Firbank et al., 2000	SunSparc (Sun Microsystems, California, USA) and Displmage package by David Plummer (University College London, UK).	Multiplying number of pixels by the corresponding voxel volumes.	Virtual phantom validation + Variability testing	
Firbank et al., 2001	Software written in Java (Sun Microsystems, California, USA).	Multiplying number of pixels by the corresponding voxel volumes.	Virtual phantom validation+ Variability testing	Mean processing time: 70 min. (vs. manual: 20min)
Majos et al., 2007 (part I)	ITK library (the Insight Software Consortium, The Insight Toolkit; http://www.itk.org)-freeware.	Multiplying number of voxels by the corresponding voxel volumes.	NR	Mean processing time: 4 min.
Majos et al., 2007 (part II)	ITK library (the Insight Software Consortium, The Insight Toolkit; http://www.itk.org)-freeware.	Multiplying number of voxels by the corresponding voxel volumes.	NR	Mean processing time: 5 min.
Kolk et al., 2008	Easy Vision 4.3 (Philips, Best, the Netherlands) In-house developed software, NOS.	NR	Variability testing+ Comparison with CT	
Comerci et al., 2013	In-house developed software, NOS.	Automatic calculation by software.	Virtual phantom validation + Variability testing	Processing time: 10 to 15 min.
Stojanov et al., 2013	Adobe Photoshop (Adobe Systems Inc., San Jose, CA).	Multiplying number of voxels by the corresponding voxel volumes.	NR	
Hoffmann et al., 2014	Amira (ThermoFisher Scientific, Massachusetts, USA).	NR	Variability testing	Mean processing time < 10min.
Schmutz et al., 2014	Amira (ThermoFisher Scientific, Massachusetts, USA) RapidForm 2006 (Inus technology, Seoul, Korea).	Automatic calculation by software.	Comparison with CT	Mean processing time: 4h with MRI vs. 1h with CT
Loba et al., 2015	ImageJ (W.Rasband, National institutes of health, Bethesda, Maryland).	Summation of area method.	NR	
Kaichi et al., 2016	Virtual Place Raijin (AZE Ltd, Tokyo, Japan).	Automatic calculation by software.	Variability testing	
Shen et al., 2018	Mimics v15.0 (Materialise, Leuven, Belgium).	Automatic calculation by software.	Phantom validation	
Tang et al., 2018	ANALYZE, GE HDAA v. 4.4 workstation (GE Healthcare).	NR	Phantom validation	

Summation of area method= multiply the 2D segmented area by the value of the slice thickness and sum all slices of the ROI.
NR: Not reported. ROI: Region of interest. NOS: Not otherwise specified.

techniques or for the purpose of subtraction. Tang et al. used water images of a Cube FSE flex sequence to manually trace the globe outer borders ^[20] (Table 3.4). Kolk et al. used T2w as well as PDw sequences to semi-automatically (MDT) measure the vitreous body, thus assessing the inner border of the globe ^[9]. They report similar measurement results for both sequences with consistent inter-preter reliability.

Optic nerve

The optic nerve is a cylindrical structure that extends from the globe to the middle cranial fossa, with an intraocular, intraorbital, intracanalicular and intracranial part. Hoffmann et al. measured the volume of the optic nerve sheath and that of the optic nerve in patients with idiopathic intracranial hypertension ^[14]. A coronal T2w sequence was obtained with a combination of a head and surface coil (Table 3.4). The optic nerve was outlined with a semi-automatic segmentation procedure and the inter-observer agreement was excellent for both the optic nerve and the optic nerve sheath volumetry. Two studies performed optic nerve volumetry as a part of subtracting procedure to analyse other ROI's, obtained through more specific sequences like PDw ^[9] and CUBE FSE flex ^[20]. Both studies used a manual outlining of the optic nerve without specifications regarding the nerve sheath.

Orbital cavity volume

The orbital cavity is a conical structure with thin walls perforated by foramina and fissures. The base entry lacks an osseous border and is outlined by a solid, curvilinear orbital margin ^[28].

Schmutz et al. compared orbital cavity segmentation on MRI with the conventional 3D bone reconstruction on CT to generate a 3D orbital cavity bony model ^[21]. They obtained T1w, isotropic MRI images with a standard head coil and defined the outer borders with a semi-automatic threshold-based segmentation procedure and manual adjustments (Table 3.4). It took 4 hours to perform the procedure on MRI compared to 1 hour with the CT-based analysis. Nishida et al., Kolk et al. and Tang et al. report a complete manual outlining of the orbital cavity by using a T1w, PDw and Cube FSE-Flex sequence ^[9,20,23]. Accuracy and procedural time was not specified.

Lacrimal gland

The lacrimal gland is located in the superior lateral portion of the orbit and is divided in a palpebral lobe and an orbital lobe. There are three papers on volumetric analysis of the lacrimal gland, including patients with Graves' orbitopathy ^[30] or sickle cell disease ^[29]. The lacrimal glands were studied with T2w, a T2w mixed turbo spin echo (TSE) sequence or the water images of a Cube FSE flex (Table 3.4), all performed in the axial plane. None of the studies used isotropic voxels. The lacrimal gland lobes were always outlined as a whole entity by manual, and not threshold-based segmentation because of its inhomogeneous intensity ^[30]. Inter-observer agreement was reported to be moderate-to-good ^[30].

Discussion

The current report provides a comprehensive overview of the recent literature on MRI-based orbital volumetry. It illustrates the historical trends and innovations of the MRI

hardware and acquisition protocols. This review illustrates that orbital muscle and fat volumetry is regularly performed for clinically relevant indications as inflammatory orbital diseases or functional problems with extraocular muscles. On the other hand volumetric studies of the lacrimal gland, globe and optic nerve are only sporadically reported and care should be taken to interpret these results.

Post-processing analysis of radiological data is gaining importance in all fields of medicine ^[31]. Objective analysis is necessary to allow definition and comparison of normalized volumetric data. While morphometry on 2-dimensional images is the simplest, the 3D volume is considered to be more accurate ^[6,27,31]. This review confirms a common evolution towards more powerful MRI devices, higher magnetic fields and the use of additional coils, which could enhance image quality. Surface coils can yield orbital images with high spatial resolution, but the signal strength decreases as the distance from the coil increases ^[18,32]. Likewise, images obtained with head coils produce a high signal-to-noise ratio allowing accurate measurements. This review illustrates a heterogeneous use of additional coils. It is not possible to determine which coil technique is superior for orbital volumetry and to what extent they influence the volumetric results. It is expected that future improvements in MRI coil technology, like the 64-channel head coil, and the introduction of increased magnetic fields with shorter echo-times will inherently affect the imaging quality hence improve measurement accuracy ^[33,34]. It would be valuable if details about additional coils were always provided in future studies to elucidate the possible advantages of these devices.

The image sequence is another component affecting volumetric measurements, as a sharp tissue contrast will improve segmentation accuracy. The included articles report a multitude of sequence protocols varying according to the ROI and the applied segmentation technique. Where some authors are able to use a single regular sequence (T1w or T2w) to analyse multiple ROI, others apply a dedicated protocol to enhance the tissue contrast facilitating the segmentation process of only one specific ROI. As studies report diverse MRI hardware vendors (GE Healthcare, Siemens, Philips, etc.), it should be pointed out that vendors can use different names for similar sequences, for example SPACE can be called CUBE (GE Healthcare, Milwaukee, Wisconsin) or VISTA (Philips Healthcare, Best, the Netherlands). Likewise, vendors can use the same name for a scanning sequence, but acquisition parameters could differ, resulting in significant deviations of the measurement results ^[18]. For this reason, care should be taken when comparing results obtained with different devices and it seems advisable to obtain consecutive scans of one patient always with the same device and scanning protocol.

Aside from the image sequence, other scanning variables could be of interest (Table 3.8). First, while most articles use anisotropic voxels, some authors suggest a 3D isotropic protocol to be more appropriate for the volumetric measurement of orbital soft tissue. Isotropic voxels allow for image reconstruction in any plane depending on the orientation of the ROI leading to more precise measurements ^[35]. Second, the additional value for the use of contrast-enhanced images is questioned. Previous studies reported that non-en-

hanced and contrast-enhanced sequences are both suitable for quantitative imaging [31,36]. However, avoiding the toxicity and cost of intravenous contrast could be an important argument for using non-enhanced images. Finally, Gaze fixation is another relevant feature during MRI scanning of the orbits. A change in globe position will alter muscle positions and volumes also changing morphology of all adjacent tissue [31]. Furthermore, the eye movements could affect image resolution and introduce measurement errors [19,31]. A limited acquisition time is one of the most important factors to avoid motion artifacts, yet advanced sequences and an increased number of sequential sequences will lengthen the scanning protocol considerably. Instructing the patient to keep the eyes gently closed – but not forced to avoid Bell's phenomenon, during scanning and limit the scanning time could reduce these artifacts. Additionally, the consistent use of fixation targets can exclude eye motion and also eliminate differences in eye position between consecutive scans.

Segmentation is an important step during volumetric analysis. This process will allow for grouping the pixels and defining the ROI boundaries, which can be accomplished by a variety of methods [37]. Manual segmentation requires the operator to trace ROIs on each consecutive section. Due to irregular morphology of orbital tissues, the manual segmentation is time-consuming and associated with high inter-operator variation [19,20]. To address these issues, semi-automated segmentation algorithms such as MDT and RG are commonly reported. With RG a seed is set in the ROI to define the reference tissue intensity, which is used by the software

to cover the whole ROI. MDT segmentation software requires a visual threshold range solely containing the target tissue to segment the ROI. These semi-automatic segmentation techniques, with MDT probably superior to RG, proved to be more convenient and at least as accurate as manual segmentation [20]. This review illustrates that orbital tissue segmentation is still challenging and time-consuming due to anatomical complexity. Currently, the manual segmentation is often reported, as the application of more advanced segmentation techniques also depends on available software, use of dedicated scanning protocols and operator expertise. More advanced imaging protocols and future developments in segmentation could lead to more automated techniques, artificial intelligence and deep learning-based approaches, which could perform high quality segmentation of orbital tissue with a short processing time [14,38]. Following segmentation, different techniques are suggested to calculate the actual ROI volume. The most popular technique is a 'summation of area' method, where the surface of each cross-section is multiplied by the slice thickness [25]. This method will inherently introduce bias because the measurement of a cross-sectional area is overestimated if the imaging plane is not perpendicular to the length axis of the ROI [6]. The drawbacks can be solved if software is used that automatically calculates the ROI volume after segmentation. This option is more practical, avoids bias and is probably more suitable for volumetric analysis.

There is currently no consensus on how to measure the muscle volume. The segmentation of a partial muscle volume will exclude all images where the muscle/

TABLE 3.8 — PITFALLS AND RECOMMENDATIONS FOR ORBITAL VOLUMETRY

		Pitfalls	Recommendation
MRI scanning characteristics	Sequence/ scanning plane	Choice of sequence may affect the ROI contrast, the segmentation procedure and the volumetric outcome.	<ul style="list-style-type: none"> - Use sequence with highest ROI contrast to enhance segmentation - Limit duration of scanning protocol. - Choose scanning plane in function of ROI - Use same MRI hardware and sequence for consecutive scanning
	Coil	Additional coils may influence image resolution and measurement accuracy	Head coil may be preferred to visualize apex and to improve procedure standardisation
	Gaze during scanning	Gaze variation can cause volume changes	Instruct patient to gently close eyes in neutral position during scanning or, preferably, use fixation target inside gantry
	Voxel	Large variation exists in proposed voxel dimensions	Aim for isotropic voxel to allow good 3D reconstruction images
Post-processing	Software	New software can be developed in house or various commercially available and free software are available	Use validated software packages and methods
	Segmentation method	Manual segmentation is largely applied in research, but impractical for routine use	More computer assisted methods allow routine use and can lower observer variability
	Volume calculation	Accuracy may differ for various methods of volume calculation	Apply automatic volume calculation by the segmentation software
	Method Validation	Many reports use non-validated methods in clinical studies	Use of validated methods or add validation part to the study
Extraocular muscles	Boundaries	<ul style="list-style-type: none"> - Muscles can be evaluated separately or together. - Complete or partial muscle volume. 	<ul style="list-style-type: none"> - Separate muscle segmentation is preferred. - Mention which muscles are included and what part of the muscle is analysed
Orbital fat	Boundaries	Practical difficulties exist with segmenting fat tissue. It is probably easier, but less accurate, to apply a subtraction method	Use of high contrast scan protocol to facilitate more automatic fat segmentation
Globe	Boundaries	Segmentation of outer border (sclera) or vitreous body will alter the volumetric outcome	Select appropriate segmentation procedure for studied ROI
Optic nerve	Boundaries	Optic nerve as well as nerve sheath can be analysed	Manual segmentation is most practical for optic nerve volumetry
Orbital cavity	Boundaries	Different definition of anterior border will affect volumetric outcome	Define anterior border to determine 'bony' volume vs. 'whole' (incl. soft tissue) volume
Lacrimal gland	Boundaries	Inhomogeneous intensity complicate (semi-) automatic segmentation	Manual segmentation is preferred for lacrimal gland volumetry

ROI: Region of interest. 3D: Three-dimensional

tendon is not clearly defined at the orbital apex and scleral insertion. This method is easier to use in daily practice, but comparison of absolute results could be problematic. The orientation of the muscle-axis was reported to be the main factor to choose the optimal scanning plane for outlining the EOM. Significant differences of muscle volume can be found when analysis is performed in a sagittal, axial or regular coronal plane (perpendicular to the midsagittal plane)^[2]. For this reason it is advised to use a 'quasi-coronal' plane, perpendicular to the long axis of the orbit thus almost perpendicular to the long axis of most EOM. On the other hand, total muscle volumetry using semi-automatic segmentation is an easier and faster procedure, although the accuracy will be determined by the segmentation precision of all individual subtracted volumes. Furthermore, it should be noted that the levator palpebrae superioris muscle is often included in the EOM volume, which can affect the volume outcomes. Volumetry of orbital fat is challenging because the fat has no defined shape of its own and fills the spaces between other structures. This makes manual outlining laborious and prone to mistakes. Semi-automatic segmentation methods in combination with dedicated scanning protocols that provide a sharp contrast between fat and adjacent tissue can provide a more feasible solution. Compared to the real volume, MDT segmentation of the orbital fat tends to underestimate^[13,20,26], while RG will rather give an overestimation^[20]. Conversely, fat volumetry by subtraction of the other orbital structures will likely give an overestimation of the true fat volume caused by difficulties to delineate smaller, non-fatty orbital structures, such as the lacrimal gland, vessels and connective tissue.

The optic nerve is a small and relatively well-defined structure, which allows easy and fast manual segmentation. Authors should specify measuring the nerve with or without the nerve sheath. When assessing the orbital cavity volume, all foramina and fissures have to be manually outlined to generate a closed surface. Additionally, the anterior border has to be defined. Some authors analyse the 'whole' orbital volume, i.e. the orbital soft tissues define the anterior border, whereas others only describe the 'bony' orbital volume, i.e. anterior border is defined by the orbital bony margins. Although a CT scan is generally considered to be superior for bony evaluations, the accuracy of an MRI scan was comparable. Nevertheless, there can be a considerable difference in procedural time related to the increased need for manual adjustments on MRI images^[21].

Despite an extensive quality control of included articles, it should be stressed that 67% (18/27) of the studies did not report any validation of the used volumetric method. That is why one should be careful when interpreting absolute volumetric values or compare outcomes of 'similar' studies. This review specifically focused on the features determining the volumetric analysis. No correlations between the volumetric outcome and clinical data were studied. It was not possible to study these correlations or to perform a meta-analysis because a large heterogeneity was noted for the used imaging protocols, selection of ROI borders and segmentation methods.

Conclusion

In conclusion, contemporary literature illustrates the clinical and scientific value for an accurate assessment of orbital tissue volumes with MRI. Various protocols have been proposed and technical innovations unfold rapidly, making comparison of results unreliable. Proper insight in the current trends and potential pitfalls is critical for planning or interpretation of volumetric studies. MRI scanning characteristics, post-processing methods and ROI-specific boundaries have to be defined in detail and the use of validated protocols is recommended. Future research should focus on standardization of imaging protocols and automation of volumetric analysis.

ACKNOWLEDGEMENTS

This work has not been submitted simultaneously to another journal and has not been published before.

All authors have read and approved this work.

No ethical approval was required.

This study received no funding. No conflicts of interest are to be disclosed.

REFERENCES

- [1] Firbank MJ, Coulthard A. Evaluation of a technique for estimation of extraocular muscle volume using 2D MRI. *Br J Radiol.* 2000 Dec;73(876):1282–9.
- [2] Tian S, Nishida Y, Isberg B, Lennerstrand G. MRI measurements of normal extraocular muscles and other orbital structures. *Graefes Arch Clin Exp Ophthalmol.* 2000;238(5):393–404.
- [3] Majos A, Grzelak P, Mlynarczyk W, Stefanczyk L. Eyeball muscles' diameters versus volume estimated by numerical image segmentation. *Eur J Ophthalmol.* 2007;17(3):287–93.
- [4] Shen J, Jiang W, Luo Y, Cai Q, Li Z, Chen Z, et al. Establishment of MRI 3D Reconstruction Technology of Orbital Soft Tissue and Its Preliminary Application in Patients with Thyroid-Associated Ophthalmopathy. *Clin Endocrinol (Oxf)* [Internet]. 2018;(Mv):0–2. Available from: <http://doi.wiley.com/10.1111/cen.13564>
- [5] Yokomachi K, Tanitame K, Takahashi Y, Awai K, Akiyama Y, Kaichi Y. Precise size evaluation of extraocular muscles using fat-suppressed fast T1-weighted gradient-recalled echo imaging and multiple gaze fixation targets. *Jpn J Radiol.* 2013;31(12):812–8.
- [6] Lennerstrand G, Tian S, Isberg B, Landau Hogbeck I, Bolzani R, Tallstedt L, et al. Magnetic resonance imaging and ultrasound measurements of extraocular muscles in thyroid-associated ophthalmopathy at different stages of the disease. *Acta Ophthalmol Scand.* 2007 Mar;85(2):192–201.
- [7] Kaichi Y, Tanitame K, Itakura H, Ohno H, Yoneda M, Takahashi Y, et al. Orbital fat volumetry and water fraction measurements using T2-weighted FSE-IDEAL imaging in patients with thyroid-Associated orbitopathy. *Am J Neuro-radiol.* 2016;37(11):2123–8.
- [8] Suh SY, Clark RA, Le A, Demer JL. Extraocular Muscle Compartments in Superior Oblique Palsy. *Invest Ophthalmol Vis Sci.* 2016;57(13):5535–40.
- [9] Kolk A, Pautke C, Wiener E, Schott V, Wolff K-D, Horch H-H, et al. Isotropic proton-density-weighted high-resolution MRI for volume measurement of reconstructed orbital fractures—a comparison with multislice CT. *Magn Reson Imaging.* 2008 Oct;26(8):1167–74.
- [10] Higashiyama T, Ohji M. Treatment with bimatoprost for exophthalmos in patients with inactive thyroid-associated ophthalmopathy. *Clin Ophthalmol.* 2018;12:2415–21.
- [11] Higgins J, Green S. *Cochrane Handbook for Systematic Reviews of Interventions* [Internet]. The Cochrane Library. The Cochrane Collaboration; 2006. Available from: <https://training.cochrane.org/handbook/> [Accessibility verified May, 2019]
- [12] Institute of Health Economics (IHE). Quality Appraisal of Case Series Studies Checklist. [Internet]. Edmonton (AB): Institute of Health Economics; 2014. Available from: <http://www.ihe.ca/researchprograms/rmd/cssqac-about/> [Accessibility verified May, 2019]
- [13] Comerchi M, Elefante A, Strianese D, Senese R, Bonavolontà P, Alfano B, et al. Semiautomatic regional segmentation to measure orbital fat volumes in thyroid-associated ophthalmopathy a validation study. *Neuroradiol J.* 2013;26(4):373–9.
- [14] Hoffmann J, Schmidt C, Kunte H, Klingebiel R, Harms L, Huppertz H-J, et al. Volumetric assessment of optic nerve sheath and hypophysis in idiopathic intracranial hypertension. *AJNR Am J Neuroradiol.* 2014 Mar;35(3):513–8.
- [15] Kolk A, Pautke C, Schott V, Ventrella E, Wiener E, Ploder O, et al. Secondary post-traumatic enophthalmos: high-resolution magnetic resonance imaging compared with multislice computed tomography in postoperative orbital volume measurement. *J Oral Maxillofac Surg.* 2007 Oct;65(10):1926–34.

- [16] Keil B, Blau JN, Biber S, Hoecht P, Tountcheva V, Setsompop K, et al. A 64-channel 3T array coil for accelerated brain MRI. *Magn Reson Med*. 2013 Jul;70(1):248–58.
- [17] Stojanov O, Stokic E, Sveljo O, Naumovic N. The influence of retrobulbar adipose tissue volume upon intraocular pressure in obesity. *Vojnosanit Pregl*. 2013 May;70(5):469–76.
- [18] Kaichi Y, Tanitame K, Itakura H, Ohno H, Yoneda M, Takahashi Y, et al. Orbital Fat Volumetry and Water Fraction Measurements Using T2-Weighted FSE-IDEAL Imaging in Patients with Thyroid-Associated Orbitopathy. *Am J Neuro-radiol*. 2016 Nov;37(11):2123–8.
- [19] Firbank MJ, Harrison RM, Williams ED, Coulthard A. Measuring extraocular muscle volume using dynamic contours. *Magn Reson Imaging*. 2001 Feb;19(2):257–65.
- [20] Tang X, Liu H, Chen L, Wang Q, Luo B, Xiang N, et al. Semi-automatic volume measurement for orbital fat and total extraocular muscles based on Cube FSE-flex sequence in patients with thyroid-associated ophthalmopathy. *Clin Radiol*. 2018;73(8):759.e11-759.e17.
- [21] Schmutz B, Rahmel B, McNamara Z, Coulthard A, Schuetz M, Lynham A. Magnetic resonance imaging: an accurate, radiation-free, alternative to computed tomography for the primary imaging and three-dimensional reconstruction of the bony orbit. *J Oral Maxillofac Surg*. 2014 Mar;72(3):611–8.
- [22] Szucs-Farkas Z, Toth J, Balazs E, Galuska L, Burman KD, Karanyi Z, et al. Using morphologic parameters of extraocular muscles for diagnosis and follow-up of Graves' ophthalmopathy: diameters, areas, or volumes? *AJR Am J Roentgenol*. 2002 Oct;179(4):1005–10.
- [23] Nishida Y, Tian S, Isberg B, Hayashi O, Tallstedt L, Lennerstrand G. Significance of orbital fatty tissue for exophthalmos in thyroid-associated ophthalmopathy. *GRAEFES Arch Clin Exp Ophthalmol*. 2002 Jul;240(7):515–20.
- [24] Nishida Y, Tian S, Isberg B, Tallstedt L, Lennerstrand G. MRI measurements of orbital tissues in dysthyroid ophthalmopathy. *Graefes Arch Clin Exp Ophthalmol*. 2001 Nov;239(11):824–31.
- [25] Bijlsma WR, Mourits MP. Radiologic Measurement of Extraocular Muscle Volumes in Patients with Graves' Orbitopathy: A Review and Guideline. *ORBIT-AN Int J ORBITAL Disord FACIAL Reconstr Surg*. 2006;25(2):83–91.
- [26] Shen J, Jiang W, Luo Y, Cai Q, Li Z, Chen Z, et al. Establishment of magnetic resonance imaging 3D reconstruction technology of orbital soft tissue and its preliminary application in patients with thyroid-associated ophthalmopathy. *Clin Endocrinol (Oxf)*. 2018 May;88(5):637–44.
- [27] Majos A, Grzelak P, Mlynarczyk W, Stefanczyk L. Assessment of intraorbital structure volume using a numerical segmentation image technique (NSI): the fatty tissue and the eyeball. *Endokrynol Pol*. 2007;58(4):297–302.
- [28] Turvey TA, Golden BA. *Orbital Anatomy for the Surgeon*. *Oral Maxillofac Surg Clin North Am*. 2012;24(4):525–36.
- [29] Buch K, Watanabe M, Elias EJ, Liao JH, Jara H, Nadgir RN, et al. Quantitative Magnetic Resonance Imaging Analysis of the Lacrimal Gland in Sickle Cell Disease. *J Comput Assist Tomogr*. 2014;38(5):674–80.
- [30] Hu H, Xu X-Q, Wu F-Y, Chen H-H, Su G-Y, Shen J, et al. Diagnosis and stage of Graves' ophthalmopathy: Efficacy of quantitative measurements of the lacrimal gland based on 3-T magnetic resonance imaging. *Exp Ther Med*. 2016 Aug;12(2):725–9.
- [31] Clark RA, Demer JL. Changes in Extraocular Muscle Volume During Ocular Duction. *Invest Ophthalmol Vis Sci*. 2016;57(3):1106–11.
- [32] Demer JL, Dushyanth A. T2-weighted fast spin-echo magnetic resonance imaging of extraocular muscles. *J AAPOS Off Publ Am Assoc Pediatr Ophthalmol Strabismus*. 2011 Feb;15(1):17–23.
- [33] Runge VM. Current technological advances in magnetic resonance with critical impact for clinical diagnosis and therapy. *Invest Radiol*. 2013;48(12):869–77.
- [34] Blamire AM. The technology of MRI - The next 10 years? *Br J Radiol*. 2008;81(968):601–17.
- [35] Velasco-Annis C, Gholipour A, Afacan O, Prabhu SP, Estroff JA, Warfield SK. Normative biometrics for fetal ocular growth using volumetric MRI reconstruction. *Prenat Diagn*. 2015 Apr;35(4):400–8.
- [36] Garau LM, Guerrieri D, De Cristofaro F, Bruscolini A, Panzironi G. Extraocular muscle sampled volume in Graves' orbitopathy using 3-T fast spin-echo MRI with iterative decomposition of water and fat sequences. *ACTA Radiol OPEN*. 2018 Jun;7(6).
- [37] Bentley RP, Sgouros S, Natarajan K, Dover MS, Hockley AD. Normal changes in orbital volume during childhood. Jo1 Bentley RP, Sgouros S, Natarajan K, Dover MS, Hockley AD Norm Chang orbital Vol Dur childhood *J Neurosurg* 2002;96(4):742-746 doi103171/jns20029640742urnal Neurosurg. 2002 Apr;96(4):742–6.
- [38] Pagnozzi AM, Fripp J, Rose SE. Quantifying deep grey matter atrophy using automated segmentation approaches: A systematic review of structural MRI studies. *Neuroimage [Internet]*. 2019;116018. Available from: <https://linkinghub.elsevier.com/retrieve/pii/S1053811919305993>

SUPPLEMENTARY MATERIALS**SUPPLEMENT A — COMPLETE SEARCH STRING****Search string PUBMED**

("orbit" [mesh] OR "eye socket" [Tiab] OR "extraocular muscles" [Tiab] OR "extraocular muscles" [Tiab] OR "optic nerve" [Tiab] OR "orbital fat" [Tiab] OR "retrobulbar fat" [Tiab])

AND

("magnetic resonance imaging" [mesh] OR "MRI" [Tiab] OR "NMR" [Tiab] OR "MR Tomography" [Tiab] OR "fMRI" [Tiab])

AND

("post processing" [Tiab] OR "post-processing" [Tiab] OR "volumetry" [tiab] OR "volumetric measurements" [Tiab] OR "analysis" [Tiab] OR "evaluation" [Tiab] OR "measurements" [Tiab] OR "sequence" [Tiab] OR "quantitative" [Tiab] OR "qualitative" [Tiab] OR "segmentation" [Tiab] OR "segment" [Tiab] OR "3D reconstruction" [Tiab] OR "signal intensity" [Tiab])

Search string Web of Science

TOPIC: (orbit OR eye socket OR extraocular muscles OR extraocular muscles OR optic nerve OR orbital fat OR retrobulbar fat)

AND TOPIC: (magnetic resonance imaging OR MRI OR NMR OR MR Tomography OR fMRI)

AND TOPIC:(post processing OR post-processing OR volumetry OR volumetric measurements OR analysis OR evaluation OR measurements OR sequence OR quantitative OR qualitative OR segmentation OR segment OR 3D reconstruction OR signal intensity)

SUPPLEMENT B — MINORS CHECKLIST FOR INCLUDED STUDIES

Author, date	Number of orbits	Clearly stated aim	Inclusion of consecutive patients	Prospective collection of data	Endpoint appropriate to the aim of the study	Unbiased assessment of the study endpoint
Firbank et al., 2000	52	2	1	0	2	1
Firbank et al., 2001	12	2	1	0	2	2
Nishida et al., 2001	28	2	0	0	2	0
Nishida et al., 2002	33	2	0	0	2	0
Szucs-Farkas et al., 2002	110	2	2	0	2	2
Ortube et al., 2006	46	2	1	0	2	0
Lennerstrand et al., 2007	84	2	0	0	2	0
Majos et al., 2007 (part I)	90	2	0	0	2	0
Majos et al., 2007 (part II)	90	2	0	0	2	0
Kolk et al., 2008	37	2	2	2	2	1
Clark et al., 2011	96	2	1	1	2	0
Clark et al., 2012	26	2	2	1	2	0
Comerci et al., 2013	48	2	1	0	2	2
Stojanov et al., 2013	200	2	1	0	1	1
Buch et al., 2014	50	2	1	1	2	1
Hoffmann et al., 2014	92	2	0	0	2	2
Schmutz et al., 2014	11	2	1	1	2	0
Loba et al., 2015	20	2	0	1	2	0
Shin et al., 2015	148	2	2	2	2	1
Clark et al., 2016	30	2	2	1	2	1
Higashiyama et al., 2016	25	2	0	0	2	2
Hu et al., 2016	90	2	2	0	2	1
Kaichi et al., 2016	78	2	1	2	2	1
Suh et al., 2016	38	2	1	2	2	1
Higashiyama et al., 2018	9	2	1	2	2	2
Shen et al., 2018	40	2	1	0	2	2
Tang et al., 2018	60	2	1	0	2	1

NA: Not Applicable; 0= not addressed; 1= partially addressed; 2= adequately addressed

Volumetry in orbital MRI

Follow-up period appropriate to the aim of the study	Loss of follow-up less than 5%	Prospective calculation of the study size	Additional criteria for comparative studies				Total
			Adequate control group	Contemporary group	Baseline equivalent of groups	Adequate statistical analysis	
2	2	0	2	2	2	2	18/24
2	2	0	1	2	2	2	18/24
2	2	0	1	2	2	2	15/24
2	2	0	1	2	2	2	15/24
2	2	0	2	2	2	2	20/24
2	2	0	2	2	2	2	17/24
2	2	0	1	2	1	2	14/24
2	2	0	NA	NA	NA	NA	8/16
2	2	0	NA	NA	NA	NA	8/16
1	1	0	2	2	2	2	19/24
2	2	0	2	1	1	1	15/24
2	0	0	NA	NA	NA	NA	9/16
2	2	0	2	1	2	2	18/24
2	2	0	2	2	2	2	17/24
2	2	0	2	2	2	2	19/24
2	2	0	2	2	2	2	18/24
2	2	0	2	2	2	2	18/24
2	2	0	NA	NA	NA	NA	9/16
2	2	0	2	2	2	2	21/24
2	2	0	NA	NA	NA	NA	12/16
2	2	0	NA	NA	NA	NA	10/16
2	2	0	2	1	2	2	18/24
2	2	0	1	2	2	2	19/24
2	2	0	2	2	2	2	20/24
2	1	0	NA	NA	NA	NA	12/16
2	2	0	2	2	2	2	19/24
2	2	0	2	2	2	2	18/24

Corresponding Author

Robin Willaert
Department of Oral and Maxillofacial Surgery
University Hospitals Leuven
Kapucijnenvoer 33, 3000 Leuven, Belgium
email: robin.willaert@icloud.com
telephone: +32 (0) 474 26 81 47
Publication references:
- Doi: 10.1016/j.ijom.2020.07.027
- PMID: 32814653

Semi-automatic MRI based Orbital Fat Volumetry: Reliability and Correlation with CT

R. WILLAERT MD, DMD^{1,2} | B. DEGRIECK MD³ | K. ORHAN DMD, MSC, PHD^{4,5} | J. DEFERM MD, DMD⁶
C. POLITIS MD, DMD, PHD^{2,4} | E. SHAHEEN MSC, PHD⁴ | R. JACOBS DMD, MSC, PHD^{4,7}

Abstract

Post-processing analysis can provide valuable information for diagnosis and planning of orbital disorders. This case-control study aims to evaluate the reliability of semi-automatic, orbital fat volumetry using magnetic resonance imaging (MRI). Two observers assessed the orbital fat volume using a standard MRI protocol (3T, T1w sequence) in 12 orbits diagnosed with Graves' orbitopathy (GO) and 10 healthy control orbits. MRI and computed tomography (CT) based analysis were compared. Intraobserver variability was good (ICC 0.88; 95%CI [0.70, 0.95]) and interobserver agreement was moderate (ICC 0.55; 95%CI [-0.09, 0.81]), which corresponds to a mean percentage difference of 1.3% and 17.9% of the total orbital fat volume. Mean differences between MRI and CT measurements were respectively 1.1 cm³ (p= 0.064, 95%CI [-0.20, 2.43]) and 1.4 cm³ (p=0.016, 95%CI [0.21, 2.56]) for the control and the GO group. MRI volumetry was strongly correlated with CT (Pearson's r= 0.7, p< 0.001). We conclude that orbital fat volumetry is feasible with a semi-automatic segmentation procedure and standard MRI protocol. Correlation with CT volumetry is good, but considerable bias may derive from observer variability and these errors should be taken into account conform the purpose of volumetric analysis. Better definition of error sources may increase measurement accuracy.

Key Words

- Computed Tomography
- Magnetic Resonance Imaging
- Graves' Orbitopathy
- Orbit
- Computer-Assisted Image Processing

AFFILIATIONS

- 1 Department of Head and Neck Surgery, Ghent University Hospital, Ghent, Belgium
- 2 Department of Oral and Maxillofacial Surgery, University Hospitals Leuven, Leuven, Belgium
- 3 Department of Radiology, Ghent University Hospital, Ghent Belgium
- 4 OMFS IMPATH Research Group, Department of Imaging and Pathology, Faculty of Medicine, KU Leuven, Leuven, Belgium
- 5 Ankara University, Faculty of Dentistry, Department of DentoMaxillofacial Radiology, Ankara, Turkey
- 6 Department of Oral and Maxillofacial Surgery, RadboudUMC, Nijmegen, The Netherlands
- 7 Department of Dental Medicine, Karolinska Institutet, Stockholm, Sweden

Introduction

Orbital fat involvement is a characteristic feature and has been widely studied in patients diagnosed with inflammatory eye disease, like Graves' Orbitopathy (GO) [1,2]. Fibroblast proliferation and adipogenesis increase soft tissue volume in the orbital cavity, contributing to proptosis and periorbital swelling, potentially leading to optic nerve compression [3-5]. In GO patients the amount of the volume increment of orbital fat is much larger than that of the extraocular muscles with the degree of exophthalmos being significantly related to orbital tissue increase [2,6]. Measurement of orbital fat can be used as an early marker to assess disease severity, activity and to monitor effectiveness of therapeutic modalities over time [2,7-9].

Therefore, orbital imaging is a valuable tool to support the diagnostic pathway, during follow-up or prior to surgery in patients with GO [8,10]. Post processing of radiological images allows for objective detection of changes in orbital tissue volume. Accuracy of morphometric measurement depends on the correct identification of intensity difference between the targeted volume and its surrounding tissues. Monitoring orbital fat volume is a challenging task because it has no defined shape of its own and merely fills the spaces between the better-defined tissues (e.g. eye ball, extraocular muscles and optic nerve) [2].

Consensus on the use of different imaging modalities has yet to be reached [8]. Computer tomography (CT) was always considered the gold standard for surgical planning due to the clear visualization of the bony orbit, fat and muscle tissue. Pre- and postoperative CT volumetric studies

have been successfully used for the assessment of orbital decompression surgery [8,11]. CT has been used to quantify the volume of extraocular muscles and orbital fat in GO [12,13]. Serial CT imaging, however, can cause radiation-induced cataract and lens opacifications limiting its clinical use in long term follow up of eye diseases [9,14]. Magnetic resonance imaging (MRI) provides excellent soft-tissue contrast, with better delineation of the orbital tissues and MRI can yield images in any plane. With the increasing use of MRI for evaluating GO, various protocols are described for a safe and accurate measurement of adipose tissue with MRI [7,9,14-16]. Initially, only determination of two dimensional measurements was feasible, but technological advances and software-assisted volumetric measurement facilitated the process for three dimensional analysis [7,9,17]. Different segmentation techniques are developed to define the tissue borders and allow quantitative analysis. Due to the irregular morphology of orbital fat, the manual segmentation (i.e. tracing the tissue on each consecutive scan) is time-consuming and associated with high inter-operator variation [16,18]. Semi-automatic segmentation techniques try to address these issues, as the software will define the tissue outlines depending on reference tissue intensity. These semi-automatic techniques still need a variable level of manual adjustments, depending on the image quality and properties of the studied tissue.

If fat volume is to be used as an indicator for diagnosis and treatment of orbital disorders, it is important that correlation between CT and MRI measurements are transparent and that the errors implicit in the measurement technique are defined.

Currently it is not clear whether findings from one imaging technique can be translated to another. Furthermore, orbital imaging with CT or MRI can be useful at different stages during follow up of the same patient. It would add great value to interpret disease evolution if results from both scans would be comparable. The measurement protocol should be easy to perform in routine clinical practice and involve post-processing software with a short learning curve. The aims of this study are (i) to analyse if it is feasible to use a standard MRI protocol and a semi-automatic segmentation technique to measure orbital fat volume in routine clinical practice and (ii) to what extent the results from MRI fat volumetry are comparable with a CT based analysis.

Materials and Methods

Data collection

In this retrospective, cross-sectional study 12 orbits of 6 patients (3 female; mean age 55 ± 16 years) diagnosed with GO were consecutively selected between January 2017 and December 2018. All patients were evaluated in an inactive disease stage according to the EUGOGO guidelines 20. Patients were only included if they received both orbital CT and MRI scan as part of routine follow-up, with a maximum of 3 months between both scans (mean interval 8 ± 10 days). For all cases, CT scan was performed for surgical planning of an orbital decompression procedure. Additionally, 5 control patients (2 female, mean age 44 ± 14 years) with 10 healthy orbits were randomly selected. Imaging was performed in the context of head trauma ($n=2$) or cerebral intervention ($n=3$). Patients were included if they were 18 years or older, received both

orbital CT and MRI scan with a maximum of 3 months interval (mean interval 16 ± 18 days). The exclusion criteria were: orbital and ocular pathology; previous ocular and periocular surgery; orbital trauma; previous radiotherapy in head and neck region; long-term use of systemic corticosteroids; and CT scans showing motion artifacts. The study adhered to the tenets of the declaration of Helsinki. Institutional review board approval and informed consents were obtained (B670201733474).

Scan protocol

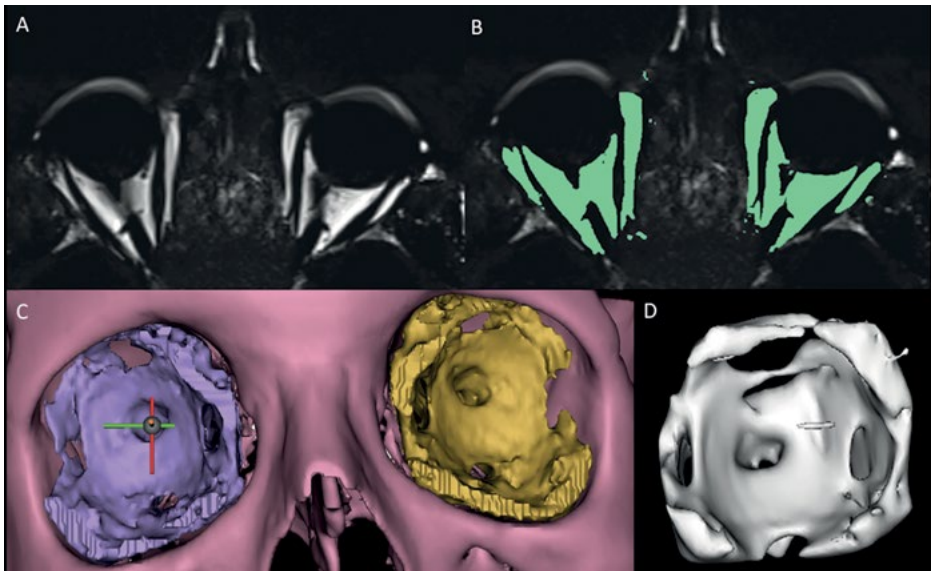
GO patients and controls were scanned with current clinical standard of care protocols. Non contrast-enhanced, T1 weighted images were obtained on a 1.5T or 3T MRI (Siemens Magnetom AVANTO or PRISMA) in axial (TE: 2.78-7.8ms; TR: 251-356ms) and sagittal planes (TE: 2.51-7.8ms; TR: 255-649ms) with standard head coil. Continuous slices of 3mm thickness were obtained. Patients were instructed to keep their eyes closed and adopt a neutral position of gaze during scanning. All CT scans were obtained through the multidetector technique with a field of view containing the orbital structures (Siemens Somatom AS). A single volume of data was acquired in the axial plane at 1-2mm thickness. All non contrast-enhanced images were recorded in Digital Imaging and Communications in Medicine 3.0 (DICOM) format, anonymized and transferred to a workstation for analysis.

Orbital fat segmentation and volume measurements

Fat volume assessment on MRI was performed on a commercially available post processing software package: Oleasphere (v3.0, Olea Medical, La Ciotat, France). The orbital fat volume of both eyes was measured on a workstation using on a 21.3-inch flat-panel color-active matrix thin-film-transistor medical display (Nio Color 3MP, Barco, Kortrijk, Belgium) with a resolution of 2048x1536 at 76 Hz and 0.2115 mm dot pitch operated at 10 bits. Two observers were trained and calibrated to analyze the orbital MRI scans of 22 orbits. To do so, they were permitted to use enhancements and orientation tools such as magnification, brightness, and

contrast to improve visualization of the landmarks. Each assessment required 15 till 30 minutes. The Oleasphere software allowed for a semi-automatic, threshold based segmentation of different orbital structures. The orbital region of interest was obtained by manual delineation of the orbital cavity on each slice that contained orbital structures. The anterior border of the orbital cavity was delineated by the anterior lacrimal crest, frontozygomatic suture, inferior orbital rim and frontal bone. A threshold based, region grow algorithm was used to segment the orbital fat tissue and excessive components (e.g. fatty orbital bone marrow) were manually erased on each slide. Segmentation was performed on the axial slices, with visual control in the other orthogonal planes.

FIGURE 4.1 — SEGMENTATION AND VOLUMETRIC ANALYSIS OF THE ORBITAL FAT



- (A) Axial slice of an orbital MRI scan (T1w, non contrast-enhanced) at the level of the optic nerve.
- (B) Orbital fat segmentation (green) using a semi-automatic, threshold-based technique.
- (C) Three dimensional reconstruction of an orbital CT scan with facial skeleton (pink) and orbital fat volume (purple and yellow) using Mimics Medical 21.0 software.
- (D) MRI based 3D reconstruction of the segmented orbital fat tissue.

After segmentation, the Oleasphere software automatically calculated the fat volume.

Fat volumetry on CT images was conducted according to the validated protocol by Regensburg and colleagues^[12]. DICOM files were uploaded into Mimics Medical 21.0 (Materialise, Leuven, Belgium). Contrast was adjusted for optimal visualization of the orbital fat. The orbital fat was identified using a multi-dimensional threshold based segmentation method with the possibility of manual adjustment on each slide. A 3D reconstruction of the orbital fat was generated and saved as a stereolithography (STL) file. The software automatically calculated the fat volume.

Variability analysis

Two observers (BD, RW) with a variable level of expertise (respectively junior radiologist and head and neck surgeon) were blinded to the patients' clinical condition and independently performed the volume measurements. One observer (RW) repeated the procedure twice on different occasions to study the intra-observer variability. Right and left orbit were examined separately.

Statistical analysis

The data were analyzed using MedCalc statistical software (Version 12.0, Ostend, Belgium). Means and standard deviations of orbital fat volumes were calculated for each observer separately. For inter- and intra-observer variability tests, the intraclass correlation coefficient (ICC) with 95% confidence interval (CI) was calculated (two-way mixed-effects model). The ICC is interpreted as following: value of 1 indicates perfect agreement; values of >0.9 are considered ideal to be used in a clinical setting. Values of 0.75 - 0.9 represent good agreement, < 0.75 and ≥ 0.5 is moderate, and <0.5 is poor reliability^[21,22]. Orbital fat volumes on MRI scans were compared with CT scans using a paired Wilcoxon signed rank test. A Mann-Whitney U test was used to compare the control and GO group for difference between MRI and CT volumetry. Bland and Altman method was used to calculate the mean difference and to evaluate the 95% limits of agreements between fat volume measurements by CT and MRI^[23]. Pearson correlation was calculated to study the correlation between the mean fat volume on MRI and CT. Mean, median and 95% confidence intervals (CI) were calculated when appropriate. Differences were considered statistically significant at P-values of < 0.05 .

TABLE 4.1 — REPRODUCIBILITY TESTING FOR ORBITAL FAT VOLUME MEASUREMENTS ON MRI

Orbital volume* (cm ³)	Observer 1	Observer 2	ICC (95%CI)	
Interobserver variability	8.5±2.0	10.3±2.4	0.55 (-0.09;0.81)	
		Observer 2a		Observer 2b
Intraobserver variability		10.3±2.4	10.3±2.1	0.88 (0.70;0.95)

* Variables are denoted as Means±SD.

ICC: Intraclass correlation coefficient, outcome values: 0= no agreement, 1= perfect agreement; CI: confidence interval

Results

Two trained observers analyzed the orbital MRI scans of 22 orbits. The mean orbital fat volume in the control group was $9.1 \pm 1.9 \text{ cm}^3$ on MRI scan compared to $10.2 \pm 2.2 \text{ cm}^3$ on the CT scan (mean difference 1.1 cm^3 , $p=0.064$, 95%CI [-0.20, 2.43]). The volume measurements for the GO group were respectively $10.3 \pm 1.6 \text{ cm}^3$ and $11.7 \pm 2.1 \text{ cm}^3$ on MRI and CT scan (mean difference 1.4 cm^3 ; $p=0.016$; 95%CI [0.21, 2.56]) (Figure 4.2). The mean difference between CT and MRI volumetry in the control group is not significant (Supplementary Table A) when compared to the GO group ($p=0.722$; 95%CI [-1.37, 1.06]).

The ICC values for orbital fat measurement are presented in Table 3.1. Intra-observer variability is good (0.88; 95%CI [0.70, 0.95]; $p < 0.001$) and interobserver agreement is moderate (0.55; 95%CI [-0.09, 0.81]; $p = 0.38$). This represents an absolute mean difference of respectively 0.13 cm^3 and 1.72 cm^3 , corresponding to a mean percentage volume difference of 1.3% to 17.9%.

Figure 4.3 illustrates the correlations between orbital fat volume measurements by MRI and CT. There is a strong positive linear correlation between the mean fat volume measurements on MRI and CT ($r=0.7$, $p < 0.001$). The Bland and Altman plot (figure 4) illustrates the mean difference of orbital fat volume measurement between CT and MRI (mean difference 1.3 cm^3 ; 95%CI [0.58, 2.07]). Relative to the mean orbital fat volume, this value corresponds to a mean percentage volume difference of 12%.

Discussion

Advances in orbital imaging and post-processing techniques with MRI and CT scan provide objective measurements to support diagnosis and treatment in orbital diseases.

CT and MRI scan both have distinct characteristics, but the use of MRI is increasing, especially when sequential imaging is needed in chronic disorders. Extensive heterogeneity in the use of different imaging modalities and highly demanding, time-consuming protocols, however, hamper the routine clinical implementation and make comparison of results difficult. If measurement of orbital fat could contribute in the routine management of orbital disorders, it is paramount to study the feasibility of fat segmentation based on standard orbital MRI scans and investigate the agreement with the CT measurements.

This study illustrates that a standard, T1 weighted orbital MRI scan can be used to estimate the orbital fat volume. A semi-automatic segmentation method is feasible in routine clinical practice by observers with a variable level of expertise. Intra-observer agreement is good. Inter-observer variability, however, is moderate leading to a relative difference up to 17.9% of the total orbital fat volume. This inter-observer variability is higher compared to earlier reports on CT based analysis^[12]. This could be explained by the definition of the tissue specific grey values at the start of the segmentation process. On the CT scan, Hounsfield units (HU) are universally used to define the tissue. These HU will stay the same in all circumstances. With the MRI based analysis, however, the observer has to define a tissue specific grey value for every patient and in every scan. For this reason a stand-

FIGURE 4.2 — RESULTS OF ORBITAL FAT VOLUMETRY ON CT AND MRI FOR GO AND CONTROL ORBITS | Means (with 95% confidence interval) and medians are provided.

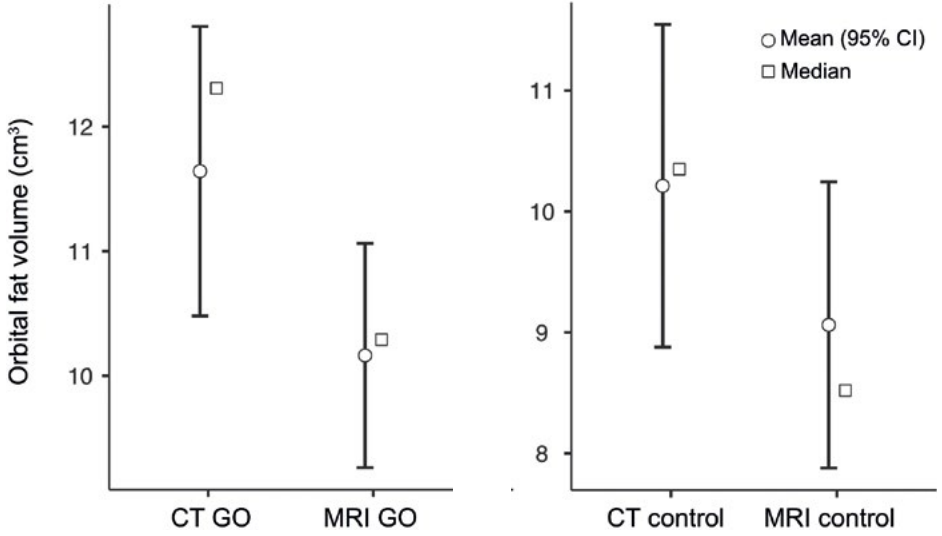
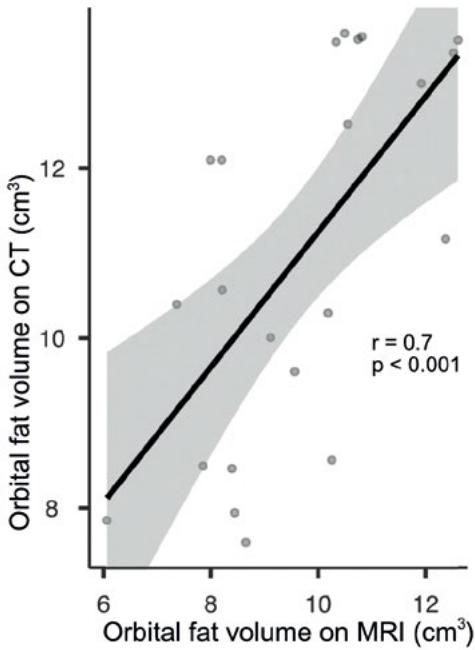


FIGURE 4.3 — SCATTERPLOT AND CORRELATION FOR ORBITAL FAT VOLUMETRY ON MRI AND CT SCAN | Pearson correlation (r) and p -value are provided.

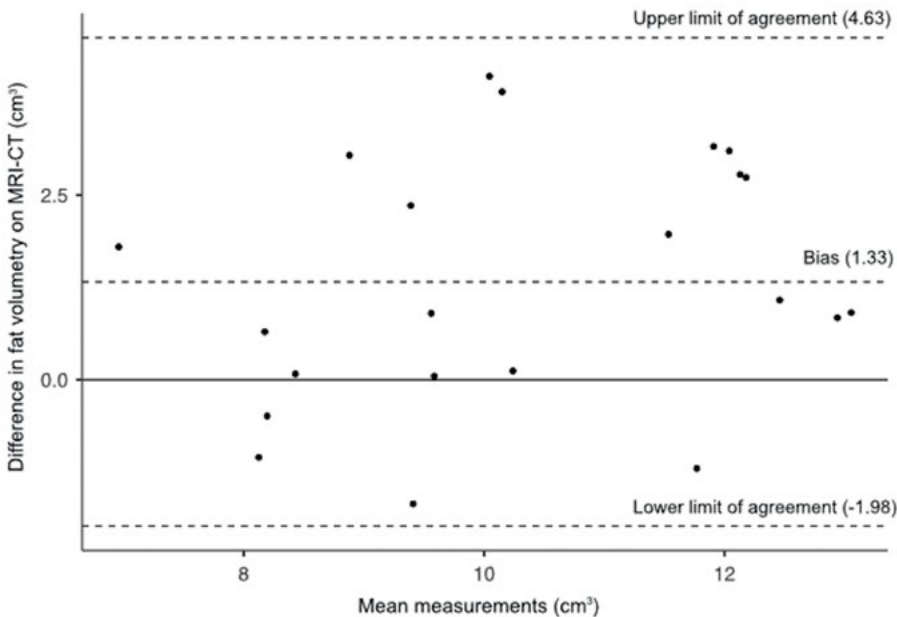


ard MRI protocol could be more prone to inter-observer differences. A strong positive correlation has been shown between fat volume measurements on MRI and CT scan. A tendency for underestimation of fat volume in MRI is observed, which corresponds with findings by Schmutz et al. who compared the orbital volume on CT and MRI [14]. The mean difference (1.3 cm³) in fat volume between MRI and CT is in agreement with earlier reports comparing the intact orbital cavity volume on CT and MRI (differences of up to 1.5 cm³), although the orbital cavity is probably easier to delineate than the fat tissue [14,24]. A volume difference greater than 1 cm³ can be considered clinically relevant as studies on orbital fat decompression report an average globe displacement of 1 mm for approximately 1 cm³ fat resection [25,26]. On the other hand, patients diagnosed with GO are reported to have an

increase in orbital fat volume of 4.2 cm³ to 6.6 cm³, which could be reliably detected by fat volumetry [27,28]. Therefore, the measurement error should be taken into account conform the purpose of volumetric analysis.

Inflammatory diseases of the orbital fat could have repercussions for imaging outcome, e.g. changing tissue intensities caused by edema or fibrosis. The success of the automatic segmentation process largely depends on differences in tissue intensities hence could be influenced by orbital diseases. When considering the possible influence of orbital tissue deformation or inflammatory disease on volume measurement, results show no significant difference in measurement error for volume calculations in the control group compared to orbits affected by Graves' disease. As this limits the causal role of or-

FIGURE 4.4 — BLAND-ALTMAN PLOT SHOWING THE MEAN DIFFERENCE (STRAIGHT LINE) AND 95% LIMITS OF AGREEMENT (DOTTED LINE) BETWEEN ORBITAL FAT VOLUME MEASUREMENT ON CT AND MRI.



bital diseases, other reasons for measurement inaccuracies could be related to the MRI protocol or segmentation method. The accuracy of volumetric measurement depends on an optimal protocol for the correct identification of intensity difference between the region of interest and its surrounding tissues^[16]. Many MRI orbital protocols have been introduced for the volumetric measurement of orbital tissues. Most studies estimate the orbital fat volume by a manual segmentation technique^[1,2,29,30]. In this approach, the region of interest have to be defined on every single slice, making it very time demanding and impractical^[31]. Due to the irregular morphology of the orbital fat, this method is associated with high inter-observer variability and is prone to bias according to the plane orientation of the scan^[16]. Other studies address this problem by segmenting all but the orbital fat tissue (EOM, globe and optic nerve) and subtract these structures (which are easier to trace) from the whole orbital volume^[2,15,32]. The resulting volume, however, will also contain other tissues like the lacrimal gland, vessels and connective tissue, which are difficult to distinguish from the fat, hence causing an overestimation of the true fat volume. More advanced methods like regional growing and multi-dimensional threshold algorithms try to overcome these problems through a semi-automatic segmentation process but require more dedicated MRI protocols^[9,16,31]. A standard MRI protocol was selected for this study to facilitate availability and make retrospective analysis more feasible. The T1 weighted sequence ensures good contrast between fat and surrounding tissues and is considered first choice in standard orbital imaging. Images were acquired with a slice thickness of 3 mm, which is

in line with universally accepted standards reported in literature^[1,2,33,34]. The non contrast-enhanced sequence allows qualitative and quantitative analysis, avoiding toxicity and cost of gadolinium^[35,36]. More advanced sequences and dedicated acquisition protocols could probably allow for more detailed analysis and enhance the post-processing possibilities^[7,9,16]. It is important to point out, however, that although this could increase opportunities in research setting, these protocols can be highly demanding (staff, scan duration, availability, etc.), which makes everyday use infeasible^[7,31]. Future research can clarify how a standard MRI protocol can be optimized (slice thickness, isotropic voxel, distance factor, etc.) for easier depiction of orbital fat, lower the measurement error and still be efficient for routine use.

To our knowledge, this is the first study to compare a semi-automatic orbital fat volume measurement on MRI and CT. Both imaging studies have specific advantages and can complement each other in the multi-modal management of orbital diseases. This report illustrates the pitfalls and shows to which degree the fat volumetry results can be matched. These insights may contribute to the increasing interest regarding the role of orbital fat tissue in the management of GO but could also give understanding to post-traumatic orbital changes. This study only includes fat volume analysis, while no correlations were performed with disease activity or severity. This issue was already extensively discussed by others and goes beyond the focus of this study^[7,9,30]. Considering the relatively small dataset, further studies will be required before these findings can be generalized. MRI measurements were compared with a CT based method,

which was previously validated and considered the clinical reference standard^[12]. It should be recognized, however, that this method also contains some error compared to the actual anatomical volumes. In future research, authors plan to optimize the MRI protocol, using anatomical specimens to compare with true tissue volume.

Conclusion In conclusion, this study illustrates the possibilities and the pitfalls of using a standard MRI protocol and a semi-automatic post-processing technique to measure the orbital fat volume. There is a good correlation with CT-based measurements, but the possible error should be considered. Moreover, the inter-observer variability has to be improved to allow for implementation as an objective outcome indicator. Enhancing the imaging protocol, with sharper delineation of tissue intensities, is believed to improve the accuracy and inter-observer agreement of MRI segmentation. Future research should focus on tissue specific MRI acquisition and post-processing techniques, keeping in mind that routine clinical use should be feasible.

ACKNOWLEDGEMENTS

This work has not been submitted simultaneously to another journal and has not been published before. All authors have read and approved this work before submitting to IJOMS.

The study adhered to the tenets of the declaration of Helsinki. Institutional review board approval and informed consents were obtained (B670201733474)

This study received no funding. No conflicts of interest are to be disclosed.

REFERENCES

- [1] Szucs-Farkas Z, Toth J, Kollar J, Galuska L, Burman KD, Boda J, et al. Volume changes in intra- and extraorbital compartments in patients with Graves' ophthalmopathy: effect of smoking. *Thyroid*. 2005 Feb;15(2):146–51.
- [2] Nishida Y, Tian S, Isberg B, Tallstedt L, Lennerstrand G. Significance of orbital fatty tissue for exophthalmos in thyroid-associated ophthalmopathy. *Graefes Arch Clin Exp Ophthalmol*. 2002;240(7):515–20.
- [3] Dolman PJ. Evaluating Graves' Orbitopathy. *Best Pract Res Clin Endocrinol Metab* [Internet]. 2012;26(3):229–48. Available from: <http://dx.doi.org/10.1016/j.beem.2011.11.007>
- [4] Kuriyan AE, Woeller CE, O'Loughlin CW, Phipps RP, Feldon SE. Orbital fibroblasts from thyroid eye disease patients differ in proliferative and adipogenic responses depending on disease subtype. *Investig Ophthalmol Vis Sci*. 2013;54(12):7370–7.
- [5] Watanabe M, Buch K, Fujita A, Jara H, Qureshi MM, Sakai O. Quantitative MR imaging of intra-orbital structures: Tissue-specific measurements and age dependency compared to extra-orbital structures using multispectral quantitative MR imaging. *Orbit (London)* [Internet]. 2017;36(4):189–96. Available from: <http://dx.doi.org/10.1080/01676830.2017.1310254>
- [6] Willaert R, Maly T, Ninclaus V, Huvenne W, Vermeersch H, Brusselselaers N. Efficacy and complications of orbital fat decompression in Graves' orbitopathy: a systematic review and meta-analysis. *Int J Oral Maxillofac Surg*. 2019 Aug;
- [7] Comerci M, Elefante A, Strianese D, Senese R, Bonavolontà P, Alfano B, et al. Semiautomatic regional segmentation to measure orbital fat volumes in thyroid-associated ophthalmopathy a validation study. *Neuroradiol J*. 2013;26(4):373–9.
- [8] Siakallis LC, Uddin JM, Miszkiel KA. *Imaging Investigation of Thyroid Eye Disease*. Vol. 34, Ophthalmic plastic and reconstructive surgery. 2018. p. S41–51.
- [9] Kaichi Y, Tanitame K, Itakura H, Ohno H, Yoneda M, Takahashi Y, et al. Orbital Fat Volumetry and Water Fraction Measurements Using T2-Weighted FSE-IDEAL Imaging in Patients with Thyroid-Associated Orbitopathy. *Am J Neuro-radiol*. 2016 Nov;37(11):2123–8.
- [10] Gonçalves A, Gebrim E, Monteiro M. Imaging studies for diagnosing Graves' orbitopathy and dysthyroid optic neuropathy. *Clinics* [Internet]. 2012;67(11):1327–34. Available from: <http://clinics.org.br/article.php?id=906>
- [11] Schiff BA, McMullen CP, Farinhas J, Jackman AH, Hagiwara M, McKellop J, et al. Use of computed tomography to assess volume change after endoscopic orbital decompression for Graves' ophthalmopathy. *Am J Otolaryngol - Head Neck Med Surg* [Internet]. 2015;36(6):729–35. Available from: <http://dx.doi.org/10.1016/j.amjoto.2015.06.005>

- [12] Regensburg NI, Kok PHB, Zonneveld FW, Baldeschi L, Saeed P, Wiersinga WM, et al. A new and validated CT-Based method for the calculation of orbital Soft tissue volumes. *Investig Ophthalmol Vis Sci.* 2008;49(5):1758–62.
- [13] Regensburg NI, Wiersinga WM, Van Velthoven MEJ, Berendschot TTJM, Zonneveld FW, Baldeschi L, et al. Age and gender-specific reference values of orbital fat and muscle volumes in Caucasians. *Br J Ophthalmol.* 2011;95(12):1660–3.
- [14] Schmutz B, Rahmel B, McNamara Z, Coulthard A, Schuetz M, Lynham A. Magnetic resonance imaging: an accurate, radiation-free, alternative to computed tomography for the primary imaging and three-dimensional reconstruction of the bony orbit. *J Oral Maxillofac Surg.* 2014 Mar;72(3):611–8.
- [15] Nishida Y, Tian S, Isberg B, Tallstedt L, Lennerstrand G. MRI measurements of orbital tissues in dysthyroid ophthalmopathy. *Graefes Arch Clin Exp Ophthalmol.* 2001 Nov;39(11):824–31.
- [16] Tang X, Liu H, Chen L, Wang Q, Luo B, Xiang N, et al. Semi-automatic volume measurement for orbital fat and total extraocular muscles based on Cube FSE-flex sequence in patients with thyroid-associated ophthalmopathy. *Clin Radiol.* 2018;73(8):759.e11–759.e17.
- [17] Kasubek J, Pinkhardt EH, Dietmaier A, Ludolph AC, Landwehrmeyer GB, Huppertz HJ. Fully automated atlas-based MR imaging volumetry in huntington disease, compared with manual volumetry. *Am J Neuroradiol.* 2011;32(7):1328–32.
- [18] Firbank MJ, Harrison RM, Williams ED, Coulthard A. Measuring extraocular muscle volume using dynamic contours. *Magn Reson Imaging.* 2001 Feb;19(2):257–65.
- [19] Bentley RP, Sgouros S, Natarajan K, Dover MS, Hockley AD. Normal changes in orbital volume during childhood. *Jo1 Bentley RP, Sgouros S, Natarajan K, Dover MS, Hockley AD Norm Chang orbital Vol Dur childhood J Neurosurg* 2002;96(4):742-746 doi103171/jns20029640742urnal Neurosurg. 2002 Apr;96(4):742–6.
- [20] Bartalena L, Baldeschi L, Boboridis K, Eckstein A, Kahaly GJ, Marcocci C, et al. The 2016 European Thyroid Association/European Group on Graves' Orbitopathy Guidelines for the Management of Graves' Orbitopathy. *Eur Thyroid J [Internet].* 2016;5(1):9–26. Available from: <https://www.karger.com/Article/FullText/443828>
- [21] Koo TK, Li MY. A Guideline of Selecting and Reporting Intraclass Correlation Coefficients for Reliability Research. *J Chiropr Med.* 2016;15(2):155–63.
- [22] Kottner J, Audige L, Brorson S, Donner A, Gajewski BJ, Hróbjartsson A, et al. Guidelines for Reporting Reliability and Agreement Studies (GRRAS) were proposed. *Int J Nurs Stud.* 2011;
- [23] Bland JM, Altman DG. Measuring agreement in method comparison studies. *Stat Methods Med Res.* 1999;8(2):135–60.
- [24] Gellrich N-C, Schramm A, Hammer B, Rojas S, Cufi D, Lagreze W, et al. Computer-assisted secondary reconstruction of unilateral posttraumatic orbital deformity. *Plast Reconstr Surg.* 2002 Nov;110(6):1417–29.
- [25] Liao SL, Huang SW. Correlation of retrobulbar volume change with resected orbital fat volume and proptosis reduction after fatty decompression for graves ophthalmopathy. *Am J Ophthalmol.* 2011;151(3):465–469.e1.
- [26] Wu CH, Chang TC, Liao SL. Results and Predictability of Fat-Removal Orbital Decompression for Disfiguring Graves Exophthalmos in an Asian Patient Population. *Am J Ophthalmol.* 2008;145(4):755–9.
- [27] Shen J, Jiang W, Luo Y, Cai Q, Li Z, Chen Z, et al. Establishment of magnetic resonance imaging 3D reconstruction technology of orbital soft tissue and its preliminary application in patients with thyroid-associated ophthalmopathy. *Clin Endocrinol (Oxf).* 2018 May;88(5):637–44.
- [28] Comerchi M, Elefante A, Strianese D, Senese R, Bonavolontà P, Alfano B, et al. Semiautomatic regional segmentation to measure orbital fat volumes in thyroid-associated ophthalmopathy a validation study. *Neuroradiol J.* 2013;26(4):373–9.
- [29] Erkok MF, Oztoprak B, Gumus C, Okur A. Exploration of orbital and orbital soft-tissue volume changes with gender and body parameters using magnetic resonance imaging. *Exp Ther Med.* 2015 May;9(5):1991–7.
- [30] Higashiyama T, Ohji M. Treatment with bimatoprost for exophthalmos in patients with inactive thyroid-associated ophthalmopathy. *Clin Ophthalmol.* 2018;12:2415–21.
- [31] Stojanov O, Stokic E, Sveljo O, Naumovic N. The influence of retrobulbar adipose tissue volume upon intraocular pressure in obesity. *Vojnosanit Pregl.* 2013 May;70(5):469–76.
- [32] Kolk A, Pautke C, Wiener E, Schott V, Wolff K-D, Horch H-H, et al. Isotropic proton-density-weighted high-resolution MRI for volume measurement of reconstructed orbital fractures—a comparison with multislice CT. *Magn Reson Imaging.* 2008 Oct;26(8):1167–74.
- [33] Majos A, Pajk M, Elgalal M, Olszycki M. Lateral rectus muscle as a new reference point in estimation of Graves' ophthalmopathy activity. 2010;16(2008):80–5.
- [34] Wu Y, Tong B, Luo Y, Xie G, Xiong W. Effect of radiotherapy on moderate and severe thyroid associated ophthalmopathy: a double blind and self-controlled study. *Int J Clin Exp Med.* 2015;8(2):2086–96.
- [35] Garau LM, Guerrieri D, De Cristofaro F, Bruscolini A, Panzironi G. Extraocular muscle sampled volume in Graves' orbitopathy using 3-T fast spin-echo MRI with iterative decomposition of water and fat sequences. *Acta Radiol Open.* 2018;7(6):205846011878089.
- [36] Daubner D, Spieth S, Engellandt K, Von Kummer R. Diagnose und differenzialdiagnose der endokrinen orbitopathie in der MRT. *Radiologe.* 2012;52(6):550–9.

SUPPLEMENTARY MATERIAL

SUPPLEMENT TABLE A — MEAN DIFFERENCE BETWEEN CT AND MRI VOLUMETRY FOR GO COMPARED TO CONTROL GROUP.

Variable* (cm ³)	GO group	Control group	p-value**	95%CI
Volume error MRI vs. CT	1.9±1.4	1.6±1.1	0.722	-1.37; 1.06

* Variables are denoted as means±SD. ** differences between the two groups were tested with the Mann-Whitney U test.
CI: confidence interval

Corresponding Author

Robin Willaert
Department of Oral and Maxillofacial Surgery
University Hospitals Leuven
Kapucijnenvoer 33, 3000 Leuven, Belgium
email: robin.willaert@icloud.com
telephone: +32 (0) 474 26 81 47

Development and Validation of an MRI Protocol for Orbital Soft Tissue Volumetry

R. WILLAERT MD, DMD^{1,2} | J. DE TOBEL MD, DMD, MSc, PhD^{1,2,3} | K. ORHAN DMD, MSc, PhD^{4,5} | S. BOGAERT MSc⁶
S. RUITERS MD⁷ | E. SHAHEEN MSc, PhD^{2,4} | R. JACOBS DMD, MSc, PhD^{4,8}

Abstract

Aim — Quantitative evaluation of orbital soft tissue volume is useful for analysing disease stages, treatment response and planning surgical treatment in various orbital disorders. Enhanced MRI methods and post-processing analysis could provide more accurate volume estimations. This study aims to develop and validate clinically feasible and accurate orbital magnetic resonance imaging (MRI) protocols for semi-automatic soft tissue volumetry. **Methods** — A qualitative assessment of 12 different orbital MRI protocols (3T, Siemens Magnetom Prisma, 4-channel loop coils and 64-channel head coil) was performed in vivo in a human volunteer, who gave informed consent. After selection of the three most dedicated MRI protocols, volumetry accuracy and reproducibility was tested ex vivo in three fresh cadaveric pig heads. Six orbits were scanned with computed tomography (CT) scan and three dedicated MRI protocols: MPRAGE, T2 SPACE ZOOMit, T1 TSE Dixon. Commercially available post-processing software (Synapse 3D and Mimics 21.0 innovation suite) was used to semi-automatically analyse the orbital soft tissue volumes (globe, extraocular muscles, orbital fat). Next, the same orbital structures were dissected to obtain a gold standard of the volumes. Volumetry was compared between the different MRI protocols, as well as between MRI, CT and the dissected volume. Intra-observer variability for the MRI-based volumetry was assessed using intra-class correlation coefficient (ICC). **Results** — Compared to the gold standard, the most accurate volumetry of the extraocular muscles (mean difference (MD) 0.17 cm³, standard error (SE) 0.06 cm³, relative volume error 7%) and globe (MD -0.33 cm³, SE 0.12 cm³, relative volume error 8%) was achieved on a T2 SPACE ZOOMit protocol. Orbital fat volumetry (MD -0.77 cm³, SE 0.15 cm³, relative volume error 15%) was most accurate with a

Key Words

- Orbit
- Computed Tomography
- Magnetic Resonance Imaging
- Computer-Assisted Image Processing
- Quantitative Evaluation

AFFILIATIONS

- 1 Department of Head and Neck Surgery, Ghent University Hospital, Ghent, Belgium
- 2 Department of Oral and Maxillofacial Surgery, University Hospitals Leuven, Leuven, Belgium
- 3 Department of Diagnostic Sciences – Radiology, Ghent University, Ghent, Belgium
- 4 OMFS IMPATH Research Group, Department of Imaging and Pathology, Faculty of Medicine, KU Leuven, Leuven, Belgium
- 5 Department of Dento-Maxillofacial Radiology, Faculty of Dentistry, University of Ankara, Ankara, Turkey
- 6 Ghent Institute for Functional and Metabolic Imaging (GIFMI), Ghent University, Ghent, Belgium
- 7 Department of Ophthalmology, University Hospitals Leuven, Leuven, Belgium
- 8 Department of Dental Medicine, Karolinska Institutet, Stockholm, Sweden

T1 TSE-Dixon protocol. MRI-based volumetry of extraocular muscles and fat correlated better (Pearson's r 0.87 ($P=0.02$) and 0.91 ($P=0.01$) respectively) with the true volume compared to CT-based measurements. Intra-observer agreement for MRI-based volumetry was ideal ($ICC > 0.9$). **Conclusion** — Accurate and reproducible volumetric analysis of orbital soft tissues is feasible when using dedicated MRI protocols. These findings can enhance the clinical implementation of orbital volumetry and facilitate evolution towards fully automated segmentation techniques.

Introduction

Imaging plays an important role in the diagnosis and management of orbital diseases and disorders. Objective morphological findings are required in unclear or asymmetric proptosis, in suspected optic neuropathy and prior to surgery^[1]. Computed tomography (CT) used to be the preferred imaging modality for orbital imaging because of good availability, short investigation time and its ability to visualize bone and soft tissues^[2,3]. The radiation exposure is, however, a disadvantage particularly when repeated scans are required in the follow-up of orbital diseases^[4-6]. Besides the lack of ionizing radiation, magnetic resonance imaging (MRI) is gaining importance for its good depiction and supreme contrast in the evaluation of soft tissues^[7-9]. Advances in MRI hardware (increasing field strength, availability of additional coils), developments of new sequences and post-processing technology make quantitative analysis increasingly valuable for diagnosis, evaluation of disease progression and treatment planning in orbital diseases. Whereas 'conventional' MRI protocols mainly provide morphological characteristics, new post-processing techniques enhance the potential of MRI as they facilitate quantitative objectification (e.g. signal intensity ratios, fractionated anisotropy, mean diffusivity and volumetric analysis). This non-invasive assessment of anatomical anomalies and tissue responses can provide clinically relevant information for understanding and differentiating orbital pathologies^[9,10]. Orbital volumetric analysis is increasingly reported for all orbital tissues and can be useful in the management of different conditions such as Graves' orbitopathy, trauma or muscles palsy^[5,11,12]. To date, various MRI proto-

cols with inherently different characteristics have been reported to perform volumetric analysis. However, there is a lack of uniformity and the proposed protocols can be time consuming with difficulties to use in routine clinical practice. When volumetric analysis is required as an objective quantitative outcome for diagnosis and treatment planning, it should be clear which scanning protocols are most suitable and which level of accuracy can be reached.

Therefore, the main objectives of this study are (I) to select the most optimal MRI scanning protocols for orbital soft tissue volumetry and (II) to assess reproducibility and measurement accuracy when using these protocols with a semi-automatic segmentation method. These developments are expected to enhance precision and practical use of orbital volumetric measurements, thus facilitating their routine incorporation for clinical as well as research purposes.

Materials and Methods

This study consisted of two stages: development and validation. In the development stage, the most suitable MRI protocols were qualitatively selected for assessing orbital tissue volumes. Followed by a validation stage to quantitatively evaluate the accuracy and reproducibility of the selected MRI protocols.

Development stage

One healthy volunteer was recruited (male, 31y). MRI scans (3T, Siemens Magnetom Prisma, Siemens Healthcare, Erlangen, Germany) were obtained with 4-channel loop coils (7 inch) or a 64-channel head coil. The volunteer was

instructed to keep the eyes closed without movement during scanning.

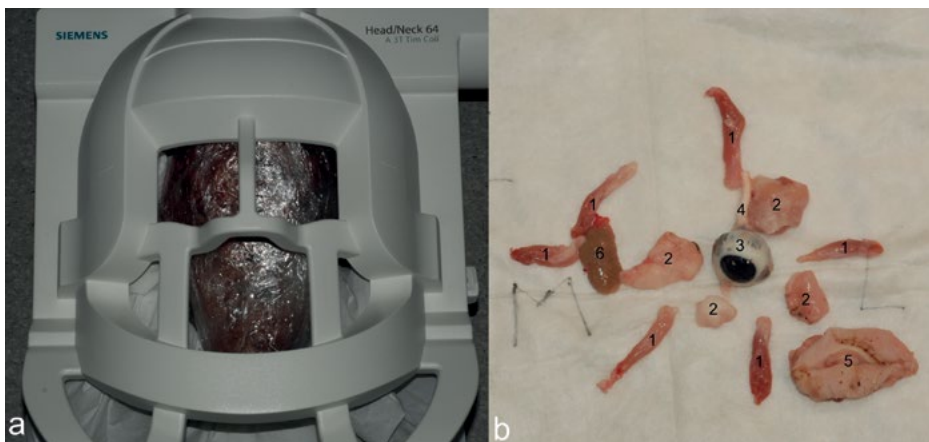
A selection of 12 MRI scanning protocols was obtained based on a comprehensive review of recent literature and suggestions by the MRI physicians and senior head and neck radiologist (Supplementary Table A). The default sequence parameters could be adjusted for the following acquisition characteristics: (1) pixel resolution, (2) slice thickness, (3) interslice gap (4) use of additional image post-processing/reconstruction filters (3D mode, distortion correction, edge enhancement, smoothing) and (5) field of view. Acquisition time for each sequence was kept as low as possible to avoid motion artifacts. All images were recorded in Digital Imaging and Communications in Medicine 3.0 (DICOM) format, anonymised and transferred to a workstation for analysis. Two observers independently performed a qualitative image analysis to evaluate resolution, soft tissue contrast, image distortion, and quality of multiplanar recon-

structions. Image quality was graded by using a 5-point Likert-like scale (1=poor, 2=suboptimal, 3=acceptable, 4=good, and 5=excellent)^[13].

Validation stage

The qualitative ratings of the 2 readers were averaged and the three most optimized MRI protocols were selected based on the qualitative analysis: MPRAGE, T2 SPACE ZOOMit and T1 TSE Dixon. Validation of these protocols was performed with three fresh cadaveric pig heads (crossbreds from Duroc and Pietrain, 10 weeks old, male). Efforts were made to maintain a physiological tissue temperature during MRI scanning to obtain the most realistic images. Next, CT scans of the cadaver heads were acquired through the multidetector technique with a field of view containing the orbital structures (Siemens Somatom AS). A single volume of data was acquired in the axial plane at 1 mm thickness. All images were recorded in DICOM 3.0 format and transferred to

FIGURE 5.1.



(a) The pig cadaver head is positioned and stabilized inside the 64-channel head coil for MRI scanning. (b) The orbital content is dissected with identification of (1) the extraocular muscles, (2) the orbital fat, (3) the globe, (4) the optic nerve, (5) skin and eyelids, (6) lacrimal gland.

a workstation for analysis. Finally, the orbital soft tissues were dissected to obtain the true volumes of the anatomical specimens. During dissection, all intra-orbital tissue was exenterated and the components of interest (orbital fat, extraocular muscles (EOM), globe) were carefully separated from other tissue (skin, lacrimal gland, optic nerve) (Figure 5.1). The volume of the anatomical specimen was assessed by submersion in a 10cc syringe with physiological saline solution.

The study adhered to the tenets of the declaration of Helsinki. Institutional review board approval and informed consent were obtained (B670201836944).

Post-processing and volumetric analysis

A senior head and neck radiologist (KO) analysed the MRI images with Synapse 3D (Fujifilm Co., Tokyo, Japan) software on two different occasions. A second observer (RW, maxillofacial surgeon) performed the analysis of the CT images using the Mimics Medical 21.0 software (Materialise, Leuven, Belgium). The workstation included a 21.3-inch flat-panel color-active matrix thin-film-transistor medical display (Nio Color 3MP, Barco, Kortrijk, Belgium) with a resolution of 2048x1536 pixels at 76 Hz. Enhancements and orientation tools such as magnification, brightness, and contrast could be used to improve visualization of the landmarks. Each assessment required 15 to 30 minutes.

The Synapse 3D software allowed for a semi-automatic, threshold based (region grow and multi-dimensional threshold) segmentation of the different orbital structures. The software automatically

recognizes muscle, fat and vitreous body, among other tissues. Intra- and extra-conal fat volumes were joined. All extraocular muscles were analysed as one volume. The globe volume was calculated by segmenting the intra-ocular fluid and vitreous body. Following the tissue segmentation, the volume was automatically measured on the workstation. A 3D reconstruction of the orbital fat, muscles and globe was generated and saved as a stereolithography (STL) file.

Tissue volumetry on CT images was conducted according to the validated protocol by Regensburg et al.^[3] using Mimics software. The specific orbital tissues were identified using a multi-dimensional threshold based segmentation method with the possibility of manual adjustment on each slice. Different masks were created for the total orbital tissue, orbital fat (intra- and extra-conal) and rectus muscles. The software automatically calculated the volume of the fat and rectus muscles. The globe volume was assessed by creating a sphere simulating the globe based on four points marking the border of the sclera and the volume of the sphere represented the globe volume^[14].

Statistical analysis

Mean differences (MD) and standard error of the mean (SE) of orbital tissue volumes (orbital fat, extraocular muscles and globe) were calculated for MRI data, CT data and the anatomical specimens. The accuracy of the different MRI sequences was determined by a comparison of the volumetric values between MRI and anatomical specimen. P-values were calculated using a paired sample t-test. Pearson's correlation coefficient was calculated to

study the correlation between the volumetric values on MRI or CT and the anatomical specimen. The intraclass correlation coefficient (ICC) using a two-way mixed-effects model was applied to study the intra-observer variability. ICC can be interpreted as following: value of 1 indicates perfect agreement; values of >0.9 are considered ideal to be used in a clinical setting. Values of $0.75 - 0.9$ represent good agreement, < 0.75 and ≥ 0.5 is moderate, and <0.5 is poor reliability^[15,16]. Right and left orbits were examined separately. Data was analysed using Statistical Package for Social Science (SPSS) (version 25.0; SPSS Inc., Chicago, IL, USA) and Jamovi (Version 1.2, retrieved from <https://www.jamovi.org>). A P-value <0.05 was considered significant.

Results Development stage results

Datasets from 12 different MRI scanning protocols were obtained from one human orbit (Supplementary Table A; Supplementary Figure A). In nine scanning protocols, the surface loop coil was used with bilateral ($n=7$) or unilateral ($n=2$) activation. The remaining three protocols were acquired with a 64-channel head coil. Pixel resolution ranged from 0.2×0.2 mm to 1.0×1.0 mm and half of the protocols contained isotropic voxels (i.e. same intensity and dimension regardless of the plane of reconstruction). Slice thickness varied from 0.5 mm to 3 mm with no or only minimal (0.6 mm) interslice gap. Different post-processing filters (e.g. 3D mode, distortion correction, smoothing) were used according to the specific acquisition protocol. Mean acquisition time was 4 min. 3 sec. (range 2 min. to 7 min. 4 sec.).

Results of the qualitative evaluation of these acquisition protocols are provided in Table 5.1. When compared to the surface coil, images obtained with the 64-channel head coil provided superior resolution of the orbital tissues (Figure 5.2). Figure 5.3 shows how selection of a distinct protocol can optimize the tissue contrast in function of the analysed region of interest. The datasets consisting of isotropic voxel size and low slice thickness provided the best multiplanar reconstructions (Figure 5.4).

Validation stage results

Table 5.2 shows details of the three selected dedicated acquisition protocols. The original T1 TSE (Turbo Spin Echo) Dixon sequence was modified to create a more isotropic voxel (from $0.6 \times 0.6 \times 1.5$ mm to $0.7 \times 0.7 \times 1.2$ mm) and the interslice gap was removed. Only the 64-channel head coil was used.

Table 5.3 and Figure 5.5 illustrate the volumetric difference when comparing the anatomical specimens to the image analysis with the different MRI protocols. Accuracy of the volumetric analysis with the T2 SPACE (sampling perfection with application-optimized contrasts by using flip angle evolution) ZOOMit protocol was superior for the extraocular muscles (MD 0.17 cm³) and the globe (MD -0.33 cm³), representing respectively 7% and 8% relative volume difference compared to the true volume. The T1 TSE Dixon protocol provided the most accurate results for the orbital fat measurements (MD -0.77 cm³, relative volume difference of 15%). Overall, MRI analysis tended to underestimate the real volume. Measurement errors were most explicit for the fat volume analysis (15 to 38% relative volume difference).

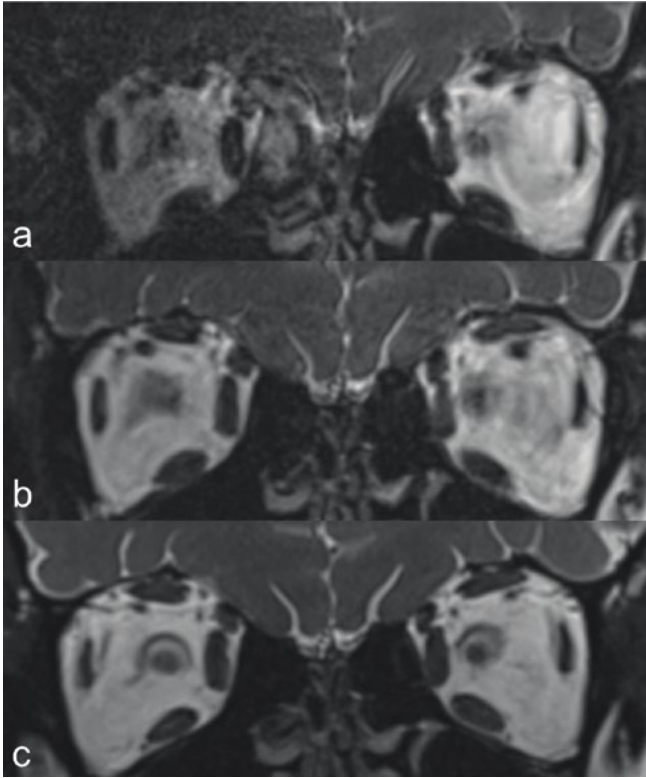


FIGURE 5.2. — INFLUENCE OF COIL SELECTION ON THE QUALITY OF ORBITAL MR IMAGES | All images were obtained with a T2 SPACE ZOOMit, isotropic voxel (0.5 mm) protocol. Image resolution improves when using the 64-channel head coil (c) compared to unilateral left loop coil (a) or bilateral loop coil (b).

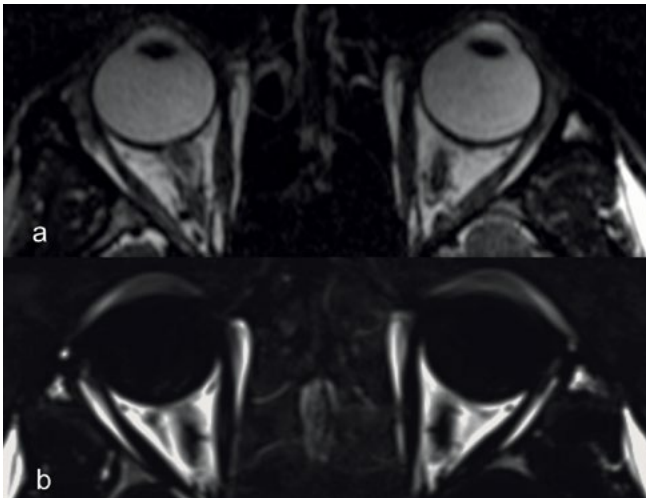


FIGURE 5.3. — TISSUE CONTRAST OPTIMISATION IN FUNCTION OF THE REGION OF INTEREST

- (a) A T2 SPACE ZOOMit sequence depicts the globe and extraocular muscles very detailed.
- (b) A T1 TSE Dixon sequence (fat images) produces a sharp contrast between the orbital fat and surrounding tissues.

Pearson correlation coefficients were illustrated in Figure 5.6 for the most accurate MRI protocols (T2 SPACE ZOOMit for EOM and globe; T1 TSE Dixon for orbital fat) and the CT, compared to the anatomical specimen. All image-based measurements, except fat volumetry on CT, illustrated a strong positive correlation with the true volume (Pearson's r

0.83-0.99). MRI volumetry of EOM and fat correlated better with the true volume compared to CT-based measurements. For the volumetric measurement of the globe, however, analysis on CT illustrated an almost perfect agreement with the volume of the anatomical specimen (Pearson's $r = 0.99$).

TABLE 5.1. — QUALITATIVE EVALUATION OF MRI SCANNING PROTOCOLS IN THE DEVELOPMENT STAGE

Sequence	Coil	Imaging Plane	Pixel (mm)	Slice thickness (mm)	Image resolution	Soft tissue contrast	Image distortion	Multiplanar reconstruction
MPRAGE	Bilateral loop coil	Coronal	0.5x0.5	0.5	3/3	3/2	No	4/3
T2 SPACE ZOOMit	Bilateral loop coil	Coronal	0.5x0.5	0.5	3/2	3/3	Inhomogeneity at right side	3/3
T1 TSE	Unilateral (L) loop coil	Transversal	0.2x0.2	1.5	2/1	2/2	Gibs ringing	1/2
T2 SPACE ZOOMit	Unilateral (L) loop coil	Coronal	0.5x0.5	0.5	3/3	3/3	Inhomogeneity and wrap around at right side	3/3
T1 SE	Bilateral loop coil	Transversal	0.3x0.3	3.0	3/2	3/3	Gibs ringing	1/2
T1 TSE Dixon	Bilateral loop coil	Transversal	0.6x0.6	3.0	3/3	4/3	No	1/1
T1 VIBE Dixon	Bilateral loop coil	Coronal	1.0x1.0	1.0	2/1	3/3	Chemical shift artifact	2/2
T1 TSE Dixon	Bilateral loop coil	Transversal	0.6x0.6	1.5	3/3	4/3	No	2/2
T2 TSE Dixon	Bilateral loop coil	Transversal	0.8x0.8	3.0	3/2	3/3	No	1/1
MPRAGE	64-channel head coil	Coronal	0.5x0.5	0.5	4/3	4/5	3D aliasing / wrap around artifact	4/3
T2 SPACE ZOOMit	64-channel head coil	Coronal	0.5x0.5	0.5	5/4	5/5	No	4/5
T1 TSE Dixon	64-channel head coil	Transversal	0.7x0.7	1.2	5/5	5/5	No	3/4

Quality rating (Observer A/B): 1: poor; 2: suboptimal; 3: acceptable; 4: good; 5: excellent.

MPRAGE: magnetization-prepared rapid gradient-echo; SPACE: sampling perfection with application-optimized contrasts by using flip angle evolution; (T)SE: (Turbo) Spin Echo; VIBE: volumetric interpolated breath-hold examination. L: Left.

TABLE 5.2. — ACQUISITION DETAILS OF THREE DEDICATED MRI SEQUENCES

Sequence	Coil	Imaging Plane	Matrix (mm)	Pixel (mm)	Slice thickness (mm)	Interslice gap (mm)	TE/TR (msec)	Scan time (min:sec)	Filter
MPRAGE	Headcoil	Coronal	263 x350 x350	0.5 x0.5	0.5	0.25	3.33 /1520	4:37	- 3D mode - Distortion correction
T2 SPACE ZOOMit	Headcoil	Coronal	263 x350 x350	0.5 x0.5	0.5	0	127 /1000	4:14	- 3D mode - Distortion correction
TI TSE Dixon	Headcoil	Axial	180 x164 x34	0.7 x0.7	1.2	0	14 /1230	6:08	- 3D mode - Distortion correction - Edge enhancement - Smoothing

TE: echo time; TR: repetition time; MPRAGE: magnetization-prepared rapid gradient-echo; SPACE: sampling perfection with application-optimized contrasts by using flip angle evolution; TSE: turbo spin echo

TABLE 5.3. — VOLUMETRIC DIFFERENCE WHEN COMPARING ANATOMICAL SPECIMEN WITH VOLUME ANALYSIS BY THE DEDICATED MRI PROTOCOLS

Measurement error (cm ³) for MRI analysis		MPRAGE	TI TSE Dixon	T2 SPACE ZOOMit
EOM	Mean difference (SE)	-0.57 (0.08)	-0.43 (0.09)	0.17 (0.06)
	95% CI	-0.76; -0.37	-0.66; -0.21	0.02; 0.31
	Relative difference	24%	18%	7%
	P-value	<0.001	0.004	0.030
Globe	Mean difference (SE)	-0.92 (0.11)	-1.10 (0.14)	-0.33 (0.12)
	95% CI	-1.21; -0.62	-1.47; -0.73	-0.65; 0.04
	Relative difference	22%	26%	8%
	P-value	<0.001	<0.001	0.070
Orbital fat	Mean difference (SE)	-1.72 (0.15)	-0.77 (0.15)	-1.8 (0.16)
	95% CI	-2.10; -1.33	-1.03; -0.44	-2.22; -1.38
	Relative difference	36%	15%	38%
	P-value	<0.001	0.001	<0.001

MPRAGE: magnetization-prepared rapid gradient-echo; SPACE: sampling perfection with application-optimized contrasts by using flip angle evolution; TSE: turbo spin echo. EOM: extraocular muscles; 95% CI: 95% confidence interval of the difference in the study sample; SE: standard error. The P-values are calculated with the paired sample t-test.

TABLE 5.4. — INTRA-OBSERVER REPRODUCIBILITY FOR MRI VOLUMETRY

	EOM	Globe	Orbital fat
ICC	0.92	0.96	0.94
95% CI	0.530-0.989	0.002-0.996	0.588-0.992

EOM: extraocular muscles; ICC: intraclass correlation coefficient (two-way mixed effects model); CI: confidence interval

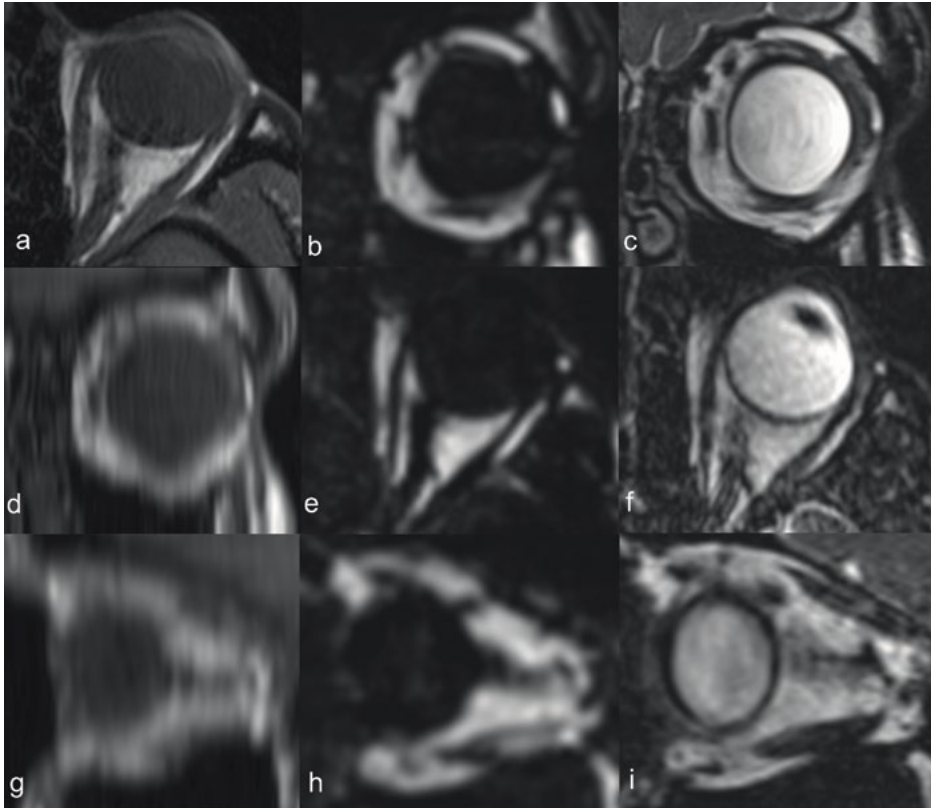
Intra-observer agreement was ideal (ICC > 0.9) for volumetric analysis using the most accurate MRI protocols (T2 SPACE ZOOMit for EOM and globe; T1 TSE Dixon for orbital fat) (Table 5.4).

Discussion

Volumetric assessment of the orbital tissues can be helpful in monitoring disease progress, to evaluate therapeutic response, for virtual treatment planning or for the definition

of normal values. MRI can be considered the optimal technique for (sequential) orbital imaging as it does not involve ionizing radiation, has excellent soft tissue contrast and can render images in any plane^[7]. MRI protocols are continuously developing and advancing, hereby increasing post-processing opportunities. The goal of this study was to find the most accurate MRI acquisition protocols to perform orbital volumetry.

FIGURE 5.4. — IMAGE QUALITY EVALUATION AFTER MULTIPLANAR RECONSTRUCTION | All images were obtained with bilateral activated surface loop coils.



Original scanning orientation (a) and reconstructed images (d, g) of a T1 SE sequence with anisotropic voxel size (0.3x0.3x3.0 mm). Original scanning orientation (b) and reconstructed images (e, h) of a T1 VIBE Dixon sequence (fat images) with isotropic voxel size (1.0x1.0x1.0 mm). Original scanning orientation (c) and reconstructed images (f, i) of a T2 Space ZOOMit sequence with isotropic voxel size (0.5x0.5x0.5 mm).

To answer this research question, the current study first screened a multitude of MRI acquisition protocols for the best image quality. In contrast to various studies advocating the use of surface loop coils for orbital imaging^[11,17,18], the images obtained with the 64-channel head coil provided superior image quality. Additionally, the qualitative analysis suggested using (nearly) isotropic voxels (0.5 to 1 mm) to obtain a good multiplanar reconstruction. This is important in volumetric measurements, as high quality reconstructions allow for accurate and simultaneous tissue segmentation in the three orthogonal planes. This could also be achieved by acquiring additional scans in every desired plane, but that would inherently lengthen the entire imaging protocol. When spatial resolution was less than 0.5 mm more artifacts like truncation or Gibbs ringing, were noticed. These artifacts, parallel to the edges of abrupt intensity change, are caused by data clipping at the edges of the acquired k-space^[19,20]. They are more common at higher field strengths with proportionally increased signal-to-noise ratio and can be reduced by either increasing the spatial resolution or by applying reconstruction filters to smoothly reduce the signal at the edges of k-space^[20]. Aliasing (or wrap-around) is another common artifact, which was also seen in the protocols used for this study. It can occur whenever any part of the body extends outside the field of view and a signal produced by this structure reaches the receiver coil^[19]. The body part outside the field of view is wrapped inside to the opposite side of the image and could mask anatomical structures. Various solutions could eliminate aliasing, e.g. filters or field of view increase, and should be discussed with the MRI technician^[19]. Image dis-

tortions due to eye movements are particularly important in orbital imaging. A change in globe position will alter muscle positions and volumes, hence, also change morphology of all adjacent tissues^[18]. A limited acquisition time is one of the most important factors to avoid motion artifacts. The T1 TSE Dixon was the lengthiest of the dedicated protocols (6 min) and this should be taken into account when subjecting a patient to multiple consecutive sequences in the same scan cycle. For this reason, especially for quantitative analysis, it can be recommended to use a fixation target during scanning.

The following dedicated 3D protocols were selected based on the findings from the qualitative analysis: (I) MPRAGE is a 3D T1 weighted sequence and is one of the most widely used sequences for brain volumetry. It is an inversion recovery fast gradient recalled-echo sequence^[21] with a very short echo and repetition time. Gradient echo techniques allow for rapid acquisition of 3D images^[22] and this sequence has been reported previously to measure the EOM and orbital fat volume with a semi-automatic segmentation method^[23,24]. (II) T2 Space ZOOMit: Space is a 3D fast spin echo sequence with variable flip-angle refocusing pulses. The sequence has been reported for detection and volumetry of brain metastasis^[21,22] and has also been described more recently to provide an accurate semi-automatic segmentation of the EOM and orbital fat volume^[12]. The ZOOMit function reduces artifacts by using a simultaneous parallel radiofrequency pulse sequence. This new technique minimizes the negative effects of folding artifacts and provides high image quality, decreased distortion and blurring, decreased motion and flow ar-

FIGURE 5.5. — ACCURACY OF THE DEDICATED MRI ACQUISITION PROTOCOLS | Boxplots with medians and means (x) represent the volumes of the anatomical specimen and volumetric analysis with the different MRI protocols. Volumetric analysis of the extraocular muscles and globe with the T2 SPACE ZOOMit protocol equals most to the anatomical specimen volume. Analysis of the fat volume is most accurate by using the T1 TSE Dixon protocol.

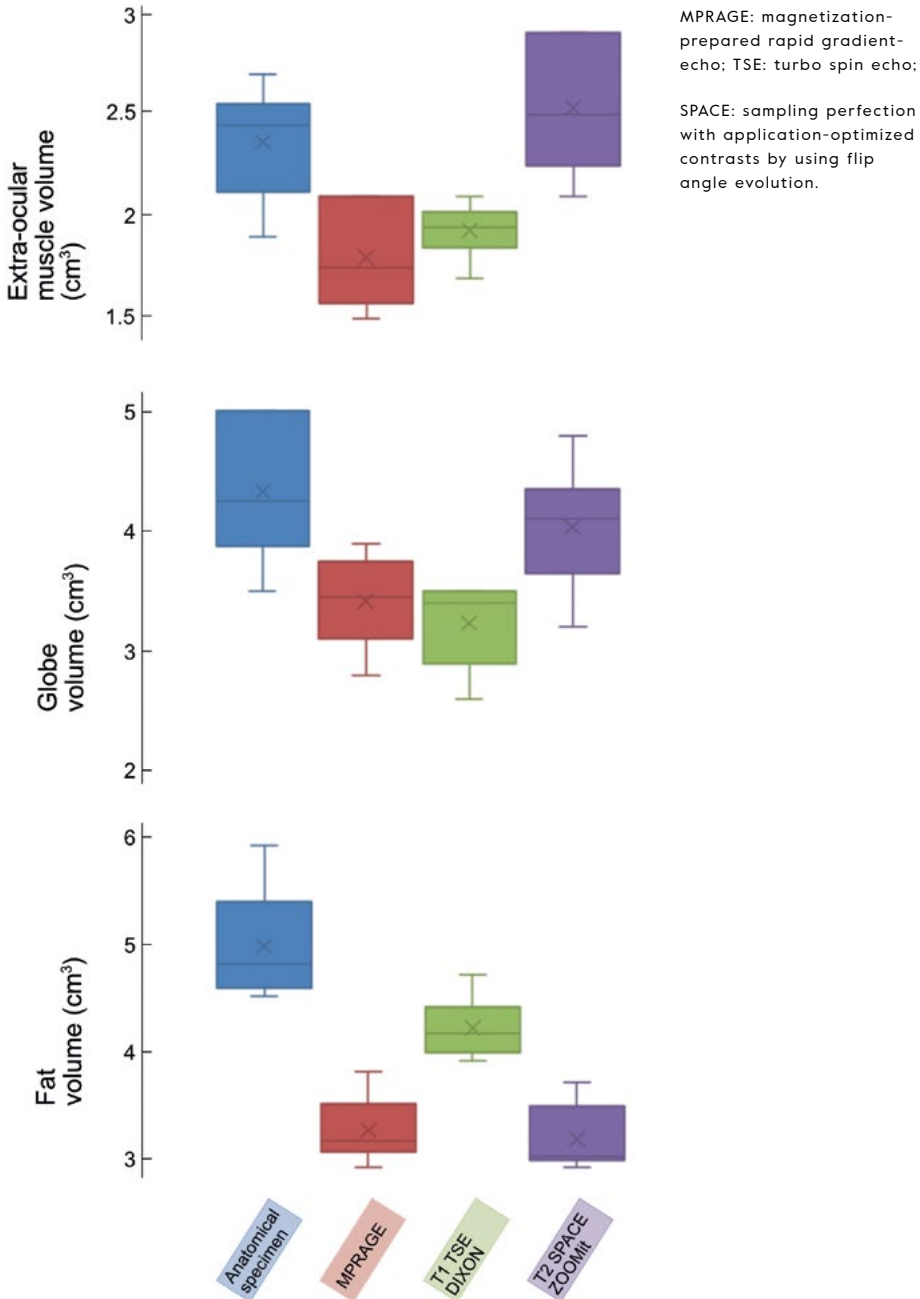
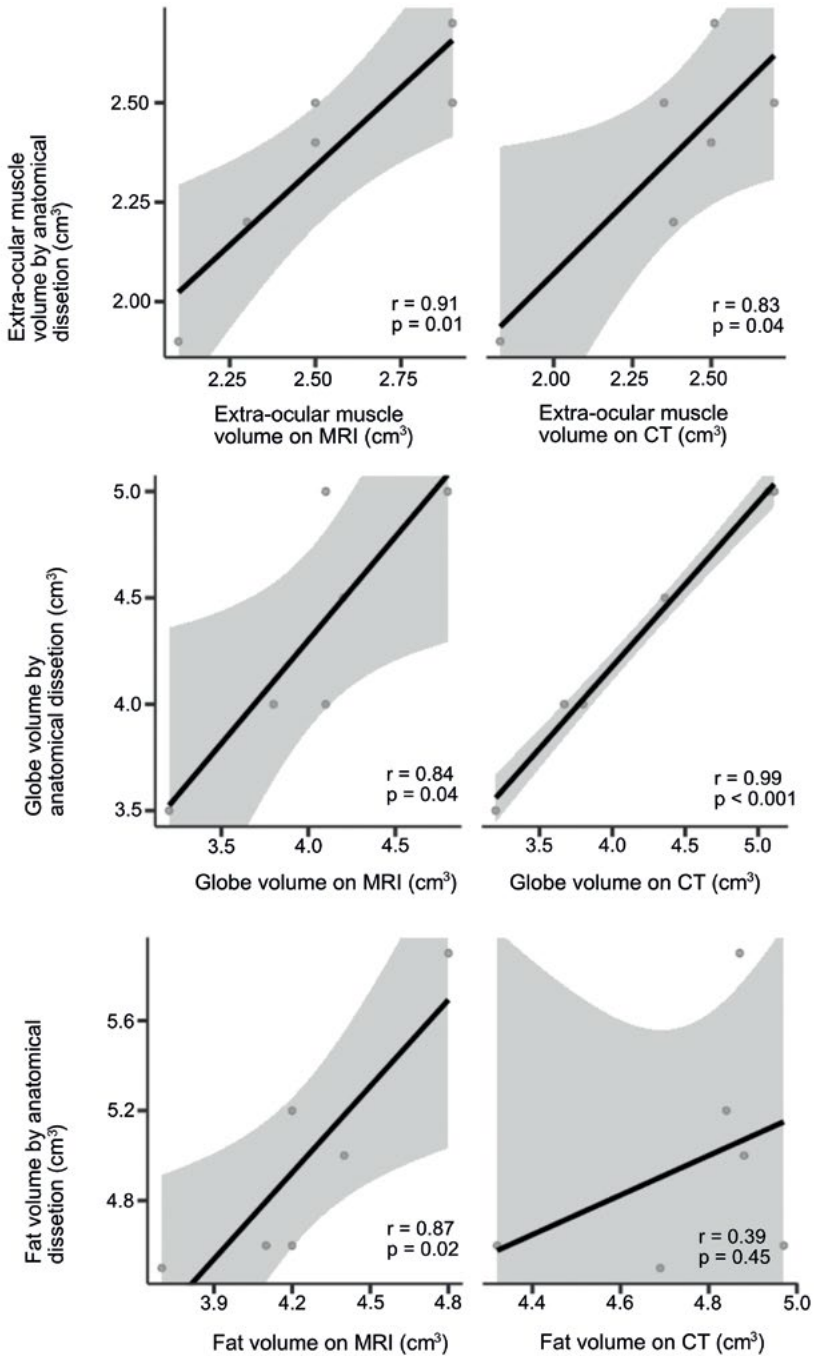


FIGURE 5.6. — SCATTERPLOT FOR CORRELATION OF VOLUMETRY ON MRI OR CT SCAN WITH THE TRUE ANATOMICAL VOLUME | Line of best fit (black) and confidence interval (grey) are illustrated. Pearson correlation (r) and p -value are provided.



tifacts, increased spatial resolution, and faster scanning. The protocol has potential to detect and evaluate smaller lesions, especially in areas prone to susceptibility artifacts and was reported for the diagnosis of optic neuritis^[25]. (III) The Dixon technique exploits the chemical shift differences of water and fat, and is able to separate water and fat proton signals to generate in-phase and out-of-phase images. These images are then used to calculate “fat-suppressed” water-only and “water-suppressed” fat-only images, rendering four series of images in a single acquisition. This saves time and the fat/water suppression is more robust with less artifacts^[26]. Other advantages of the Dixon technique are that it can be acquired in T1, T2 and proton density and with spin echo as well as gradient echo techniques. This technique has been proven successful for orbital fat volumetry in Graves’ orbitopathy^[5].

Many studies report the use of various MRI protocols for orbital volumetry, but few studies actually use a validated protocol. Tang et al. used both fatty and lean phantoms to assess accuracy with a Cube Fast Spin Echo flex sequence (3D T1 weighted sequence)^[12]. They reported a measurement error of 9.2% to 12.6% for a semi-automatic segmentation in the fatty phantoms and 10.3% to 14.1% in the lean phantoms. Shen et al. described and validated a T1 weighted Fast Spin Echo (comparable to MPRAGE) MRI protocol on a phantom consisting of butter and chicken wings^[23]. They reported an absolute relative error of 2.8% to 4.6% for fat volumetry and 0.7% to 4.1% for muscle volumetry. The use of phantom models allows for an optimal assessment of the true volume, but bypasses the difficulties asso-

ciated with segmentation of orbital tissues in a clinical setting, explaining the lower error values. In particular, the segmentation of the orbital fat is prone to variability because fat fills the spaces between other tissues and has no defined shape of its own^[17]. This probably explains the largest error for fat volumetry (mean relative difference 15%) in the current study. Use of the T2 SPACE ZOOMit sequence was most favourable for the estimation of the EOM (mean relative difference of 7%) and globe volume (mean relative difference of 8%), which is in line with previous reports^[12,23,24]. Except for the EOM volume, the current study confirms earlier studies stating that MRI tends to underestimate the true volume^[7,12,23]. Semi-automatic volume measurements with the selected MRI protocols showed to be very reproducible. This is an important finding because the successive changes in tissue volume have more clinical relevance compared to the absolute values of a single measurement. It has to be noted that morphometric discrepancies may occur when different sequences are used. This is confirmed by this study, even for well-defined structures as the globe. There are several implications for the clinical practice. First, consecutive scanning for orbital diseases should ideally be performed with the same scanning protocol. Second, one must be very cautious when comparing volumetric measurements obtained with different sequences. Moreover, comparison of absolute volumetric values between different studies is not recommended as the measurement error could exceed other detectable sources of volumetric change.

Different vendors may provide variable acquisition protocols, with the same

or different labels, e.g. SPACE can be called CUBE (GE Healthcare, Milwaukee, Wisconsin) or VISTA (Philips Healthcare, Best, the Netherlands). Application of these different protocols may result in different outcomes, although the same trend can be expected. Moreover, every acquisition protocol has some default parameters and it is not always possible to modify these without restrictions or causing additional artifacts (e.g. when aiming for isotropic voxels). This should be clarified with the service engineer, technician and radiologist before implementing a specific volumetry protocol in clinical practice.

The current study findings illustrate that MRI measurements for EOM and fat correlate better to the true volume than CT-based measurements. This is most pronounced for orbital fat volume and emphasizes the value of using the most optimal protocol (T1 TSE Dixon). This protocol results in a strong contrast between fat and other tissue, hereby optimizing the semi-automatic segmentation process and outcome accuracy. Regarding the globe volume, the correlation between MRI and anatomical specimens was lower than compared with the CT. The reason could be that the MRI-based segmentation outlined the inner border of the globe rather than the outer border, which was measured with CT volumetry and also when calculating the anatomical volume by submersion.

Some limitations should be considered when interpreting the results. The number of orbits to analyse the measurement accuracy was limited. Although efforts were made to maintain the normal body temperature in the cadaveric tissue, temperature changes could influence

MRI signals, introducing measurement bias. The orbital volume of the investigated cadavers is 2 to 3 times smaller than in human orbits, which demanded longer segmentation time. No imaging protocols with admission of intravenous contrast were used in this study. The non contrast-enhanced sequences, however, allowed for quantitative volumetric analysis, avoiding toxicity and cost of gadolinium^[27,28].

Conclusion

In conclusion, the current study illustrates that volumetry of orbital tissues is clinically feasible, accurate and reproducible when using dedicated MRI protocols. It is critical to select the most optimal sequence and acquisition parameters as different protocols can cause variable volumetric outcomes. The most optimal volumetry protocols are hereby suggested (T2 SPACE ZOOMit for EOM and globe; T1 TSE Dixon for orbital fat), but future studies should confirm these recommendations by integrating these protocols in clinical practice. Furthermore, the study results could serve as a basis to initiate fully automated segmentation techniques enhancing post-processing accuracy and practical implementation.

ACKNOWLEDGEMENTS

The authors want to express their gratitude to Dr. J. Fransen for his contribution during dissection of the cadaveric specimens.

This research did not receive any specific grant from funding agencies in the public, commercial, or not-for-profit sectors.

The authors declare that they have no conflict of interest.

All procedures performed in the study were in accordance with the ethical standards of the institutional and/or national research committee (Ethical review board University Hospital Ghent, reference number B670201836944) and with the 1964 Helsinki declaration and its later amendments or comparable ethical standards.

Informed consent was obtained from the participant included in the study.

REFERENCES

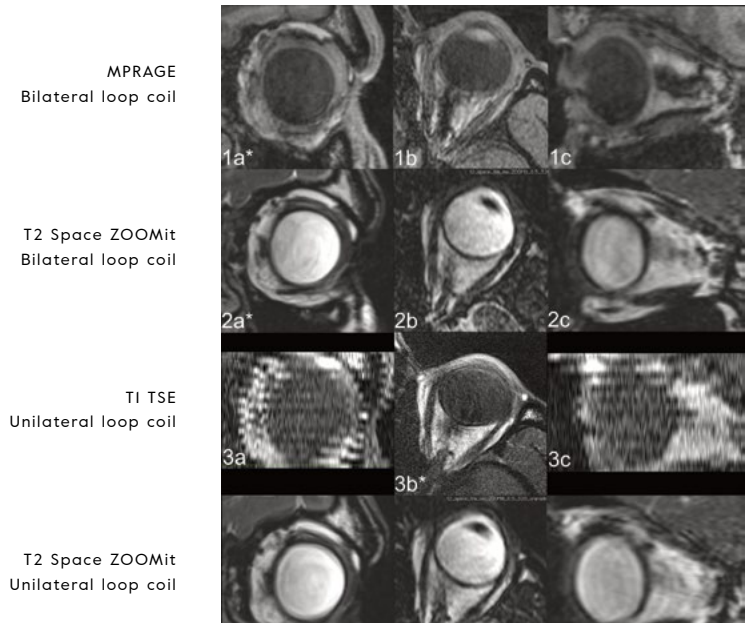
- [1] Müller-Forell W, Kahaly GJ. Neuroimaging of Graves' orbitopathy. Vol. 26, Best Practice and Research: Clinical Endocrinology and Metabolism. 2012. p. 259–71.
- [2] Siakallis LC, Uddin JM, Miszkil KA. Imaging Investigation of Thyroid Eye Disease. Vol. 34, Ophthalmic plastic and reconstructive surgery. 2018. p. S41–51.
- [3] Regensburg NI, Kok PHB, Zonneveld FW, Baldeschi L, Saeed P, Wiersinga WM, et al. A new and validated CT-Based method for the calculation of orbital Soft tissue volumes. *Investig Ophthalmol Vis Sci.* 2008;49(5):1758–62.
- [4] Tan JSP, Tan KL, Lee JCL, Wan CM, Leong JL, Chan LL. Comparison of eye lens dose on neuroimaging protocols between 16- And 64-section multidetector CT: Achieving the lowest possible dose. *Am J Neuroradiol.* 2009;30(2):373–7.
- [5] Kaichi Y, Tanitame K, Itakura H, Ohno H, Yoneda M, Takahashi Y, et al. Orbital Fat Volumetry and Water Fraction Measurements Using T2-Weighted FSE-IDEAL Imaging in Patients with Thyroid-Associated Orbitopathy. *Am J Neuro-radiol.* 2016 Nov;37(11):2123–8.
- [6] Schmutz B, Rahmel B, McNamara Z, Coulthard A, Schuetz M, Lynham A. Magnetic resonance imaging: an accurate, radiation-free, alternative to computed tomography for the primary imaging and three-dimensional reconstruction of the bony orbit. *J Oral Maxillofac Surg.* 2014 Mar;72(3):611–8.
- [7] Firbank MJ, Coulthard A. Evaluation of a technique for estimation of extraocular muscle volume using 2D MRI. *Br J Radiol.* 2000 Dec;73(876):1282–9.
- [8] Tian S, Nishida Y, Isberg B, Lennerstrand G. MRI measurements of normal extraocular muscles and other orbital structures. *Graefes Arch Clin Exp Ophthalmol.* 2000;238(5):393–404.
- [9] Watanabe M, Buch K, Fujita A, Jara H, Qureshi MM, Sakai O. Quantitative MR imaging of intra-orbital structures: Tissue-specific measurements and age dependency compared to extra-orbital structures using multispectral quantitative MR imaging. *Orbit (London).* 2017;36(4):189–96.
- [10] Majos A, Grzelak P, Mlynarczyk W, Stefanczyk L. Eyeball muscles' diameters versus volume estimated by numerical image segmentation. *Eur J Ophthalmol.* 2007;17(3):287–93.
- [11] Suh SY, Clark RA, Le A, Demer JL. Extraocular Muscle Compartments in Superior Oblique Palsy. *Invest Ophthalmol Vis Sci.* 2016;57(13):5535–40.
- [12] Tang X, Liu H, Chen L, Wang Q, Luo B, Xiang N, et al. Semi-automatic volume measurement for orbital fat and total extraocular muscles based on Cube FSE-flex sequence in patients with thyroid-associated ophthalmopathy. *Clin Radiol.* 2018;73(8):759.e11-759.e17.
- [13] Gaddikeri S, Mossa-Basha M, Andre JB, Hippe DS, Anzai Y. Optimal Fat Suppression in Head and Neck MRI: Comparison of Multipoint Dixon with 2 Different Fat-Suppression Techniques, Spectral Presaturation and Inversion Recovery, and STIR. *Am J Neuroradiol.* 2018;39(2):362–8.
- [14] Willaert R, Shaheen E, Deferm J, Vermeersch H, Jacobs R, Mombaerts I. Three-dimensional characterisation of the globe position in the orbit. *Graefes Arch Clin Exp Ophthalmol.* 2020;
- [15] Koo TK, Li MY. A Guideline of Selecting and Reporting Intraclass Correlation Coefficients for Reliability Research. *J Chiropr Med.* 2016;15(2):155–63.
- [16] Kottner J, Audige L, Brorson S, Donner A, Gajewski BJ, Hróbjartsson A, et al. Guidelines for Reporting Reliability and Agreement Studies (GRRAS) were proposed. *Int J Nurs Stud.* 2011 Jun;48(6):661–71.
- [17] Nishida Y, Tian S, Isberg B, Tallstedt L, Lennerstrand G. Significance of orbital fatty tissue for exophthalmos in thyroid-associated ophthalmopathy. *Graefes Arch Clin Exp Ophthalmol.* 2002;240(7):515–20.
- [18] Clark RA, Demer JL. Changes in Extraocular Muscle Volume During Ocular Duction. *Invest Ophthalmol Vis Sci.* 2016;57(3):1106–11.
- [19] Stadler A, Schima W, Ba-Ssalamah A, Kettenbach J, Eisenhuber E. Artifacts in body MR imaging: Their appearance and how to eliminate them. *Eur Radiol.* 2007;17(5):1242–55.
- [20] Dietrich O, Reiser MF, Schoenberg SO. Artifacts in 3-T MRI: Physical background and reduction strategies. *Eur J Radiol.* 2008;65(1):29–35.
- [21] Danieli L, Riccitelli GC, Distefano D, Prodi E, Ventura E, Cianfoni A, et al. Brain Tumor-enhancement visualization and morphometric assessment: A comparison of MPRAGE, SPACE, and VIBE MRI techniques. *Am J Neuroradiol.* 2019;40(7):1140–8.
- [22] Kato Y, Higano S, Tamura H, Mugikura S, Umetsu A, Murata T, et al. Usefulness of contrast-enhanced T1-weighted sampling perfection with application-optimized contrasts by using different flip angle evolutions in detection of small brain metastasis at 3T MR imaging: Comparison with magnetization-prepared rapid acquisition. *Am J Neuroradiol.* 2009;30(5):923–9.

- [23] Shen J, Jiang W, Luo Y, Cai Q, Li Z, Chen Z, et al. Establishment of magnetic resonance imaging 3D reconstruction technology of orbital soft tissue and its preliminary application in patients with thyroid-associated ophthalmopathy. *Clin Endocrinol (Oxf)*. 2018 May;88(5):637–44.
- [24] Firbank MJ, Harrison RM, Williams ED, Coulthard A. Measuring extraocular muscle volume using dynamic contours. *Magn Reson Imaging*. 2001 Feb;19(2):257–65.
- [25] Seeger A, Schulze M, Schuettauf F, Ernemann U, Hauser TK. Advanced diffusion-weighted imaging in patients with optic neuritis deficit – value of reduced field of view DWI and readout-segmented DWI. *Neuroradiol J*. 2018;31(2):126–32.
- [26] Santos Armentia E, Martín Noguero T, Suárez Vega V. Advanced magnetic resonance imaging techniques for tumors of the head and neck. *Radiol (English Ed [Internet])*. 2019;61(3):191–203. Available from: <https://doi.org/10.1016/j.rxeng.2019.03.005>
- [27] Garau LM, Guerrieri D, De Cristofaro F, Bruscolini A, Panzironi G. Extraocular muscle sampled volume in Graves' orbitopathy using 3-T fast spin-echo MRI with iterative decomposition of water and fat sequences. *Acta Radiol Open*. 2018;7(6):205846011878089.
- [28] Daubner D, Spieth S, Engelland K, Von Kummer R. Diagnose und differenzialdiagnose der endokrinen orbitopathie in der MRT. *Radiologe*. 2012;52(6):550–9.

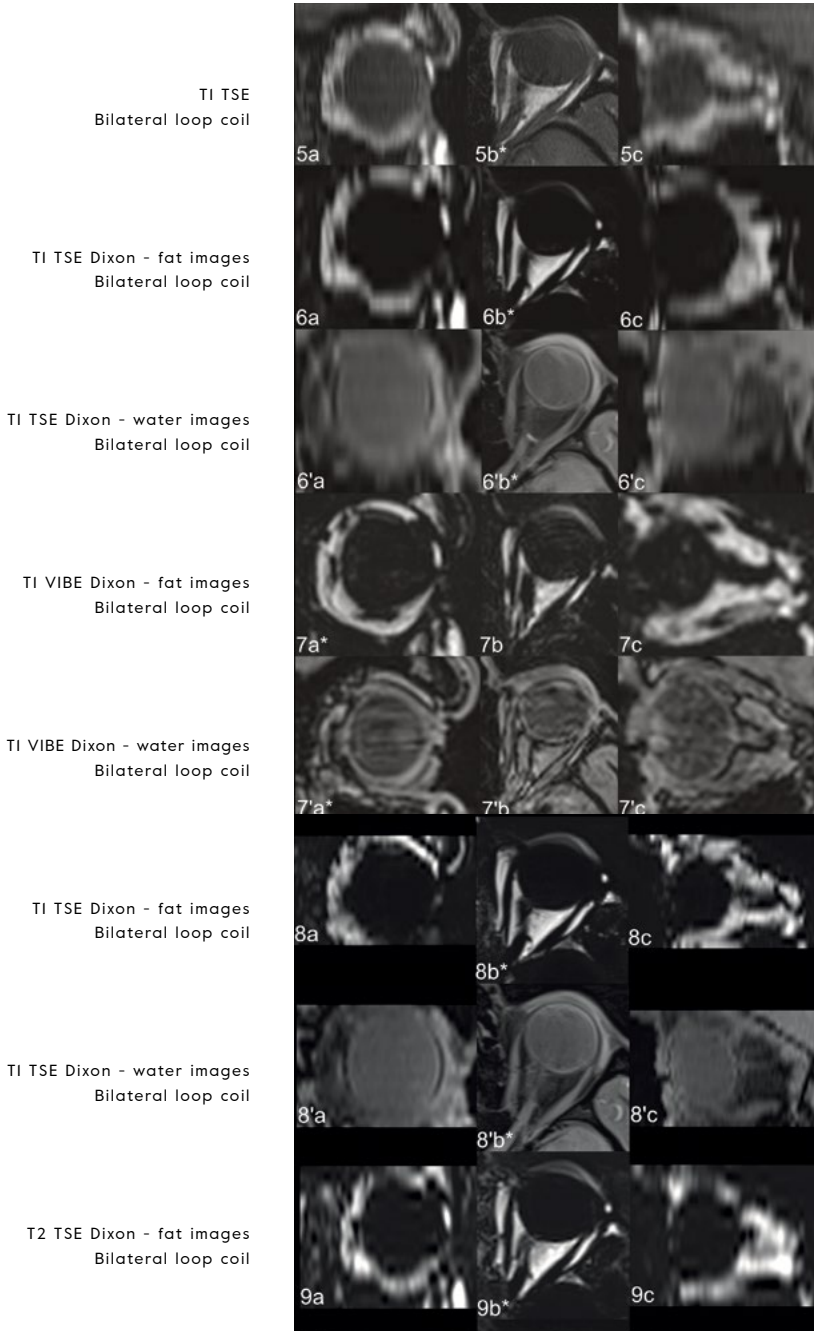
SUPPLEMENTARY MATERIAL

SUPPLEMENTARY FIGURE A —IMAGES OBTAINED IN THE DEVELOPMENT STAGE | The left orbit is displayed at the level of maximum globe dimension in the (a) coronal, (b) axial and (c) sagittal plane. The original scanning plane is marked (*) and the other images are the orthogonal reconstructions.

(Figure A is continued on the next page)

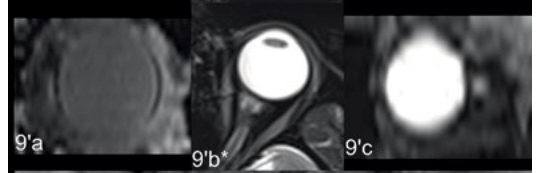


SUPPLEMENTARY FIGURE A CONTINUED

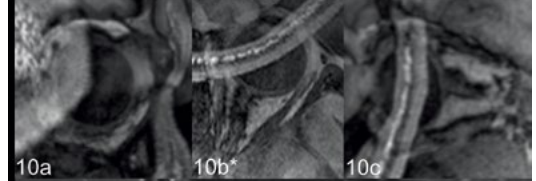


SUPPLEMENTARY FIGURE A CONTINUED

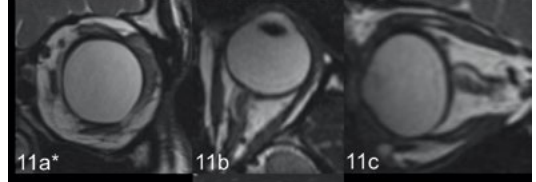
T2 TSE Dixon - water images
Bilateral loop coil



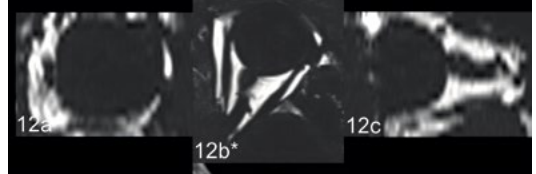
MPRAGE
64-channel head coil



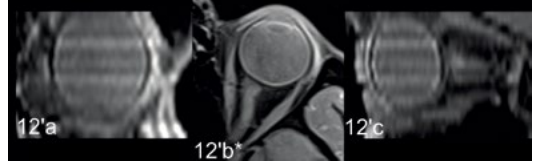
T2 Space ZOOMit
64-channel head coil



T1 TSE Dixon - water images
64-channel head coil



T1 TSE Dixon - water images
64-channel head coil



SUPPLEMENTARY TABLE A — ACQUISITION DETAILS OF 12 DIFFERENT MRI PROTOCOLS USED IN THE DEVELOPMENT STAGE

Sequence	Coil	Imaging Plane	Matrix (mm)	Pixel (mm)	Slice thickness (mm)	Interslice gap (mm)	TE/TR (msec)	Scan time (min:sec)	Filter
MPRAGE	Bilateral loop coil	Coronal	263x350x350	0.5x0.5	0.5	0.25	3.33/1520	4:37	- 3D mode - Distortion correction
T2 SPACE ZOOMit	Bilateral loop coil	Coronal	263x350x350	0.5x0.5	0.5	0	127/1000	4:14	- 3D mode - Distortion correction
T1 TSE	Unilateral (L) loop coil	Axial	80x80x36	0.2x0.2	1.5	0	15/682	5:52	/
T2 SPACE ZOOMit	Unilateral (L) loop coil	Coronal	263x350x350	0.5x0.5	0.5	0	127/1000	7:35	- 3D mode - Distortion correction
T1 SE	Bilateral loop coil	Axial	263x350x350	0.3x0.3	3.0	0	17/525	2:01	/
T1 TSE Dixon	Bilateral loop coil	Axial	180x180x54	0.6x0.6	3.0	0.6	12/580	4:13	- Edge enhancement - Smoothing
T1 VIBE Dixon	Bilateral loop coil	Coronal	380x214x20	1.0x1.0	1.0	0.2	(1) 2.46 (2) 3.69 /5.60	3:20	- 2D mode - Distortion correction
T1 TSE Dixon	Bilateral loop coil	Axial	180x164x34	0.6x0.6	1.5	0.3	14/797	4:25	- Edge enhancement - Smoothing
T2 TSE Dixon	Bilateral loop coil	Axial	210x210x50	0.8x0.8	3.0	0.3	82/4000	2:50	- 2D mode - Distortion correction - Edge enhancement - Smoothing
MPRAGE	64-channel head coil	Coronal	263x350x350	0.5x0.5	0.5	0.25	3.33/1520	4:37	- 3D mode - Distortion correction
T2 SPACE ZOOMit	64-channel head coil	Coronal	263x350x350	0.5x0.5	0.5	0	127/1000	4:14	- 3D mode - Distortion correction
T1 TSE Dixon	64-channel head coil	Axial	180x164x34	0.6x0.6	1.2	0.3	14/1230	6:08	- 3D mode - Distortion correction - Edge enhancement - Smoothing

TE: echo time; TR: Repetition time; MPRAGE: magnetization-prepared rapid gradient-echo; SPACE: sampling perfection with application-optimized contrasts by using flip angle evolution; (T)SE: (Turbo) Spin Echo; VIBE: volumetric interpolated breath-hold examination. L: Left.

Discussion

The orbit comprises a complex architecture of soft tissues and bone. Disease-related changes in the orbital structure cause severe problems, such as pain, diplopia, impaired vision and globe displacement. Imaging of the soft tissues of the orbit is mandatory for diagnosis and surgical planning. It produces an objective representation and enables a detailed analysis of the individual orbital structure.

The position of the globe in the orbit is a key element when studying the orbital architecture. Significant changes of the globe position result in limited eye movement, enoftalmos, proptosis or globe displacement. Accurate documentation of the globe position can improve the understanding of pathophysiological mechanisms and provide essential information to plan rehabilitative surgery.

As current measurement methods contain important drawbacks^[1-3], new approaches that could reliably document the globe position are required for objective evaluation. The first article of this thesis validates a new method to three-dimensionally define the globe position. Optimal reproducibility was illustrated with high inter- and intraobserver agreement on separate analysis in X, Y and Z axis. This technique also defines an Euclidean movement of the globe as a combination of the shift on each individual axis. Moreover, the amount of change is positively correlated with the severity of preoperative proptosis and the size of the Euclidean shift exceeded the movement on each axis. To the best of our knowledge, the resulting Euclidean shift of the globe is not yet described in literature. We believe that the Euclidean movement of the globe can be used in orbital decompression surgery to monitor the outcome and to detect unusual 3D shifting of the globe. Future investigations are needed to clarify its clinical role and confirm whether the resulting 3D position change is sufficiently reliable to interpret globe position changes.

The position of the globe is determined by the orbital cavity (bony framework) on one hand and the amount of tissue occupying this cavity, thus supporting the globe on the other hand. As orbital fat constitutes more than half of the soft tissue volume, it plays an important role in defining the globe position^[4,5]. The volume of fat can be shifted, as seen in orbital fractures and bony decompression surgery, increased due to thyroid eye disease, or decreased after radiotherapy or fat decompression surgery. Imaging studies of the volume and position of the intra- and extraconal fat in relation to the globe are of value to tailor the outcome of reconstructive surgery that aims to restore the normal globe position. The second article of this thesis reviews orbital fat decompression surgery for the reduction of proptosis in thyroid eye disease^[6-10]. Some authors describe a linear association between anteroposterior globe position and fat volume^[9]. Others suggest an

equation, that includes patient age and gender amongst other variables (e.g. preoperative diplopia) to calculate the globe shift following orbital decompression. However, there are three important remarks. First, these studies describe the anterior-posterior (X-axis) globe position change only. As the fat volume changes in three dimensions, it is reasonable to believe that the globe position can vary correspondingly. Second, the suggested associations rely on observation studies. Interpretation in terms of causal and individual prediction remains difficult. Many confounding factors such as ethnic anatomical differences, the role of patient subgroups (inflammatory diseases vs. traumatic events) and site of fat volume change (post- or pre-equatorial fat) still remain controversial^[10-12]. Third, the studies were based on clinical exophthalmometry and were not assessed by imaging analysis of the globe position and fat volumetry.

Using imaging data for quantification of orbital tissue volume could improve understanding of the underlying mechanisms and support a predictable treatment strategy. Furthermore, fat volumetry could be helpful in monitoring disease progression and therapeutic response and to define normal values. Post-processing analysis of radiological data is gaining importance in all fields of medicine^[13]. Two-dimensional measurements are easy and can estimate the tissue volume, but calculating the true 3D volume is considered to be more accurate^[14-16]. Both Computed Tomography (CT) and Magnetic Resonance Imaging (MRI) are routinely performed imaging modalities to study the orbital region. Whilst CT is the gold standard for the bony orbit, volumetric studies on orbital tissue have been largely studied with validated CT protocols^[4]. On the other hand, MRI techniques are rapidly expanding, hereby increasing post-processing opportunities. Nowadays MRI is considered the optimal technique for (sequential) orbital soft tissue imaging. It does not involve ionizing radiation, has excellent soft tissue contrast properties and can render images in any plane^[17]. The third article in this thesis illustrates that orbital muscle and fat volumetry is often performed for various indications and can be clinically relevant. On the other hand, volumetric studies of the lacrimal gland, globe and optic nerve are only sporadically reported. Care should be taken when interpreting the results. The wide differences in imaging modalities and the complex, time-consuming protocols of MRI hamper its routine clinical implementation and make comparison of results difficult. There is currently no consensus on performing MRI-based volumetry and the protocols continuously evolve, making it difficult to select the most reliable technique.

A standard T1 weighted sequence is widely available and is generally included in an orbital MRI scan protocol. If volumetric measurement of orbital tissue could contribute in the routine management of orbital disorders, it is meaningful to study the feasibility of this sequence. The fourth study of this thesis investigates the reliability of an MRI-based volumetry of orbital fat and explores the concordance with CT-based measurements. The authors conclude that a semi-automatic segmentation method is feasible in routine clinical practice by observers with a variable level of expertise. Intra-observer agreement is good, though inter-observer variability is moderate. These insights justify the use of retrospective analytic studies on the condition that images are taken with an identical

protocol, using the same hardware and software and preferably, be evaluated by the same observer.

To make comparison of results between studies more reliable, there is a need for standardized imaging and post-processing protocols. Uniformous imaging data and validated post-processing analysis facilitate long-term follow-up and multicenter collaboration. The accuracy of volumetric measurements depends on the correct identification of tissue intensity of the region of interest (ROI) and its surrounding structures ^[5,18]. In the final study of this thesis, the authors used qualitative and quantitative volumetric analysis methods to define the most accurate MRI acquisition protocols. Two dedicated imaging protocols are suggested for volumetric analysis of the orbital fat, extraocular muscles and globe. The study showed that MRI-based measurements for muscles and fat correlate better with the true volume than CT-based measurements. This emphasizes the value of using a protocol that results in a strong contrast between the ROI and other tissues, hereby optimizing the semi-automatic segmentation process and outcome accuracy. Other findings demonstrate that morphometric discrepancies may occur if different sequences are used. This also involves the globe. There are, however, several important implications for routine clinical practice. First, consecutive scanning for orbital diseases should ideally be performed with the same scanning protocol. Second, volumetric measurements can only be compared when obtained with identical scanning protocols. And finally, as the measurement error could exceed other detectable sources of volumetric change, absolute volumetric values have limited value between different studies.

Limitations

There are several limitations in this thesis that should be addressed. Orbital diseases may cause severe psychological impairment ^[19], hence surgical outcome and treatment successes go beyond objective measurements or image analysis. Quality of life assessment may provide a valuable approach to rectify the variability in clinical measurements and image post-processing. However, despite accumulating evidence of its importance, this tool is not yet applied in routine clinical practice. Further research is required to intensify the clinical implementation of quality of life assessment as a parameter to evaluate outcome in orbital surgery ^[6,7].

Relatively small datasets are used to support the study findings. First, this can be attributed to the search for a homogeneous study population. Various techniques for orbital surgery are practiced, the choice depending on a surgeon's experience, institutional tradition and specific conditions of the patient. To minimize bias, only patients with equal pathology and type of surgery were included. Second, before applying one new method in a large population, the authors decided to explore the feasibility and accuracy of multiple imaging methods on a limited sample. This methodology allowed to select the most suitable technique, however, validation on large study populations is required before our findings can be generalized.

As illustrated in this thesis, orbital imaging and post-processing analysis can be performed with CT as well as MRI scanning. Both have distinct indications as well as disadvantages that have to be taken into account. The globe position analysis (Article 1) was performed on consecutive CT scans. Although low-dose scan protocols can be used, the cumulative radiation dose could be harmful to orbital structures, causing adverse effects to the lens and retina ^[20]. In the pediatric population, there is the concern of potential malignancy. CT scan is the preferred modality for surgical planning due to the optimal visualization of the bony orbit and volumetric studies have been successfully used for the outcome assessment of orbital reconstructive surgery ^[21]. CT scan is the gold standard for traumatic injuries and/or during the perioperative period, thus legitimating repeated scans and facilitating the use of this protocol. However, monitoring the long-lasting disease, such as thyroid eye disease, may require repeated scans to evaluate the globe position and the cumulative dose could be of concern. Orbital imaging with an MRI scan offers an increased precision and superior depiction of the orbital soft tissues without radiation exposure. On the contrary, MRI always played a secondary role in the bony evaluation of the orbit, for example after orbital trauma. New developments in MRI protocols, such as black bone sequences, allow adequate identification of the bony contours and could make MRI a valuable radiation-free alternative for bony analysis ^[22]. A drawback for MRI is the presence of ferromagnetic foreign bodies whose displacement and/or heating may cause severe secondary injury ^[23,24]. Compared to a CT scan, the procedural time for MRI imaging takes considerably longer. This is important for the orbit as motion artifacts from eye movements decrease image resolution and cause measurement errors ^[16,25]. The use of fixation target inside the gantry can prevent eye movement during scanning and allows to obtain the same scanning position for consecutive scans, though these are not widely available.

Detailed MRI protocols are suggested in this thesis. Notably, MRI hardware companies may apply different names for similar sequences and acquisition parameters, all of which may result in significant deviations of the measurement outcome ^[26]. Moreover, each acquisition protocol contains several default parameters which cannot be modified without restrictions or causing additional artifacts. Before implementing a suggested orbital protocol, the details should be clarified with the service engineer, technician and radiologist. Also, care should be taken when comparing results obtained with different devices and it seems advisable to obtain consecutive scans with the same device and scanning protocol for the individual patient.

Future challenges

This thesis describes the spectrum of possible studies with orbital MRI and CT accommodating diagnosis and treatment of orbital disorders. Each imaging modality has its distinct indications and advantages but go alongside in the future. As health care resources must be used concisely, the complementarity of these techniques should be further investigated to enhance a multimodal approach. Ideally, only the optimal imaging

technique should be performed for a certain indication or disease stage, but information from consecutive scans should be fully comparable, contributing to the whole picture.

Regarding the clinical applications of the investigated techniques, this thesis focused on patients diagnosed with Graves' orbitopathy. The various orbital components that can be involved, the challenging disease progression and complexity of treatment make this a suitable condition for the current research purposes. Moreover, the techniques can be useful in the management of other conditions such as orbital fractures, anophthalmic socket syndrome, orbital tumors and congenital malformations. One important prerequisite to implement the morphometric measurements in clinical decision making would be the characterization of normal and aberrant values according to age and gender.

Detailed analysis and more sophisticated post-processing modalities increase the research potential, though can be highly demanding ^[18,27]. Staff must be trained to implement and analyse new imaging protocols. Investments in time as well as finances are necessary to obtain up-to-date hard- and software ^[13,28]. These practical burdens were overcome in research setting, however, could impede routine use in clinical practice. Clear protocols and close cooperation between radiologists, engineers, technicians and clinicians are mandatory to achieve valuable revenue regarding the clinical outcome. Moreover, implementation of the principles of deep learning and artificial intelligence could lead to more automated segmentation techniques, which could make the image analysis more accessible in clinical practice ^[29,30].

The ultimate goal of clinical research is to provide better patient care. High quality image analysis of the orbital soft tissues can be used to build an integrated virtual model. The more reliable the input, the more realistic a virtual model can diagnose abnormalities and simulate an intervention. Virtual models can be used to accommodate multidisciplinary discussions, for patient communication or to adjust a treatment plan. Like in many parts of society the virtual (r)evolution is advancing steadily in medicine. Software applications are more accessible (freeware and open source software) and 3D technology is becoming mainstream. It is challenging but imperative to bring expertise from diverse domains (fundamental researchers, computer scientists, clinicians, surgeons) together and create a common language. This concentration of knowledge is the way forward to generate creativity and explore new grounds.

Conclusions

New technologies are emerging fast around the globe. The orbit plays a central role in the face and various pathological conditions can affect its complex architecture. Imaging analysis could provide a more individual approach by implementing objective and patient-specific morphometric measurements in the diagnostic process and surgical management. This thesis provides insights in the value of post-processing analysis. It illustrates the pitfalls and potential of contemporary MRI techniques and gives practical knowledge for implementation in clinical practice.

REFERENCES

- [1] Segni M, Bartley GB, Garrity JA, Bergstralh EJ, Gorman CA. Comparability of proptosis measurements by different techniques. *Am J Ophthalmol*. 2002;133(6):813–8.
- [2] Ramli N, Kala S, Samsudin A, Rahmat K, Zainal Abidin Z. Proptosis - Correlation and Agreement between Hertel Exophthalmometry and Computed Tomography. *Orbit*. 2015;34(5):257–62.
- [3] Bingham CM, Sivak-Callcott JA, Gurka MJ, Nguyen J, Hogg JB, Feldon SE, et al. Axial Globe Position Measurement: A Prospective Multicenter Study by the International Thyroid Eye Disease Society. *Ophthal Plast Reconstr Surg*. 2016;32(2):106–12.
- [4] Regensburg NI, Kok PHB, Zonneveld FW, Baldeschi L, Saeed P, Wiersinga WM, et al. A new and validated CT-Based method for the calculation of orbital Soft tissue volumes. *Investig Ophthalmol Vis Sci*. 2008;49(5):1758–62.
- [5] Nishida Y, Tian S, Isberg B, Tallstedt L, Lennerstrand G. Significance of orbital fatty tissue for exophthalmos in thyroid-associated ophthalmopathy. *Graefes Arch Clin Exp Ophthalmol*. 2002;240(7):515–20.
- [6] Cheng AM, Wei YH, Tighe S, Sheha H, Liao SL. Long-term outcomes of orbital fat decompression in Graves' orbitopathy. *Br J Ophthalmol*. 2018;102(1):69–73.
- [7] Li EY, Kwok TY, Cheng AC, Wong AC, Yuen HK. Fat-removal orbital decompression for disfiguring proptosis associated with Graves' ophthalmopathy: safety, efficacy and predictability of outcomes. *Int Ophthalmol*. 2015;35(3):325–9.
- [8] Liao SL, Huang SW. Correlation of retrobulbar volume change with resected orbital fat volume and proptosis reduction after fatty decompression for graves ophthalmopathy. *Am J Ophthalmol*. 2011;151(3):465–469.e1.
- [9] Prat MC, Braunstein AL, Dagi Glass LR, Kazim M. Orbital fat decompression for thyroid eye disease: retrospective case review and criteria for optimal case selection. *Ophthal Plast Reconstr Surg*. 2015;31(3):215–8.
- [10] Wu CH, Chang TC, Liao SL. Results and Predictability of Fat-Removal Orbital Decompression for Disfiguring Graves Exophthalmos in an Asian Patient Population. *Am J Ophthalmol*. 2008;145(4):755–9.
- [11] Ivekovic R, Novak-Laus K, Tedeschi-Reiner E, Masnec-Paskvalin S, Saric D, Mandic Z. Full-thickness anterior blepharotomy and transpalpebral fat decompression in Graves' orbitopathy. *Coll Antropol*. 2005;29 Suppl 1:33–6.
- [12] Kazim M, Trokel SL, Acaroglu G, Elliott A. Reversal of dys-thyroid optic neuropathy following orbital fat decompression. *Br J Ophthalmol*. 2000;84(6):600–5.
- [13] Runge VM. Current technological advances in magnetic resonance with critical impact for clinical diagnosis and therapy. *Invest Radiol*. 2013;48(12):869–77.
- [14] Majos A, Grzelak P, Mlynarczyk W, Stefanczyk L. Assessment of intraorbital structure volume using a numerical segmentation image technique (NSI): the fatty tissue and the eyeball. *Endokrynol Pol*. 2007;58(4):297–302.
- [15] Lennerstrand G, Tian S, Isberg B, Landau Hogbeck I, Bolzani R, Tallstedt L, et al. Magnetic resonance imaging and ultrasound measurements of extraocular muscles in thyroid-associated ophthalmopathy at different stages of the disease. *Acta Ophthalmol Scand*. 2007 Mar;85(2):192–201.
- [16] Clark RA, Demer JL. Changes in Extraocular Muscle Volume During Ocular Duction. *Invest Ophthalmol Vis Sci*. 2016;57(3):1106–11.
- [17] Firbank MJ, Coulthard A. Evaluation of a technique for estimation of extraocular muscle volume using 2D MRI. *Br J Radiol*. 2000 Dec;73(876):1282–9.
- [18] Tang X, Liu H, Chen L, Wang Q, Luo B, Xiang N, et al. Semi-automatic volume measurement for orbital fat and total extraocular muscles based on Cube FSE-flex sequence in patients with thyroid-associated ophthalmopathy. *Clin Radiol*. 2018;73(8):759.e11–759.e17.
- [19] Wiersinga WM. Quality of life in Graves' ophthalmopathy. *Best Pract Res Clin Endocrinol Metab* [Internet]. 2012 Jun;26(3):359–70. Available from: <http://dx.doi.org/10.1016/j.beem.2011.11.001>
- [20] Khan DZ, Lacasse MC, Khan R, Murphy KJ. Radiation Cataractogenesis: The Progression of Our Understanding and Its Clinical Consequences [Internet]. Vol. 28, *Journal of Vascular and Interventional Radiology*. Elsevier; 2017. p. 412–9. Available from: <http://dx.doi.org/10.1016/j.jvir.2016.11.043>
- [21] Siakallis LC, Uddin JM, Miszkil KA. Imaging Investigation of Thyroid Eye Disease. Vol. 34, *Ophthalmic plastic and reconstructive surgery*. 2018. p. S41–51.
- [22] Schmutz B, Rahmel B, McNamara Z, Coulthard A, Schuetz M, Lynham A. Magnetic resonance imaging: an accurate, radiation-free, alternative to computed tomography for the primary imaging and three-dimensional reconstruction of the bony orbit. *J Oral Maxillofac Surg*. 2014 Mar;72(3):611–8.
- [23] Kubal WS. Imaging of Orbital Trauma. *RADIOGRAPHICS*. 2008;28(6):1729–39.
- [24] Freund M, Hahnel S, Sartor K. The value of magnetic resonance imaging in the diagnosis of orbital floor fractures. *Eur Radiol*. 2002 May;12(5):1127–33.
- [25] Firbank MJ, Harrison RM, Williams ED, Coulthard A. Measuring extraocular muscle volume using dynamic contours. *Magn Reson Imaging*. 2001 Feb;19(2):257–65.
- [26] Kaichi Y, Tanitame K, Itakura H, Ohno H, Yoneda M, Takahashi Y, et al. Orbital Fat Volumetry and Water Fraction Measurements Using T2-Weighted FSE-IDEAL Imaging in Patients with Thyroid-Associated Orbitopathy. *Am J Neuro-radiol*. 2016 Nov;37(11):2123–8.

Discussion

- [27] Comerci M, Elefante A, Strianese D, Senese R, Bonavolontà P, Alfano B, et al. Semiautomatic regional segmentation to measure orbital fat volumes in thyroid-associated ophthalmopathy a validation study. *Neuroradiol J*. 2013;26(4):373–9.
- [28] Blamire AM. The technology of MRI - The next 10 years? *Br J Radiol*. 2008;81(968):601–17.
- [29] Pagnozzi AM, Fripp J, Rose SE. Quantifying deep grey matter atrophy using automated segmentation approaches: A systematic review of structural MRI studies. *Neuroimage* [Internet]. 2019;116018. Available from: <https://linkinghub.elsevier.com/retrieve/pii/S1053811919305993>.
- [30] Hoffmann J, Schmidt C, Kunte H, Klingebiel R, Harms L, Huppertz H-J, et al. Volumetric assessment of optic nerve sheath and hypophysis in idiopathic intracranial hypertension. *AJNR Am J Neuroradiol*. 2014 Mar;35(3):513–8.
-

Summary

The orbit is a bony cavity containing the eye globe, which is embedded in a cuff of soft tissues including fat and muscles amongst others. Disorders of the orbital architecture, for example due to inflammatory diseases or facial trauma, can cause globe displacement, problems with vision and facial disfigurements leading to functional, social and aesthetic impairment.

Orbital imaging studies like computer tomography (CT) and magnetic resonance imaging (MRI) are valuable tools to support the diagnostic pathway, to objectify observations during follow-up or to assist the surgical planning. Advancements in image post-processing are expanding the potential of a more detailed analysis and a patient-specific approach. This thesis aims exploring the role of intra-orbital structures through a study of the post-processing capabilities.

Determining the globe position is a prerequisite when studying an orbital disease. Different clinical and radiological methods are described though all have inherent shortcomings. The first study of this thesis establishes a CT-based method to measure a change of the globe position in three-dimensions. This technique is accurate, precise and illustrates the globe displacement in every dimension. The downside, however, is the need for consecutive CT scans hence exposing the patient to radiation effects. MRI is a

radiation free alternative and displays an excellent soft tissue contrast. The authors plan to proceed studying this method by implementing an MRI-based analysis of the globe position.

The larger part of the orbital tissue consists of fat. The second study illustrates that changes of the orbital fat evoke displacements of the globe. This could lead to a variable degree of double vision, although the mechanisms of action are unclear. Interestingly, it was illustrated that removal of orbital fat was relatively safe and can be considered an effective treatment for patients suffering from exophthalmos. Imaging studies could be of great value to measure the orbital fat volume. Abnormal amounts of fat could be detected and a treatment plan could be modified to the patient-specific situation. A CT-based analysis of the orbital fat volume has been previously described and validated. Because MRI is believed to produce a superior depiction of the soft tissues, the third study of this thesis explored the current literature to investigate the possibilities of soft tissue volumetry with MRI. This review reveals a myriad of MRI-based techniques for orbital volumetric analysis. Large heterogeneity exists related to the study hardware, imaging protocols and volumetric analysis. Because there is currently no consensus on the preferred MRI technique, care should be taken when comparing results obtained with different protocols. Moreo-

ver, it is unclear to which degree the CT-based analysis is equivalent to a volumetric assessment on MRI.

For this reason, the authors investigated in a fourth study if volumetry on a regular MRI protocol would be feasible and comparable to a validated CT-based method. Provided that post-processing software is available, this report illustrates that volumetric analysis on a regular T1 weighted protocol is feasible in routine clinical practice. Correlation with CT-based volumetry is good. It should be taken into account however, that considerable bias may derive from observer variability and these errors could impede the clinical relevance in certain pathological conditions.

Using the best suitable MRI protocol could optimize measurement accuracy. In the final study of this thesis, various MRI techniques are qualitatively and quantita-

tively evaluated and correlated to a volumetric assessment on CT as well as to the true anatomical specimen. Two protocols are suggested for optimal orbital fat, muscle and globe volume assessment. These findings could enhance post-processing accuracy; nevertheless future studies should confirm these recommendations by evaluating the suggested protocols in larger cohorts.

To summarize, this thesis focuses on the post-processing opportunities as a bridging tool from the clinical assessment and imaging to the diagnosis and treatment planning in orbital disorders. Insights in the potential and pitfalls of post-processing analysis can enhance the implementation in clinical practice and research projects. The goal is to provide objective documentation of the orbital content so to improve understanding of the pathophysiological mechanisms and advance patients-specific approaches.

Samenvatting

De oogkas of orbita is een benige holte in het aangezichtsskelet die de oogbol beschermt en daarnaast ook plaats biedt aan andere weefsels zoals spieren en vet. Onder meer ontstekingsziekten of een aangezichtstrauma kunnen de structuur van de orbitale weefsels aantasten. Dit kan leiden tot een veranderde positie van de oogbol, visus problemen of misvormingen van het gelaat wat gepaard kan gaan met functionele, sociale en esthetische bezwaren.

Computer tomografie (CT) en magnetische resonantie (MR) zijn beeldvormingsonderzoeken die een belangrijke waarde hebben bij orbitale aandoeningen. Zij spelen een rol in het bepalen van de diagnose, maar zijn ook van belang bij het opsporen van veranderingen tijdens de opvolging van een ziekte of om de heelkundige behandeling voor te bereiden. Specifieke bewerking van deze beelden laat een meer gedetailleerde analyse toe die kan bijdragen tot een meer patiënt gericht behandeltraject. De nadruk van deze thesis ligt op het nagaan van de mogelijkheden om de beeldvorming te bewerken zodat meer inzicht kan verkregen worden in de rol van de verschillende orbitale weefsels.

De positie van de oogbol in de oogkas is een belangrijke parameter bij het onderzoek van een orbitale aandoening. Er bestaan verschillende methoden om de positie te bepalen met klinische meetinstrumenten of rechtstreeks op de beeld-

vorming. Elk van deze instrumenten hebben echter hun beperkingen. In het eerste onderzoek van deze thesis wordt een nieuwe methode voorgesteld om de veranderingen in de positie van de oogbol in 3 dimensies te documenteren. Deze methode is zeer nauwkeurig, maar veronderstelt opeenvolgende CT scans en stelt de patiënt dus bloot aan röntgenstraling. De MR scan vermijdt deze straling en kan tevens alle orbitale weefsels zeer gedetailleerd weergeven. In de toekomst zullen de auteurs nagaan of de MR scan als alternatief kan gebruikt worden om deze nieuwe meetmethode toe te passen.

Naast de oogbol, bestaat het grootste deel van de orbitale weefsels uit vet. Een tweede studie van deze thesis toont aan dat volumewijzingen in het vet een belangrijke verandering in de oogbolpositie kunnen aantonen. Dit kan in bepaalde situaties leiden tot dubbelzicht bij de patiënt, maar meer onderzoek is nodig om de oorzakelijke mechanismes hiervoor te kunnen achterhalen. Het onderzoek toont verder aan dat het verwijderen van orbitaal vet veilig kan gebeuren en een effectieve behandeling kan zijn wanneer patiënten klachten hebben van een te ver naar voor gepositioneerde oogbol. In deze context zou het nameten van het vetvolume op beeldvorming een grote meerwaarde kunnen betekenen. Wanneer een te groot vetvolume kan worden gedetecteerd, zou dit een behandelplan op maat van de patiënt kunnen ondersteunen. Een meet-

methode waarbij gebruik gemaakt wordt van een CT scan werd reeds voorgesteld. Echter, om de hierboven aangehaalde redenen van straling en omdat een MR scan de weke weefsels nauwkeuriger kan beschrijven, zou een MR onderzoek beter geplaatst kunnen zijn voor het meten van het orbitale vet. Een derde luik van deze thesis omvat een nazicht van de huidige literatuur omtrent de mogelijkheden om weefselvolumes te berekenen op basis van orbitale MR beeldvorming. In dit overzicht wordt duidelijk dat uiteenlopende technieken zijn beschreven, maar het is onduidelijk welke toestellen, richtlijnen of volumemetingen meest geschikt zijn. Het ontbreken van gelijkvormigheid tussen de verschillende studies maakt het niet mogelijk om resultaten te vergelijken of om een normale waarde te bepalen. Daarenboven is het onduidelijk in welke mate de metingen op MR overeenkomen met gelijkaardige metingen op de CT scan.

Om deze reden werd in een vierde studie van deze thesis nagegaan of het mogelijk is het vetvolume te bepalen op een standaard MR scan en in welke mate dit resultaat overeenstemt met metingen gebaseerd op een CT scan. Mits goede software voorhanden is, illustreert dit onderzoek dat het vetvolume relatief eenvoudig kan bepaald worden op een T1 gewogen MR scan. Dit resultaat stemt goed overeen met gelijkaardige metingen op een CT scan. Men moet echter indachtig zijn dat deze metingen een zekere foutmarge kunnen bevatten naargelang verschillende onderzoekers de metingen doen. Afhankelijk van de ernst van verandering veroorzaakt door de ziekte, kan deze foutmarge de klinische relevantie van het onderzoek teniet doen.

Indien de standaard MR scan wordt vervangen door een meer gespecialiseerd MR onderzoek zouden deze foutmarges kunnen verkleinen. Een laatste onderzoek in deze thesis gaat na welke MR technieken meest geschikt zijn voor volumemetingen in de orbita. Door middel van kwalitatieve en kwantitatieve analyses wordt nagegaan welke technieken het meest nauwkeurig zijn in vergelijking met de CT gebaseerde metingen en het ware volume na weefseldissectie. Twee specifieke protocollen worden voorgesteld om volumemetingen van orbitaal vet, spieren en de oogbol zo nauwkeurig mogelijk uit te voeren. Toekomstig onderzoek is noodzakelijk om deze resultaten te bevestigen in grotere aantallen en zo een uniforme meetmethode te kunnen introduceren.

Kort samengevat, deze thesis benadrukt de mogelijkheden bij het bewerken van de beeldvorming om, naast het klinisch onderzoek, de diagnose en behandeling bij orbitale aandoeningen beter te kunnen ondersteunen. Kennis van de kracht, maar ook van de valkuilen is noodzakelijk om deze bewerkingen uit te voeren binnen de klinische praktijk alsook in het kader van onderzoeksprojecten. Het doel is bij te dragen aan een objectieve documentatie van de orbitale structuren zodat ziekteprocessen beter kunnen beschreven worden en een nog meer patiënt gerichte behandeling mogelijk wordt.

Personal contributions

Article 1 – Three-dimensional characterisation of the globe position in the orbit.

R. Willaert, E. Shaheen, J. Deferm, H. Vermeersch, E. Jacobs, I. Mombaerts

Contributors RW and ES shared the first authorship and contributed equally. Design and conduct of the study by RW and ES. ES constructed various digital models for measuring the globe position, which were evaluated and validated by RW. Collection, analysis, management and interpretation of the data by RW, ES, JD and IM. Preparation of the manuscript by RW, ES and IM. Critical revision of the manuscript was performed by JD, RJ, HV and IM. Review and final approval of the manuscript by all the authors.

This article was published as: Willaert R, Shaheen E, Deferm J, Vermeersch H, Jacobs R, Mombaerts I. Three-dimensional characterisation of the globe position in the orbit. *Graefes Arch Clin Exp Ophthalmol*. 2020 March 05. <https://doi.org/10.1007/s00417-020-04631-w>

Article 2 – Efficacy and complications of orbital fat decompression in Graves' orbitopathy: a systematic review and meta-analysis.

R. Willaert, T. Maly, V. Ninclaus, W. Huvenne, H. Vermeersch, N. Brusselsaers

Design and conduct of the study by RW, TM and NB. Collection, analysis, management and interpretation of the data by RW, TM and VN. Preparation of the manuscript by RW, TM and WH. Critical revision of the manuscript was performed by VN, WH, HV and NB. Review and final approval of the manuscript by all the authors.

This article was published as: Willaert R, Maly T, Ninclaus V, Huvenne W, Vermeersch H, Brusselsaers N. Efficacy and complications of orbital fat decompression in Graves' orbitopathy: a systematic review and meta-analysis. *Int J Oral Maxillofac Surg*. 2019. <https://doi.org/10.1016/j.ijom.2019.08.009>

Article 3 – A Systematic Review on Volumetric Analysis in Orbital MRI.

R. Willaert, M. Degraeve, J. Deferm, K. Orhan, I. Mombaerts, R. Jacobs, N. Brusselsaers

Design and conduct of the study by RW and MD. Collection and analysis of the data by RW and MD. Management and interpretation of the data by RW, JD and KO. Preparation of the manuscript by RW, IM and NB. Critical revision of the manuscript was performed by JD, RJ and IM. Review and final approval of the manuscript by all the authors.

**Article 4 – Semi-automatic MRI based Orbital Fat Volumetry:
Reliability and Correlation with CT.**

R. Willaert, B. Degrieck, K. Orhan, J. Deferm, C. Politis, E. Shaheen, R. Jacobs

Design and conduct of the study by RW, BD and KO. Data collection by RW, ES and JD. Analysis, management and interpretation of the data by RW, KO and ES. Preparation of the manuscript by RW, ES and JD. Critical revision of the manuscript was performed by BD, ES, CP and RJ. Review and final approval of the manuscript by all the authors.

This article was published as: Willaert R, Degrieck B, Orhan K, Deferm J, Politis C, Shaheen E, Jacobs R. Semi-automatic magnetic resonance imaging based orbital fat volumetry: reliability and correlation with computed tomography. *Int J Oral Maxillofac Surg.* 2020 Aug 17:S0901-5027(20)30288-5. doi: 10.1016/j.ijom.2020.07.027.

**Article 5 – Development and Validation of an MRI Protocol
for Orbital Soft Tissue Volumetry.**

R. Willaert, J. De Tobel, K. Orhan, S. Bogaert, S. Ruiters, E. Shaheen, C. Politis, R. Jacobs

Design and conduct of the study by RW, JDT, KO and ES. Collection, analysis, management and interpretation of the data by RW, ES, SB and SR. Preparation of the manuscript by RW, ES and JDT. Critical revision of the manuscript was performed by SR, RJ, CP and SB. Review and final approval of the manuscript by all the authors.

Acknowledgements

Most people would agree that I am not a man of many words, that's why this section certainly is a great opportunity to express the often unspoken gratitude.

First to my Soul Mate, for continuously forcing me out of my comfort zone and comfort me when I am forced to change track or have to overcome an unforeseen burden.

Full recognition and thanks are due to the important contributions of my promotors:

- Prof. Em. Dr. H. Vermeersch for initiating this project, stimulating the creative thinking and for his enthusiasm that was the fuel to keep the fire going.
- Prof. Dr. N. Brusselaers for her sincere commitment, valuable comments and guidance throughout the entire process.
- Prof. Dr. R. Jacobs for setting the research goals, designing a clear path and providing the invaluable network of people to accomplish this.
- Prof. Dr. I. Mombaerts to share her tremendous expertise and meticulous reviewing, lifting the overall quality to a higher level.

A special recognition should be given to Ir. E. Shaheen for bridging the gap between the clinical practice and computer science. Your striving for novelty and high quality research work was an essential motor during the whole process.

My sincere thanks to all co-authors for their continuous efforts, patience and scientific input. Every one contributed to her or his expertise and the end result could never be achieved without their significant work. We made every effort to minimize errors and inaccuracies. If any did occur, we apologize.

I want to acknowledge Prof. dr. C. Politis for facilitating this research work during my years of clinical training. The continuous and structural support for scientific work in the field of oral and maxillofacial surgery must be highly appreciated.

I also want to express my gratitude to Janine Kopatz for her expert skills, dedication and patience regarding the editing process.

And lastly, I owe a great debt of gratitude to my parents for performing probably the most difficult task: they never meddle with what I am doing, but they always give me the confidence and the courage to pursue my goals. And not to forget, my parents-in-law for their unrestrained hospitality throughout the years.

Curriculum vitae

PERSONAL DATA

name Robin Willaert
date of birth May 30th, 1986
place of birth Veurne, Belgium
nationality Belgian
profession Medical Doctor

CONTACT

address Dept. Oral and Maxillofacial Surgery
University Hospital Leuven
Herestraat 49, 3000 Leuven

e-mail robin.willaert@uzleuven.be
robin.willaert@icloud.com

phone +32 16 34 12 69
+32 16 33 24 62

fax +32 16 34 24 37

PROFESSIONAL CAREER*Education*

2013 – 2017	Master in Maxillofacial Surgery, KU Leuven, Leuven, Belgium
2006 – 2013	Bachelor and Master in Medicine, KU Leuven, Leuven, Belgium (Summa cum laude, highest distinction)
2004 – 2009	Bachelor and Master in Dentistry KU Leuven, Leuven, Belgium (Magna cum laude, great distinction)
1998 – 2004	Latin-Mathematics, College Veurne, Veurne, Belgium

Surgical training

2016 – 2017	Dept. Head, Neck & Maxillofacial Surgery (Prof. Dr. H. Vermeersch) Ghent University Hospital, Ghent, Belgium
2015 – 2016	Dept. Maxillofacial Surgery (Dr. T. Hoppenreijns) Rijnstate hospital, Arnhem, The Netherlands
2014 – 2015	Dept. Head, Neck & Maxillofacial Surgery (Prof. Dr. H. Vermeersch) Ghent University Hospital, Ghent, Belgium
2013 – 2014	Dept. Maxillofacial surgery (Prof. Dr. C. Politis) University hospital Leuven, Leuven, Belgium

Fellowship

2020	Dept. Oral and Maxillofacial Surgery (Prof. Dr. R. Rikhotso) Chris Hani Baragwanath Hospital, Johannesburg, South Africa
2019	Dept. Plastic and Reconstructive Surgery (Dr. S. Jirawatnotai) Lerdsin Hospital, Bangkok, Thailand
2017 – 2018	Dept. Head, Neck & Maxillofacial Surgery (Prof. Dr. H. Vermeersch) Ghent University Hospital, Ghent, Belgium

PUBLICATIONS

*Articles in journals
indexed in ISI Web
of Science*

Shaheen E, **Willaert R**, Miclotte I, Coropciuc R, Bila M, Politis C. A novel fully automatic design approach of a 3D printed face specific mask: proof of concept. PLOS ONE. 2020. In press (accepted 20th November 2020)

Willaert R, De Tobel J, Orhan K, Bogaert S, Ruiters S, Shaheen E, Politis C, Jacobs R. Development and Validation of an MRI Protocol for Orbital Soft Tissue Volumetry. Submitted to European Journal of Radiology.

Willaert R, Degrieck B, Orhan K, Deferm J, Politis C, Shaheen E, Jacobs R. Semi-automatic magnetic resonance imaging based orbital fat volumetry: reliability and correlation with computed tomography. Int J Oral Maxillofac Surg. 2020.17:S0901-5027(20)30288-5. doi: 10.1016/j.ijom.2020.07.027.

Deferm JT, Baan F, Schreurs R, **Willaert R**, Maal T, Meijer G. Digital surface scanning in flap perfusion. Int J Oral Maxillofac Surg. 2020. S0901-5027(20)30202-2. doi: 10.1016/j.ijom.2020.05.015.

Willaert R, Shaheen E, Deferm J, Vermeersch H, Jacobs R, Mombaerts I. Three-dimensional characterisation of the globe position in the orbit. Graefes Arch Clin Exp Ophthalmol. 2020 March 05. <https://doi.org/10.1007/s00417-020-04631-w>

Willaert R, Maly T, Ninclaus V, Huvenne W, Vermeersch H, Brusselaers N. Efficacy and complications of orbital fat decompression in Graves' orbitopathy: a systematic review and meta-analysis. Int J Oral Maxillofac Surg. 2019. <https://doi.org/10.1016/j.ijom.2019.08.009>

Willaert R, Nevens D, Laenen A, Batstone M, Politis C, Nuyts S. Does intensity-modulated radiation therapy lower the risk of osteoradionecrosis of the jaw? A long-term comparative analysis, Int J Oral Maxillofac Surg. 2019. <https://doi.org/10.1016/j.ijom.2019.04.018>

Willaert R, Opdenakker Y, Sun Y, Politis C, Vermeersch H. New technologies in rhinoplasty: A comprehensive workflow for computer-assisted planning and execution. PRS global open. 2019. DOI: 10.1097/GOX.

Ceulemans L.J., Deferm N.P., Deferm S, **Willaert R.A.**, Deferm J.T., Vanhoenacker F.M. Unusual Cause of Mechanical Ileus: Abdominal Cocoon Syndrome. Journal of the Belgian Society of Radiology. 2016. 100(1), p.36

PUBLICATIONS*Articles in journals
not indexed in ISI Web
of Science*

Willaert R, Van Bever PJ, Knockaert B, Verhaeghe W, Huvenne W, Vermeersch H. Kaakbotnecrose : achtergrond en recente inzichten voor de algemeen practicus. Tijdschrift voor Geneeskunde. 2016. 72:906-911.

Verhaeghe W, Demey N, Knockaert B, **Willaert R**, Vermeersch H. Fracturen van het aangezichtsskelet. Tijdschrift voor Geneeskunde. 2016. 72:900-905.

Knockaert B, Verhaeghe W, **Willaert R**, Jacobs K, Vermeersch H. Dentogene infecties. Tijdschrift voor Geneeskunde. 2016. 72:894-899.

Publications in books

None

Theses

“Hyperbaric medicine: indications for head and neck pathology”
2013, Thesis Master in Medicine
Promotor: Prof. Dr. C. Politis

“Patient indications and motivation in orthognathic surgery”
2009, Thesis Master in Dentistry
Promotor: Prof. Dr. G. Willems

SCIENTIFIC ACTIVITIES*International congresses
oral presentations***“Evaluation of the globe position -Validation of a new method”.**

Willaert R, Shaheen E, Deferm J, Jacobs R, Vermeersch H, Mombaerts I.
77th PRS KOREA 2019. Seoul, Korea.

“Virtual rhinoplasty”.

Willaert R, Opendakker Y, Sun Y, Politis C, Vermeersch H.
77th PRS KOREA 2019. Seoul, Korea.

“Evaluation of different MRI protocols for orbital soft tissue segmentation”.

Willaert R, Orhan K, Detobel J, Bogaert S, Ruiters S, Shaheen E, Jacobs R.
ESHNR 2019, Clinisi, Italy.

“Fat decompression in endocrine orbitopathy”.

Willaert R, Maly T, Ninclaus V, Huvenne W, Vermeersch H, Brusselaers N.
24th EACMFS conference 2018. Munich, Germany.

“New technological advances in rhinoplasty”.

Willaert R, Opendakker Y, Sun Y, Politis C, Vermeersch H.
8th European Rhinoplasty Course 2018. Brussels, Belgium.

“The use of piezosurgery in rhinoplasty”.

Willaert R, Vermeersch H.
8th European Rhinoplasty Course 2018. Brussels, Belgium.

“Piezosurgery in rhinoplasty”.

Willaert R, Vermeersch H
7th European Rhinoplasty Course 2017. Brussels, Belgium.

*National congresses
oral presentations***“Lacrimal trauma and management”.**

Willaert R, Deferm J, Ninclaus V, Knockaert B, Verhaeghe W, Vermeersch H.
KBVSMFH 2016, Brussels, Belgium.

“Anterior segment osteotomy”.

Willaert R, Brouns J, Hoppenreijns
T. KBVSMFH 2015, Brussels, Belgium.

“Orbital decompression in facial trauma”.

Willaert R, Knockaert B, Verhaeghe W, Huvenne W, Ninclaus V, Vermeersch H.
KBVSMFH 2014, Brussels, Belgium.

SCIENTIFIC ACTIVITIES*National congresses
oral presentations***“Extra-oral implants and episthesis”.**

Willaert R, Ureel M, Knockaert B, Verhaeghe W, Huvenne W , Bonte K, Deron P,
De Cubber J, Vermeersch H.
KBVSMFH 2014, Brussels, Belgium.

“Hyperbaric medicine: fact and fiction”.

Willaert R, Politis C.
ASBL 2013, Luik, Belgium.

“IMRT in head and neck cancer”.

Willaert R, Nevens D, Laenen A, Politis C, Nuyts S.
KBVSMFH 2012, Brussels, Belgium.

“The abdominal cocooning syndrome”.

Ceulemans L, Deferm N, Deferm S, Willaert R, Deferm J, Vanhoenacker F.
Belgian Surgical Week 2012, Spa, Belgium.

SCIENTIFIC COURSES**Cadaveric workshop on Rhinoplasty.**

Siriraj Hospital, 07/2019, Bangkok, Thailand.

17th Annual Asian course in head and neck surgery.

Hands-on training in microvascular surgery.

02/2019, Bangkok, Thailand.

8th European rhinoplasty course.

03/2018, Brussels, Belgium.

55th International course for stepwise flap raising.

02/2018, Aachen, Germany.

SASMFOS surgical flap raising cadaver hands on workshop.

09/2017, Cape town, South Africa.

7th European rhinoplasty course.

04/2017, Brussels, Belgium

Advances in computer-assisted microvascular craniomaxillofacial reconstruction.

11/2016, London, United Kingdom.

Advances and innovations in CMF trauma course.

11/2016, London, United Kingdom.

6th AOCMFS advanced course on orbital reconstruction.

05/2016, Birmingham, United Kingdom.

AOCMF course-principles in craniomaxillofacial fracture management.

12/2014, Davos, Switzerland.

SERVICES*Scholarly Services***Lecture “CBCT in maxillofacial surgery”**

Course for CBCT in Dentistry Part I. 10/2017, Ghent, Belgium.

Lecture “Iatrogenic necrosis of the jaw”

Alumni Conference University Hospital Ghent. 11/2015, Ghent, Belgium.

Lecture “Airway anatomy in obstructive sleep apnoe”

Ortho Leuven Conference. 11/2014, Leuven, Belgium.

Lecture “Oral biopsy-technique”

Alumni Conference-LUTV. 12/2013, Leuven, Belgium.

Lecture “Impaired jaw opening”

Alumni Conference-LUTV. 03/2013, Leuven, Belgium.

*Promotorship***Co-promotor master thesis Medicine**

Ine Strubbe (2016, 2017).

“Radiographic evaluation in Graves’ Orbitopathy”

Matthias Quisqater (2016, 2017).

“Orbital decompression procedures: review of the literature”

*External reviewer***International Journal of Oral and Maxillofacial Surgery**

European Journal of Radiology – Tijdschrift voor geneeskunde

*Community Services***Dental camp**

MEDORA, 2019, Chitwan, Nepal.

Oral surgery and maxillofacial reconstruction

SEE AND SMILE, 2018, Loikaw, Myanmar.

Teaching activities at dept. plastic and reconstructive surgery

CORSU, 2017, Kisubi, Uganda.

Dental camp

MEDORA, 2017, Maikaisingh, Nepal.

Dental camp

MEDORA, 2016, Maikaisingh, Nepal.

MEMBERSHIPS

KBVSMFH

Royal Belgium Society of Stomatology and Maxillofacial Surgery

EACMFS

European Association for Cranio Maxillo Facial Surgery

IAOMS

International Association of Oral and Maxillofacial Surgeons

